A Study of Orientated Crystal Growth on Inert and Active Substrates.

By

D.M.Evans, B.Sc., A.Inst.P.

A Thesis Submitted for the Degree of Doctor of Philosophy in the University of London.

Applied Physical Chemistry Laboratories,
Imperial College of Science and Technology,
London, S.W.7.

November, 1950.

Contents.

Abstract.

The method of electron diffraction, which is ideally suited to the study of some of the fundamental problems of crystal growth, is applied to the study of the structure of films deposited on active and inactive substrates, chemical reactions with polycrystalline and single-crystal substrates, and strain effects in chemically formed surface layers.

The structure of one-degree oriented films of iron, lead sulphide, and zinc, formed by the condensation of the vapour on inert substrates, is investigated and the manner in which the orientation of the deposit crystals is influenced by the main experimental conditions is elucidated, with particular regard to the effect of oblique incidence of the vapour stream and the effect of the surface texture, both of which have been inadequately investigated hitherto.

The influence of the substrate on the orientation of the oxidation product of polycrystalline zinc specimens is illustrated, while the results obtained with deposits formed by chemical reaction on the cleavage face of a zinc single-crystal and with deposits formed by condensing zinc from the vapour on to the cleavage face of rock-salt lead to a new insight into the nature and stability of two-degree oriented films.

PART I. INTRODUCTION.

1. General Introduction.

Since the discovery by Davisson and Germer (1927) and Thomson (1927) of the diffraction of electrons by crystals, Thomson's photographic technique has led to the extensive use of high voltage electrons as a means of investigating the atomic structure of matter in thin films and gases. Owing to the scattering and absorption of electrons by matter being very much greater than that of X rays even films only a few atoms thick can give clear diffraction patterns, and the immediate surface regions of massive materials can be studied without the diffraction pattern being confused, as in X-ray diffraction, by the presence of stronger contributions from the rest of the underlying material. The method of electron diffraction is thus ideally suited to the study of some of the fundamental problems of crystal growth in surface layers and it has been applied, by various workers, to the study of the structure of films deposited on solid or liquid substrates (from solution, from the vapour, or by electrodeposition etc.), molecular structure, catalysis, wear and lubrication, anodic processes, photo-electric properties, chemical reactions and corrosion.

In the experiments described below, the Finch type of camera was used for recording the electron diffraction patterns

at voltages of the order of 60 KV. The camera and the technique have been described by Finch, Quarrell and Wilman (1935) and the general theory of the diffraction of electrons by Finch and Wilman (1937), Thomson and Cochrane (1939), and von Laue (1948).

In the present study of crystal growth the structure of one-degree oriented films, formed by the condensation of the vapour on various substrates is investigated. The results elucidate the manner in which the main experimental conditions influence the structure of the films, with particular regard to the effect of oblique incidence of the vapour stream and the effect of the surface texture, both of which have been inadequately investigated hitherto. For these experiments zinc, lead sulphide and iron were especially suitable in view of their different structures and properties; these experiments are described in Part II. The orientation of the oxide and sulphide reaction products formed from the one-degree oriented zinc deposits is described in Part IV and shows the relation of this orientation to that of the zinc substrate.

The experiments described in Parts III and IV lead to a new insight into the nature and stability of two-degree oriented deposits on single-crystal substrates. Instructive examples of epitaxy were observed in the case of zinc oxide on a zinc cleavage face (Part IV) and in the case of zinc deposits

condensed in vacuo on rocksalt cleavage faces (Part III). The results on the oxidation of ZnS (Part V) show for the first time how the strain due to the misfit of the lattices of the substrate and the deposit at the interface is relieved by a kind of deformation - now recognised for the first time as a process of rotational slip. The relation of the direction of the rotational slip to the applied stress was investigated further by appropriate unidirectional abrasion of ZnS cleavage faces (see Part V) and electropolished copper (110) faces (see Part VI).

Before describing the above experiments which lead to these new advances an account is given of the previous work in these fields of the structure and orientation of deposits, epitaxy, deposition by chemical reaction, and stresses in chemically formed surface layers.

2. Crystal growth in thin films condensed from the vapour on inert substrates.

Metals deposited on glass at liquid air temperatures have been shown to be amorphous (Gen, Zelmanoff and Schalnikoff 1933; Hass, 1937), while some metals have been shown to be amorphous in very thin films at room temperature. For instance Was (1939) obtained diffuse ring patterns from gold films when the thickness was $\sim$ 70 A., but the film showed crystalline structure on thickening.

The amorphous state of deposited metals has most often

been observed in the case of antimony and arsenic. The amorphous phase of arsenic formed by electrodeposition has been observed by Finch and Sun (1936), while the amorphous phase of antimony formed by electrodeposition has been observed by Hass (1937) and by Finch, Wilman and Yang (1947). The amorphous phase of sublimed arsenic has been observed by Greiling and Richter (1949), while the amorphous phase of antimony condensed from the vapour has been observed by Levinstein (1949).

With these exceptions, thin metal films formed by condensation of the vapour on to substrates at room temperature are confirmed by electron diffraction to be crystalline in nature, and are characterised by properties which differ considerably from those of the bulk metal. Extensive studies on resistivities, for example, can now be interpreted, in the light of electron diffraction results, as showing that the resistivity of a thin film is considerably greater than that of bulk metal mainly because of the discontinuous crystal structure of the film, and that the ratio of resistivity of a film to that of bulk metal depends on the mean thickness and the type of film. The properties of thin films also vary considerably according to the experimental conditions of their formation. The factors which are most frequently cited as causes for such variations are the atomic velocity and the number of atoms impinging on the surface per second, the type

of substrate and the temperature during deposition, the thickness of the film, and the degree of vacuum maintained in the chamber. The influence of these factors will now be considered briefly.

The dependence of deposit structure on the velocity of the impinging atoms. Miayamato (1933) has developed a theory according to which a potential barrier at a surface would permit only fast atoms to reach the surface, while slower atoms would be reflected. Beek, Smith and Wheeler (1940) have suggested that preferred orientation of films, formed by atoms evaporated in a gaseous atmosphere, might be caused by the decreased velocity of the atoms after colliding with gas atoms. Bateson and Bachmeyer (1946) have attributed the poor quality of some evaporated non-reflecting coatings to atoms of low velocity. In order to study the effects of atomic velocity on the film structure Levinstein (1949) investigated the effects of different velocities using a mechanical velocity selector and found that whereas antimony (whose vapour was found to consist of polyatomic molecules as well as atoms) produced films whose grain size seemed to vary with the size of the molecule forming the antimony film, in general velocity variations within thermal ranges did not affect the structure of metal films.

The rate of condensation on the substrate. From theoretical

considerations the rate of condensation may be expected to have considerable bearing on film structure. It has been shown by many workers (Wood, 1916; Chariton and Seminov, 1924; Cockcroft 1928) that when the vapour beam density is below a certain critical value, films cannot be formed. This critical density is a function of the substrate temperature and varies widely for different metals. Frenkel (1924) has explained this by assuming that atoms arriving at the substrate move over the surface and eventually re-evaporate from the substrate if the temperature is high enough. When a collision occurs between two of the atoms which are moving on the surface an atom pair is formed which has a much longer lifetime on the surface than a single atom. Such pairs then act as nuclei of condensation. The critical beam density thus depends on the lifetime of a particular metal atom on a particular surface. Levinstein (1949) showed that metals with low melting points showed the greatest dependence on the rate of evaporation. He found that zinc and cadmium films could not be formed at all at low rates of evaporation; when the rate of evaporation was high, films were formed quite readily.

The effect of substrate temperature on the mobility of the deposit atoms. The tendency of condensed atoms to migrate on surfaces has been deduced from measurements of resistance of extremely thin metal films (Appleyard, 1937), from thermionic (Bratain and Becker, 1933) and photoelectric (Bosworth, 1935)

measurement upon composite surfaces and from optical observations (Andrade and Martindale, 1935) and electron diffraction results (Hass, 1937; Was, 1939). The electron diffraction method is well suited to the investigation of the mobility of atoms (or molecules) over surfaces and it has been shown by Kirchner (1932), Finch and Wilman (1937) and Finch (1938), that atoms (or molecules) were able to move over the surface of the supporting foil such that they were drawn together forming crystals of considerable size. Picard and Duffendeck (1943), using the electron microscope, studied thin films of Cd, Cu, Au, Mg and Zn formed by evaporation and condensation on collodion substrates in vacuum, the substrate temperatures being controlled. Zinc formed a bluish splotchy surface on the uncooled glass surface showing relatively large crystals with considerable space between them (the evaporation was over a period of 3 to 4 minutes). The non uniform appearance of these surfaces at room temperature and the appearance of these metals in the shadow of obstacles in the evaporating chamber showed that the atoms were reflected from glass surfaces, losing some of their energy upon impact until their energy became less than the latent heat of evaporation of the metal from glass. They would then migrate over the surface until the stable crystalline forms were developed, leaving large areas of blank substrate between particles. This tendency of condensed atoms to migrate on the substrate until

fairly large 3-dimensional agglomerates are formed has been illustrated by Weber (1941,1944,1948) with thin bismuth films evaporated on to pyrex and formvar in vacuum. Analysis of the electron diffraction patterns showed that the very thin bismuth films ($\sim$ 20 atom layers in thickness), while initially composed of small crystals, grew rapidly upon ageing into larger crystals.

The nature and temperature of the substrate exerts, as a rule, a preponderating effect on both the crystal size and orientation. If, however, the substrate surface has no regularity of atomic arrangement (e.g. glass, polished metals etc) or if it has such regularity (e.g. a crystal surface) but does not exert strong forces of attraction on the deposit atoms then the deposit crystals are randomly disposed unless the deposit atoms have sufficient mobility and cohesive attraction to aggregate into monatomic sheets having minimum free energy. In this case deposit crystals are built up with such a densely populated net plane parallel to the surface though otherwise randomly disposed ("one-degree orientation"). Such substrates are termed "inert" in that they exert no orientating influence on the deposit other than as a supporting surface.

If the mobility of the substrate atoms is low the crystal size tends to be small, and orientation is usually weak or absent; but if the substrate is maintained at a sufficiently high temperature during condensation, orientation is more likely to occur.

The following one-degree orientations have been observed in evaporated films:- (001) orientation in cadium iodide (Kirchner, 1932); (111) in barium (Burgers and Dippel, 1934), (111) in thick calcium fluoride films (Burgers and van Amstel, 1936); (100) in aluminium and other face-centred cubic metals (Beeching, 1936). However, Quarrell (1937) suggested there was some evidence that face-centred cubic metals sometimes took up an orientation with (110) planes parallel to the surface, while Germer observed (111) orientation in aluminium films. Crystals of some of the cubic ionic compounds have been found to possess a strong preference for cube face orientation e.g. NaF (Germer, 1939). Strong (111) orientation has been observed in Sb films by many workers (Hass, 1942; Lotmar, 1948). Bannan and Coogan (1949) observed (111) orientation of calcium fluoride on different types of glass at 25°C.; at 110°C. there was no (111) orientation but strong (110) orientation. Dixit (1933) concluded that at higher temperatures one-degree orientations may occur such that planes of lower population density are parallel to the substrate, but his experimental results were inadequate to support this theory.

The effect of inclining the vapour stream to the substrate. Burgers and Dippel (1934) found that the orientation axis in calcium fluoride films was normal to the substrate when the vapour stream was normal to the surface but slightly inclined

towards the vapour stream when this was at very oblique incidence (the [111] axis was tilted by 10° for an angle of incidence of 65°). Experiments on the absorbtion of iodine by these films suggested that the (111) planes formed the most prominent boundary planes, which are therefore in the form of flat plates. Burgers and van Amstel (1936) observed a similar partial tilt of the [111] orientation axis towards the vapour stream, in films of barium condensed on flat copper discs. Beeching (1936) found that the [100] orientation axis in aluminium films was inclined to the vapour stream by about 15° when the angle of incidence of the vapour was 45°. Nelson (1937) found that iron evaporated from a tungsten filament and deposited on glass and other surfaces invariably oriented with (111) planes parallel to the surface for normal incidence. He suggests, rather vaguely, that the [111] orientation axis tended towards the vapour stream when this was at oblique incidence, but no details are given.

Burgers and Dippel (1934) and Thomson and Cochrane (1939) (and Thomson, 1948) explained the influence of the direction of the vapour stream by supposing the crystals grew by atoms arriving on a face, moving over it until they came to the edge and then prolonging the face (Volmer, 1932; Burgers and Dippel, 1934); such plane crystal faces normal to the vapour stream will then receive more atoms per unit area on these faces and so grow faster than the others where

similar faces are inclined to the vapour stream. However, planes parallel to the surface have the advantage that they can grow laterally in all directions. Thomson concludes that the partial tilt of the orientation axis observed by Burgers and Beeching is due to a compromise between these opposing tendencies

It is difficult to see how this compromise is reached and in view of the somewhat scanty experimental results available, the author carried out a detailed investigation of the effects of inclined vapour streams, over a wide range of angles of incidence for substances of differing structure and properties viz. iron (body-centred cubic); lead sulphide (face-centred cubic) and zinc (close-packed hexagonal). The results (described in Part II) show the effect of oblique vapour streams on crystal orientation and surface texture, and the real explanation of the previous results of Burgers and Beeching is given.

3. Epitaxy.

It is well known that crystals grown upon a crystalline substrate may sometimes be oriented parallel to one another and to a well-defined crystallographic direction of the substrate. The classical case is that of sodium nitrate on calcite; the two are isomorphous and the sodium nitrate grows from solution with its axes parallel to those of calcite. Many other cases are known, for growth both from solution and

from melts, for electrolytically deposited crystals and for crystals grown from the vapour. Isomorphism is not essential.

Royer (1928) applied the results of X-ray diffraction determinations of crystal structures to define the conditions under which epitaxy occurs, and investigated microscopically many examples in growth from solution. He showed that "epitaxy" (as he called this phenomenon) depends upon the simple relation between the form and dimensions of the two-dimensional cells in the net planes of the substrate and deposit crystals at the junction face.

Lassen (1934), Lassen and Brück (1935), Brück (1936), Kirchner and Lassen (1935), Kirchner and Cramer (1938), and Goche and Wilman (1939) studied the epitaxy of metals deposited by condensation from the vapour on rocksalt in vacuo, using the method of electron diffraction. Bruck interpreted his results by postulating that the distance of atoms between the substrate and the deposit crystal averaged over a cell tends to be a minimum, but in view of the different electrical character of the Na and the Cl atoms in the surface it seems doubtful if much weight can be attached to this.

Finch and Whitmore (1938) concluded from their experiments on the growth of $NaNO_3$ on various natural and polished faces of calcite that the orientation is wholly determined by the atomic arrangement on the substrate surface and that the forces determining epitaxy are short-range.

Thomson and Cochrane (1939) and Thomson (1948) consider the existence of steps and cracks in the surface of the substrate crystal is in many cases a determining factor. They consider that as atoms are deposited they group themselves in rows along these steps, which become a zone axis for the deposit. Some prominent face containing such densely-populated rows then grows out over the substrate surface and thus the orientation is established. However, Drabble (1949) showed that the scratches on glass played only a secondary part when methylene blue crystals were grown on a scratched glass surface; the crystals grew in random azimuthal distribution, though some were able to develop their characteristic "needle" shape when their length was along the scratches. Wilman (1950) concluded from the evidence of "rotational slip" in crystals that cracks and steps, whether microscopic or even only one atom high, play a secondary part in determining the orientation.

Rüdiger (1937) found that metals deposited on to rock-salt and other single-crystal substrates showed epitaxy only if the temperature of the substrate during deposition was above a critical temperature.

Undoubtedly temperature plays an important part in epitaxial growth since an increase in temperature increases the vibration amplitude of the surface atoms in the substrate and thus facilitates migration of the deposited atoms. At room temperature on most single-crystal substrates the crystals of

the deposit are either randomly disposed, or they exhibit one degree of orientation; on heated substrates the atoms arriving on the surface are more mobile and thus can move to positions of low potential energy and at the same time aggregate together in close-packed sheets on the smooth substrate so that densely packed crystal planes tend to grow parallel to the substrate. If the mobility of the deposit atoms over the substrate, as distinct from the mobility over the deposit crystals, is high enough a second degree of orientation develops from the initial stage of parallel growth between atom rows of similar packing density at the interface.

Seifert (1937), in his work on oriented overgrowth of ionic partners, came to the conclusion that one-dimensional lattice fitting for a row of closely spaced ions is sufficient to give rise to oriented overgrowths. Wilman (1940) also found that a preferred orientation can exist where there is a similarity of specing in one row of closely packed units in each lattice.

From the theoretical point of view epitaxial growth is an atomic problem and the elements of an atomic theory of crystal growth have been laid down by Volmer, Stranski, Becker and Döring; new contributions have been made by Frank, Burton and Cabrera (see Discn. Faraday Soc., "Crystal Growth", 1949). This theory applies explicitly to growth from the vapour, but can probably be applied in principle to growth from solution.

Since crystal orientations are determined by forces between one atomic layer and the next, in order that there shall be a definite orientation in a crystalline overgrowth on a crystalline substrate there must be formed, as the initial stage, an immobile monolayer of regular atomic pattern (called a nucleus). If the formation of a monolayer is regarded as a process of adding atom to atom, it is possible, if the influence of the substrate is strong, and the lattice dimension differences $\lesssim 15\%$, for these (foreign) atoms to take up the same positions on the substrate as would atoms belonging to the same substance as the substrate. The resulting monolayer is therefore homogeneously deformed to fit on the substrate, thus forming a nucleus. A theory has been developed (Frank and van der Merwe, 1949) which led to predictions regarding the necessary conditions under which such an orientated nucleus can be formed. This nucleus acts as a substrate for the formation of another atomic layer on it, provided that the binding between deposit atoms is not weaker than their binding on to the substrate. If the atomic pattern of the nucleus, and hence that of the substrate, resembles the atomic pattern of a plane in the normal lattice of the deposit (e.g. when the two lattices are isomorphic), it is possible for a stable, macroscopically thick oriented film to grow by repetition of this process of atomic layer formation. Since the formation of a monolayer is really

a process of adsorption on the substrate, it is the pattern of potential troughs (i.e. positions of minimum potential energy) of the deposit atoms in the substrate field, rather than the atomic pattern of the substrate surface, which must resemble the atomic pattern in the plane of the deposit.

The binding in the adsorption process is of various types e.g. ionic, homopolar, through a hydrogen bond, through dipoles, etc. Willems (1943) concludes that, for oriented overgrowth to take place, there must exist the possibility of a strong chemical bond between the units of overgrowth and the corresponding units of the substrate and he confirmed this experimentally in particular cases.

According to Van der Merwe (1949) the "limiting misfits" in the case of ionic overgrowths might be expected to be greater than for metallic overgrowths, since the compressibilities of the former are much greater than those of the latter. In particular, oriented overgrowths with very large misfits is observed in the case of oxides and halides - a fact accounted for by the particularly high compressibilities of these large anions.

As is apparent from the above discussion the determining factors are the nature and distribution of the force fields at the substrate in relation to the kind of atoms arriving at the surface. Closeness of fit between parallel

atom row spacings cannot be regarded as the sole factor determining the orientation relationship developed between substrate and epitaxial layer since, in some cases, a different orientation from that actually occurring would result in a better fit between parallel rows. For example, silver grows on a rocksalt cube face with cube faces and axes parallel to those of the rocksalt (e.g. Lassen, 1934; Bruck, 1936). A much better fit would be with cube faces parallel, but with the silver cube edges parallel to the rocksalt cube-face diagonal. This fit would ,however, reduce the co-ordination number of alternate Ag atoms, and thus be less stable than the one actually observed, in which the co-ordination of the Ag atoms on the rocksalt face is similar to that in AgCl (Drabble,1949).

The paper by van der Merwe (1949) includes a comprehensive survey of all published cases of epitaxy up till that time (1949).

A new and interesting case of epitaxy is zinc deposited on a rocksalt cleavage face described and discussed in Part III.

4. The structure of deposits formed by chemical reactions on solid surfaces. The above discussions have been confined to the case of growth on a surface, the component atoms or molecules of which do not enter into the structure of the growing crystal, but support the primary deposit layer, and which may or may not through their own arrangement fully determine its orientation,

according to whether the substrate surface is inert or active. We now consider the more complex case of growth at a surface in which the crystal building units are the products of chemical interaction between molecules arriving from outside the surface and the atoms of the surface itself. We will confine the discussion to the oxidation of surfaces by oxygen and sulphur atoms.

Epitaxial crystal growth can only occur in those cases where the mobility of the oxygen over the surface is sufficiently high for it to move from its point of arrival at the surface to an appropriate site where it is finally held. A low mobility and high degree of retention of oxygen molecules arriving at the surface favour the formation of oxide layers whose crystal orientation is not related to that of the metal; and the oxide layer may even be amorphous, e.g. the spontaneously formed amorphous oxide layer formed on aluminium crystals. Indeed recent work in this laboratory has shown that the oxide film formed on an anodically polished copper single crystal face exposed to air at room temperature is also amorphous (Finch, 1950)

Metal surfaces immediately combine with oxygen to form an oxide layer of a molecular order of thickness. The subsequent rate of growth in thickness of this layer depends on the rate with which further oxygen can gain access to the metal, either by penetration of oxygen (Pilling and Bedworth, 1923; Valensi, 1935; Evans, 1948) or by the migration of metal atoms

through the spontaneously formed oxide layer (Pfeil, 1929; Wagner, 1933; Bordeen, Brattain and Schockley, 1946).

Studies on epitaxial growth of crystalline layers of metallic oxidation products such as oxides, halides, sulphides and selenides suggests that in many cases the initial layer must itself be epitaxially arranged i.e. each adsorbed molecule (or atom) of oxygen takes up the same type of relative position in regard to the arrangement of the surface metal atoms. Thus an epitaxial primary oxide layer formed on a metal single crystal is itself a single crystal.

The efficiency of such a layer in protecting a metal surface from further attack can be expected to increase with the density of packing of the constituent atoms of the oxide. For instance, the spontaneously formed oxide layer on the cleavage surface of a zinc single crystal is of a molecular order of thickness. In this face the zinc and consequently all the adsorbed oxygen atoms are closely packed together. No further oxidation occurs in dry air at normal temperature even after prolonged exposure. Other faces of a zinc single-crystal, however, particularly of lesser density of packing, do not show a similar resistance.

It has long been known that the oxidation rate is not the same for different crystal faces (Tammann, 1930; Mehl and Mc.Candless, 1937; Lustman and Mehl, 1942) for tarnishing

reactions at low temperatures, giving oxide layers a few thousand angstroms thick. Bénard (1948) investigated the oxidation of iron and copper after a long oxidation time and high temperature and classified the crystal planes of Cu according to the decreasing rate of oxidation thus:- 210, 221, 211, 111,100,123. This does not agree with the above contention that the oxidation rate increases with decreasing density of metal atoms on the surface i.e. (111), (100), (110), (311) etc. Mott and Cabrera (1949) point out that this is probably due to the imperfections of the surface, the rate of oxidation on different crystal faces depending on the concentration of "dislocations" (Frank, 1949) per unit area of each crystal face.

All oxides are at least partly polar and the charges on the metal and oxygen ions must be strongly attracted to the substrate metal. Strong cohesive forces between metal and oxide must exist, whether or not the lattice parameters of the metal and of the oxide are equal or nearly equal. Whether the initial film of oxide will take a pseudomorphic form; the strain effects at the interface (due to the difference in lattice parameters) and the possible relief of this strain are discussed in Part V.

A survey of the experimental data on oxidation is given in a book by Evans (1948) while the "Pittsburgh International Conference on Surface Reactions" (1948) includes papers which discuss some of the theoretical implications of

surface reactions. A review of the theory of the oxidation of metals is also given by Cabrera and Mott (1949).

While the oxides of most metals have been studied by electron diffraction, in a large number of cases the metallic substrate was randomly oriented resulting in randomly disposed oxide crystals (e.g. Smith, 1936; Bound and Richards, 1939; Hickman, 1948). While these results give information on the rate of oxidation and the structure of the oxides formed it tells little of the influence of the substrate on the formation of the oxide. A better understanding of the substrate effects is obtained by studies of the relationship of the orientation of oxide films and metals when the oxidation of oriented polycrystalline and single crystal specimens are examined by electron diffraction.

Oxidation of oriented polycrystalline deposits. Burgers and van Amstel (1936) studied the oxidation of polycrystalline barium specimens and found that the direction of closest packing of the metal atoms in the face-centred oxide lattice was closely parallel to a corresponding direction in the body-centred metal lattice (i.e. a [111] direction). Nelson (1937) studied the air-formed film of Fe_3O_4 on polycrystalline iron in (111) orientation and he suggested that the (100) plane in the oxide was parallel to the (100) plane of iron with [110] in the (100) oxide plane parallel to the [100] in the (100) plane of the

iron, this orientation being reasonable on the basis of matching the atomic positions in the cube faces.

The oxidation (by oxygen and sulphur vapours) of oriented polycrystalline zinc deposits is described in Part IV.

Oxidation of single-crystal faces. Strong two-degree orientation of the crystal lattices of the reaction product on a single-crystal substrate has been observed in electron diffraction studies of the oxidation of copper (Thomson, 1931; Yamaguti, 1938), zinc-blende (Yamaguti, 1935; Aminoff and Broome, 1936), stibnite (Miyake, 1938), palladium (Fordham and Khalsa, 1939), molybdenite (Uyeda, 1938), lead sulphide (Elleman, 1948), iron (Mehl, Mc Candless and Rhines, 1934), antimony (Acharya, 1948), and other crystals. Finch and Quarrell in their electron diffraction study of crystalline zinc deposits exposed to air observed two structures, one being the normal structure of undistorted zinc oxide and the other a similar structure with the lattice dimensions unnaturally short parallel to the surface and unnaturally long at right angles to it.

The parallel growth of ZnO on the $\{0001\}$ cleavage face of Zn has been studied by Wilman (1947) and by Acharya (1948) and discussed by Finch (1950). The zinc cleavage face was spontaneously covered with a very thin film of oxide on exposure to air (as had previously been observed by Finch and Quarrell,

1934). This initial layer protects the metal from further oxidation, since it was only after prolonged heating at 400°C. that the film of oxide changed appreciably. However, when the cleavage faces were exposed by Acharya (1948) for a short time to mild attack by H_2S vapour (or treated with benzene containing thiophene) they rapidly gave rise, at 400°C., to a layer of zinc oxide in (101) orientation in addition to the (001) orientation. It was suggested that the (101) orientation arose through the effect of the sulphur compounds modifying in some manner, the growth of the oxide layer. It may be noted that Vernon (1924) observed that polycrystalline copper surfaces exposed to sulphur were more readily oxidised than pure copper.

Further experiments on the oxidation of a zinc cleavage face are described in Part IV.

The formation of zinc oxide on zinc blende has been studied by many workers. Aminoff and Broome (1936, 1938) oxidised (001), (111), and (110) faces of zinc blende by heating the crystals in air, while Yamaguti (1935) oxidised the (110) cleavage face. The orientations are discussed by Seifert (1940) In the zinc blende each zinc ion is surrounded by four tetrahedrally placed sulphur ions. The S ions round a zinc are first replaced by oxygen ions and the oxide crystal then grows as a hexagonal lattice, the c axis of the latter being normal to a tetrahedral face and the other axes being tetrahedral edges.

Uyeda, Takagi and Hagihara (1941) extended these results to the study of the formation of the oxide on the 111, $\overline{111}$, 110 and 100 faces in the natural and etched states and also on the cleaved 110 surface.

Further experiments on the oxidation of the etched and unetched cleavage face of zinc blende are described in Parts IV and V.

5. Stress in the growth of oxide layers.

Oxide crystals must be in a constrained condition since they have to occupy space previously occupied by the metal, and, as was first pointed out by Pilling and Bedworth (1923) the volume occupied by unconstrained oxide is, in the case of heavy metals, greater than that of the metal producing it. At right angles to the surface, expansion of the oxide particles is possible, but parallel to the surface there can be no relief of constraint. Consequently, the first crystal of oxide must be in a state of compression parallel to the surface - possibly with compensating elongation at right angles. As the oxide phase extends, whether laterally or in depth, this distorted crystal structure is likely to be continued, since it requires less energy then to produce, spontaneously, nuclei representing the stable form. Thus we may expect that a film of distorted oxide will come to cover the whole surface, and

that the constrained structure will be continued when that film proceeds to thicken, unless mechanical breakdown brings about stress-relief. There is strong evidence for the distortion of the crystal structure. Finch and Quarrell (1934, 1939) found that ZnO on the basal plane of Zn had a pseudomorphic structure; the normal oxide structure is squashed into congruence with that of the zinc underneath (the percentage difference in lattice dimensions between ZnO and Zn along the $[10\bar{1}0]$ in the basal plane is 20%). Similar tendencies were observed in overgrowths of MgO on Mg (Finch and Quarrell, 1939) and in the experiments of Finch and Sun (1936) where the abnormal crystal orientations of very thin films were in general such that the atomic population density in the orientation plane of the deposit approached that in the substrate surface.

Numerous other investigators, such as Mehl (1934), Schwab (1947), and Capdecombe (1945) have established crystallographic relationships between the film and the basis, such relationships implying a state of strain since the lattice dimensions, in general, will not be such as to permit continuity of structure without some modification of the unconstrained values.

Whether the initial spontaneously formed monolayer of oxide will take up the lattice parameter of the metal underneath or whether it will correspond to the lattice parameter of the undistorted oxide depends on various factors: 1) the

distribution and intensities of forces between the substrate surface and the oxide layer, 2) the compressibility of the oxide material (the more compressible the oxide the more likely it will be to take up the distorted form), 3) the degree of misfit between the two lattices. Frank and van der Merwe (1949) conclude that if the degree of misfit is less than 15%, the film will, in its state of lowest energy, take up the lattice parameter of the substrate, if it is greater than 15%, it takes up very nearly its own unconstrained lattice parameter.

It may be pointed out that the calculations of van der Merwe are based on the premise that the first atomic layer of the deposit is distorted so as to take up the undistorted lattice parameter of the substrate. This cannot be so, because not only must the surface layer of atoms of the substrate be distorted also but the transition from the undistorted lattice parameters of the substrate to those of the deposit must necessarily take place over several such atomic layers.

In the case of the growth of ZnO on Zn the misfit is 20% and yet pseudomorphic growth was observed. This is undoubtedly due to the fact that very thin films show a much higher compressive strength than the bulk material (e.g. Mott, 1949).

The large strain permissible in thin layers thus cannot persist into films of indefinite thickness - a fact well established in experiments which show that pseudomorphic growth

was no longer observed in sufficiently thick films (e.g. Finch and Quarrell, 1934, 1939). Thickening of films must necessarily be accompanied by transition processes which tend to make the bulk deposit strain free. The film can only assume its unstrained lattice parameter either by breaking away from the surface through plastic deformation or by recrystallisation.

This strain transition process may, or may not, result in a loss or change of the initial orientation. If the process takes place through slip in planes parallel to the substrate (Neuhaus and Willems, 1940, 1943) such a loss is not likely to occur. If however the slip takes place simultaneously in planes inclined to each other, a loss is likely to occur. This would seem to be the case in the experiments of Finch and Sun since the regular orientation became random with sufficient film thickness. This transition process can, however, also take place through the growth of an unstrained bulk film on the thin strained part of the overgrowth at the interface. Detailed calculations by Menzer (1938) (which was confirmed by Goche and Wilman (1939) in the case of Ag) on observations of Ag and Ni films on NaCl showed that the losses of the deposit consisted largely of small crystallites having (221) faces parallel to the substrates. The bulk of the film, growing on these crystallites, is twinned on the (111) faces with respect to the crystallites and has an orientation parallel to that of NaCl. The corresponding misfits in the contact plane thus

also lie within the tolerance limit, which is not the case for the misfits suggested by the orientation of the bulk of the overgrowth.

U.R.Evans (1948) suggests two possible mechanisms whereby mechanical breakdown can occur - either gliding can take place resulting in the extrusion of wedge-shaped portions, or the film can leave the basis locally forming "blisters".

Cabrera and Mott (1949) suggest that the explanation of the kinks in the oxidation curve shown for Cu by Garforth (1949) is due to recrystallisation caused by the strain in the oxide layer. It is of interest to note in this connection that Cahn (1949) has observed that bent metal single crystals are particularly liable to a special type of recrystallisation in which the elastic stresses in successive narrow regions of the lattice are eliminated, each region taking up the mean of the range of orientation originally present in it; the effect is called "polygonisation" to distinguish it from primary recrystallisation by nucleation and growth.

Wilman (1950) demonstrated the common occurrence of "rotational slip" as a new kind of deformation process in crystals. It is defined as the slipping of one part of a crystal on a neighbouring part, so that the two atomic sheets which slide over one another are densely populated planes, as in translational slip, but rotationally displaced about an axis

normal to their plane to one of a series of definable new positions where metastable equilibrium can occur. The rotation of ZnO crystals, grown by heating a cleavage of zinc blende in air, described in Part V constitutes the first clear example of rotational slip caused by epitaxial stresses (Evans and Wilman, 1950). This conclusion is confirmed by the results obtained on the uni-directional abrasion of a zinc blende cleavage face (Part V) and extensive rotational slip is demonstrated by the abrasion of electro-polished (110) faces of a copper single crystal (Part VI).

PART 2.

ONE-DEGREE ORIENTED FILMS FORMED BY CONDENSATION OF THE VAPOUR ON INERT SUBSTRATES.

1. Experimental Details.

The deposits were prepared in a Pyrex test tube, 20 cms. long and 4 cm. diameter, stoppered by a rubber bung through which passed a short 1 cm. diameter glass tube, leading through a wide bore tap to a Cenco-Hyvac pump capable of reducing the pressure to 10^{-3} mm. of Hg. The small volume of the apparatus and the short pumping line resulted in this final pressure being attained within a few minutes. Two long brass rods passed through the bung served as leads for the filament, which was heated by the passage of A.C. current from the secondary winding of a transformer, the current being controlled by a resistance in series.

In the case of zinc and iron a tungsten filament was used, attached to the brass leads by clips. The zinc was heated in a crucible until molten, skimmed several times, and the tungsten filament immersed in it. On withdrawal the zinc clings to the filament with only a very thin film of ZnO on the outside. The Zn vaporises without melting. The atoms are emitted in straight lines from the source apart from

slight diffusion by the residual air in the tube, and condense on the substrate and the walls of the glass tube.

The thin skin of ZnO remains on the filament after the zinc has evaporated (due to its very low vapour pressure). In the case of iron it was found more convenient to wrap some pure iron wire tightly round the tungsten filament. On heating the tungsten to white heat the iron first melts (M.Pt. 1527°C.) then evaporates at a convenient rate.

In the case of lead sulphide a small portion of the mineral was enclosed in a nickel gauze strapped between the brass rods. PbS sublimes in vacuum at 500°C.

The specimens of glass were portions of microscope slides; they were first washed in benzene then placed in a mixture of alcohol and nitric acid, washed in distilled water and dried on a clean filter paper. This treatment provided a satisfactory grease-free surface.

In all the above cases it was advisable, though perhaps not always necessary, to evaporate some of the material off the filament before placing the substrate beneath it. This reduces the possibility of contamination of the specimens by any foreign substances which may be on the filament.

When the direction of the incident vapour stream was desired to be normal to the substrate the substrate was arranged to be perpendicularly beneath the source of atoms.

The size of the zinc blob on the filament (or PbS in the Ni gauze) was made as small as possible the criterion being that there would have to be sufficient of the substance to form a film of the required thickness at the appropriate distance from the filament.

For the investigations on the effects of inclined vapour streams the glass substrates were usually in the form of 2 cm. long strips distant about ½ cm. from the vapour source They were arranged as shown in Figure 1 so that the atoms impinged on the surface at angles of incidence (with the nromal to the surface) varying from 0° at normal incidence to about 80° at the extreme end of the specimen. Care was taken to identify particular parts of the substrate corresponding to different angles of incidence when scanned by the electron beam.

2. Electron diffraction patterns from polycrystalline specimens

In considering the diffraction pattern by transmission of a polycrystalline specimen, it can be regarded as equivalent to a single crystal rotated through the same range of orientation as exists in the specimen. If there are many crystals with random distribution in the path of the beam a pattern of rings results, analogous to the X-ray Hull-Debye-Scherrer or "powder" pattern. Unlike the X ray powder pattern, its electron diffraction prototype is usually due to

crystals each of which gives rise to a pseudo-cross-grating pattern of spots, characteristic of the crystal setting. Any diffraction spot, however, only attins its maximum intensity at the position corresponding to reflection of the primary beam in the corresponding net plane at the Bragg angle; hence Bragg's law gives the angular radii, 2θ, of the maxima of the diffraction rings in the pattern and since these angles are small for fast electrons we have to close approximation

$$d_{hkl} = \frac{\lambda L}{R_{hkl}}$$

where L is the camera length and R_{hkl} the radius of the hkl diffraction ring.

One-degree orientation in which the crystals have net planes of a particular type parallel to the surface is defined by stating either the indices of these net-planes or those of the lattice row normal to this plane. Such a lattice row is called the orientation or "fibre" axis. The natural undisturbed orientation developed in most crystalline layers during deposition on inert substrates are best studied by the reflection method, where the electron beam strikes the surface at nearly grazing incidence; the pattern in this case is due to transmission through the projecting crystals which the electron beam can traverse without appreciable energy loss, and slightly more than half of the diffraction pattern is cut off by the opaque specimen.

A graphical way of defining the positions of the diffractions is to use the fact that any diffraction hkl must lie at the intersection of the hkl ring with the corresponding h' th order layer line due to the lattice row parallel to the orientation axis [uvw] where h' = hu + kv + lw. The layer lines, in this case, are practically straight and equidistant with spacing $\lambda L/T$ where T is the lattice point spacing along [uvw]. These layer lines are parallel to the shadow edge and the orders of diffraction from [uvw] lie in the plane of incidence, hence the indices of the orientation can be obtained.

If the one-degree orientation is very strong then the pattern consists of short well defined arcs or spots; if the orientation is weak then these spots are spread into arcs along the rings. The angular spread of a spot along the ring radius is a measure of the strength of the orientation i.e. it is a measure of the degree of exactness with which the crystallites tend to be orientated with a plane parallel to the surface; the shorter the arcs the easier it is to determine the mean orientation. In some deposits several types of orientation occur simultaneously.

The particular case of zinc which has a close-packed hexagonal structure is described further in Part II (6).

3. Experimental Results. Iron on glass.

Normal Incidence. Figure 2 shows the electron diffraction pattern obtained from an opaque iron film deposited on glass. The iron was evaporated from an iron wire heated directly by an electric current. The evaporation was continued for a few minutes, with the specimen about $\frac{1}{2}$ cm. from the source of atoms. The pattern in symmetrical about a line perpendicular to the shadow edge and shows that a (111) plane was parallel to the surface, i.e. the 222 diffaction in the plane of incidence. All the maxima due to the body-centred cubic iron fall on well defined layer lines whose spacing corresponds to the distance between atoms in the [111] rows. The strong arc in the plane of incidence at 2.87 cm. from the central spot is the 222 arc of α Fe.

The pattern contains some arcs which do not fall on the layer lines; in particular an intense elongated spot between the first and second layer line and others inside the first layer line. The additional arcs and their relative intensities are in good agreement with the pattern to be expected from Fe_3O_4 (the oxide film being formed due to exposure after deposition) since it forms very readily even at low pressure). The orientation seems similar to that observed by Nelson (1937).

Oblique Incidence. Whereas the diffraction patterns corresponding to normal incidence were symmetrical, with the [111] axis normal to the surface, it was found that when the vapour stream was inclined to the surface the [111] axis was tilted towards the vapour by various amounts.

A tilt of the [111] axis by 9° towards the vapour stream was recorded for an angle of incidence of 52° (measured from the normal to the surface) when the electron beam was at right angles to the direction of the vapour stream. The pattern with the electron beam at right angles to this, i.e. in the plane of incidence of the vapour stream, was symmetrical with the [111] axis in the plane of incidence of the pattern. This specimen was produced by slowly evaporating the iron directly off a heated iron wire, the total time of evaporation being about 1½ hours. It was found more convenient to evaporate the iron from a heated tungsten filament since the iron wire had a tendency to fuse. All the following specimens were made this way, the evaporation time being between 30 and 60 seconds.

It was observed by scanning specimens with the electron beam at right angles to the direction of the incident vapour that there was a variation in the tilt of the orientation axis along the length of the specimen, the tilt decreasing slightly with increased angles of incidence of the vapour stream. This effect was then investigated in greater detail.

Figure 3 shows a tilt of 19° of the [111] axis towards the vapour stream corresponding to an angle of incidence of 37°. Figure 4 shows a tilt of only $8\frac{1}{2}$° for an angle of incidence of 62° in the same specimen. The azimuth at right angles to these patterns gave a pattern (Figure 5) which is symmetrical about the plane of incidence. These results are shown graphically in Curve B (Figure 6).

Figures 7,8,9,10,11,12 were all obtained from another specimen of iron deposited on glass which had been abraded with 4/0 emery paper on a rotating disc. Figures 8,9,10,11,12 were taken with the beam at right angles to the direction of the vapour stream and corresponded to angles of incidence at 28°, 48°, 62°, 70°, 73° respectively. Figure 7 was taken at right angles to this in the symmetrical azimuth. The glass was arranged so that the vapour stream, when inclined, was at right angles to the scratches produced by the abrasion. This sequence of results is shown graphically by Curve A (Figure 6).

A specimen of iron on glass etched with HF (showing the etched pits visibly) gave a tilt of the [111] axis of 11° for an angle of incidence of 45°.

The straight line drawn on the graph plots the tilt of the orientation axis which would be observed if it aligned itself with the direction of the vapour stream i.e. for an angle of incidence of 30° (say) the axis would be tilted by 30°

from the normal so as to lie along the vapour stream.

Figures 13, 14, 15, 16, were all obtained from another specimen formed under similar conditions as the previous specimens. The pattern from the region where the vapour stream was at normal incidence showed that the iron was oriented with the (110) planes parallel to the surface. Figures 13,14,15,16 corresponded to angles of incidence of 37°, 55°, 64°, 68° respectively with the beam at right angles to the direction of the vapour stream, the observed tilts of the [110] axis being 9½°, 9-1/4°, 9°, 9° respectively. These results are shown graphically in Figure 17. At right angles to this azimuth (i.e. with the electron beam along the vapour stream direction) the pattern was observed to be symmetrical with the 220 arc in the plane of incidence i.e. with the [110] orientation axis perpendicular to the substrate.

4. Experimental Results. Lead Sulphide on glass.

A small portion of lead sulphide mineral was used for the evaporation. It had a tendency to fly off in fragments on heating so it was enclosed in a nickel gauze strapped between the filament leads. The PbS sublimed at ~ 500°C, a practically opaque film ~ 3000 Å. being obtained for an evaporation period of ~1 minute. The effect of oblique vapour streams was investigated in a number of specimens. The results obtained were very similar to those obtained with iron in so far as the

orientation axis was perpendicular to the substrate (ordinary glass) at normal incidence and was only partially tilted towards the vapour stream at oblique incidence. Figure 18 shows the strong (100) orientation obtained with the [100] orientation axis tilted towards the vapour by 8°; this corresponds to an angle of incidence of 24°. Figure 19 shows a tilt of the [100] axis by exactly the same amount for an angle of incidence of 56° from the same specimen. These results are shown graphically in Figure 20.

5. Summary and Discussion of Results obtained from Iron and PbS

The structure of opaque films of iron deposited on glass from the vapour was investigated by means of electron diffraction. The effects of different rates of evaporation were investigated together with the effect of inclining the vapour stream to the substrate over the whole range of angles of incidence on glass surfaces in various conditions.

(111) orientation was found most frequently as has been observed by Nelson (1937) with evaporated films and by Finch and Sun (1936) with films formed by electrodeposition. An article by König (1948) on the oxidation and recrystallisation of, and the Faraday effects in, iron in thin layers produced by evaporation in vacuo is, at present, unobtainable, but it has been abstracted (König, 1949).

When the vapour stream was normal to the surface the orientation axis [111] was perpendicular to the substrate. When the vapour stream was inclined to the surface the [111] axis slightly tilted towards the vapour stream direction, the amount of the tilt depending on the angle of incidence of the vapour.

The manner in which this tilt is dependent on the angle of incidence is shown by curves B and A (Figure 6), in which the tilt of the [111] axis is plotted as ordinate and the angle of incidence as abcissae, the points on the graphs corresponding to single specimens of iron on ordinary glass and scratched glass respectively. The [111] axis is perpendicular to the substrate for normal incidence (i.e. the tilt is 0° for an angle of incidence of 0°); the curves then fall considerably below the straight lines which correspond to the orientation axis aligning itself along the vapour stream direction. They show an increase in the tilt of the [111] axis as the angle of incidence increases up to a region corresponding to an angle of incidence of $\sim 30°$, the tilt then falls off with increased angle of incidence, being only $\sim 5°$ at an angle of incidence of 70°.

These graphs correspond to specimens formed by depositing iron (evaporated from a tungsten filament) on to glass, the films of iron being opaque to light, and the evaporation times being ~ 45 secs. The points corresponding to

the results for iron evaporated directly from a heated iron wire with an evaporation time of 1½ hours (the film being approx. of the same thickness) and to those of iron evaporated on to the surface of etched glass lie inside the region between curves A and B showing no marked difference in the general effect. This indicates that the evaporation time, or rather the rate of evaporation, is not a critical factor; neither is the coarse texture (relative to atomic dimensions) of the glass surface, presumably because only the tips of the coarse projections are accessible to the electron beam and contribute to the diffraction pattern.

All but one of the 15 specimens examined showed (111) orientation. Only one case was observed which was different from this, although the experimental conditions were apparently the same; Figures 13,14,15,16 were obtained from this specimen, showing (110) orientation. At normal incidence the [110] axis was perpendicular to the substrate; when the vapour stream is inclined to the surface the [110] axis was inclined towards it by an amount which is considerably less than its inclination to the normal, the plotted curve (tilt of [110] as ordinate, angle of incidence abcissae) falling well below the straight line (Figure 17). The curve rises to a tilt of the [110] axis of ~10° for an angle of incidence of approximately 30°; it then flattens out with increasing angles of incidence showing practically the same tilt (9°) for angles of incidence up to 70°.

It is interesting to note that Finch and Sun (1936) and Finch, Wilman and Yang (1947) observed (110) orientation of iron electrodeposited on to various substrates in addition to the more commonly occurring (111) orientation.

Cube face orientation was observed with lead sulphide deposited on glass at room temperature. Elleman (1948) observed cube face orientation of PbS on cleavage faces of rocksalt below 150°C. and Wilman (1948) observed usually a mixture of (001) and (110) orientations both in PbS chemically precipitated at room temperature and that condensed from the vapour on pyrex at 450°C. The [100] orientation axis was found to be perpendicular to the substrate for normal incidence and only partially inclined towards the vapour stream direction at inclined incidence in a manner very similar to that of iron (particularly the case of (110) orientation as comparison of Figures 17 and 20 show) since the tilt of the orientation axis increased with increased angle of incidence for small angles of incidence (up to 20°) then remained constant over the range of angles from 24° to nearly 60° the observed tilt being only 8° (Figure 20).

Now it is well known that glass has a remarkably smooth surface as shown by the electron microscope (Williams and Wyckoff, 1945) there being no perceptible differences in this fine-scale smoothness between glass surfaces which are

commercially rouge-polished or fire-polished. But the surface of all amorphous substrates are wavy rather than flat on the atomic scale with which we are concerned. The results obtained by the author with iron evaporated on to glass are explained as being due to the effect of this undulating nature of the substrate:-

When a metal is evaporated in a sufficiently good vacuum, the metal atoms will travel in straight lines from the filament and some will be deposited on to the substrate. If a metal is used which does not migrate after deposition, its thickness will be greatest on those aspects of the surface which face the oncoming atoms, and there will be regions of the substrate that will be shielded so as to receive little or no metal. When "shadowing" is used for electron microscopy a vacuum of at least 0.1 u should be maintained (since sharp shadows are required) but a somewhat poorer vacuum is sufficient for optical shadowing, almost any vaporisable metal being capable of producing acceptable shadows for optical examination. Chromium was one of the first metals to be used successfully for shadowing (Williams and Wyckoff, 1946); the properties of iron are very similar.

When the iron atoms strike the surface at normal incidence all parts of the surface are almost equally favoured for deposition; the crystals grow in an orientation with a

particular plane (usually the (111) plane) parallel to the surface and the orientation axis is then perpendicular to the surface as illustrated in Figure 21a. However when the vapour stream strikes the surface obliquely parts of the surface receive a low density of atoms owing to their obliquity (see Figure 21b) or even are "shadowed" by the mounds on the surface (see Figure 21c) resulting in the portions of the mounds facing the vapour stream receiving the greatest portion of the deposited metal (we know that the iron atoms do not migrate to such an extent as to fill the depressed portions of the surface).

The metal crystallites on these portions of the surface are oriented parallel to the surface immediately beneath them so that the net effect is, averaged over the section of the surface scanned by the electron beam, a tilt of the mean orientation axis towards the vapour stream (see Figure 21). It can readily be seen from Figure 21 that this results only in a partial tilt of the orientation axis towards the vapour stream.

A similar explanation is obviously applicable to the observed partial tilt of the [110] orientation axis in the case of iron and the [100] axis in the case of lead sulphide deposited on glass.

The above explanation may also account for the fact that the curves are not only considerably below the straight lines but, in the case of curves A and B, show a decrease in

the angle of tilt with increased angle of incidence. When the vapour stream becomes more inclined to the surface only the extreme tips of the mounds will be in a position to receive the vapour so that the orientation axis will, necessarily, be less inclined to the normal to the mean surface (Figure 21c). The film does, undoubtedly, become thinner in those regions which correspond to greater obliquity due to the greater distance from the source of atoms, but care was taken to ensure an adequate thickness of the metal in these regions, so it seems unlikely that this is the dominant effect at the more oblique angles, although it may well have been a contributory factor in these cases (i.e. corresponding to curves A and B).

The above experiments thus lead to the conclusion that when only a partial tilt of the orientation axis occurs towards the vapour stream the crystals are oriented with a densely packed atom plane parallel to the substrate surface, but differently inclined parts of the undulating surface receive different amounts of deposit material per unit area. This natural explanation, quite apart from any need to assume facet development (Burgers and Dippel, 1934; Thomson, 1948), suffices to account for the partial tilt of the orientation axis observed with calcium fluoride by Burgers and Dippel (1934); with barium by Burgers and van Amstel (1936); and with Al by Beeching (1936).

6. Theoretical determination of the diffraction patterns corresponding to various one-degree orientations of zinc.

In order to determine the orientations of the zinc specimens, charts were plotted showing the positions of the diffraction spots for particular orientations. The positions of the arcs in the patterns obtained are compared with these charts to enable the exact orientation (or orientations) to be determined. It must be realised that the spots are broadened into arcs in the diffraction patterns and that there is a difference ~~variation~~ in intensity of the arcs due to (1) a general diminution in intensity with increasing reflection angle (2) the difference of intensity of the various arcs due to the relative positions of the atoms in space - the "structure factor", (3) the variation in the number of equivalent sets of planes contributing to a particular diffraction spot.

The structure factor of zinc (close-packed hexagonal) results in the following "forbidden diffractions" :- 001, 003, 005, 111, 113, 115, etc. These rings are omitted from the charts. In drawing the charts all the equivalent planes are taken into account for each ring, but the spots are drawn of equal intensity (there will be variations in intensities of the spots on the same ring due to the different number of co-operating planes contributing their diffractions to each particular spot).

All the charts are drawn to the scale such that $R_{110} = 5$ cm.

<u>One-degree (100) orientation</u>. (Figure 22). The normal [uvw] to the plane (hkl) for a hexagonal lattice is such that

$$u : v : w = (2h + k) : (h + 2k) : 3/2\, l/(c/a)^2$$

for (100) orientation, $u : v : w = 2 : 1 : 0$

Now lattice row [uvw] has lattice translation T, where

$$T = \sqrt{\Sigma u^2 a^2 + 2\Sigma uvab \cos\gamma}$$

which for the hexagonal system reduces to

$$T = \sqrt{u^2 a^2 + v^2 a^2 + w^2 c^2 - uva^2}$$

so that [210] has $T = \sqrt{3}a$.

layer line spacing $\lambda l/T = \lambda L/\sqrt{3}a$.

Now put $R_{110} = 5$ cm. so that $R_{110} = 5 = \lambda L/d_{110} = \lambda L/(a/2)$

i.e. $(\lambda L/a) = 2.5$

so that the <u>layer line spacing</u> $= 2.5/\sqrt{3} = 1.44$ cm.

and $h' = hu + kv + lw = 2h + k$.

The rings are drawn (such that $R_{110} = 5$ cm.) and the layer lines drawn with the above spacing. The values h' are worked out for reach ring taking into account all the equivalent planes (e.g. $\{11\bar{2}\}$ gives $(11\bar{2}2)$, $(1\bar{2}12)$, $(\bar{2}112)$, $(\bar{1}\bar{1}22)$, $(\bar{1}2\bar{1}2)$, $(2\bar{1}\bar{1}2)$); the intersections of the layer line with this particular value of h' with the corresponding ring gives rise to a diffraction spot.

The calculations are similar for the other orientations

One-degree (101) orientation. (Figure 23).

u:v:w = 1:½:0.127; h' = h + ½k + 0.217 l

Layer line spacing = 2.62 cm.

One-degree (001) orientation. (Figure 24).

u:v:w = 0:0:1; h' = l

Layer line spacing = 1.34 cm.

One-degree (112) orientation. (Figure 25).

u:v:w = 1:1:0.289; h' = h+k+0.289 l

Layer line spacing = 2.203 cm.

One-degree (201) orientation. (Figure 26)

u:v:w = 2:1:0.217; h' = 2u + v + 0.217 w.

Layer line spacing = 1.406 cm.

One-degree (105) orientation. (Figure 27).

u:v:w = 1:½:1.084; h' = h + ½k + 1.084 l

Layer line spacing = 1.14 cm.

One-degree (135) orientation. (Figure 28).

u:v:w = 1:1.4:0.4335; h' = 1 + 1.4 l + 0.4335 l

Layer line spacing = 1.68 cm.

Indexing of rings by the method of Hull and Davey.

Hexagonal crystals involve a cell edge (a) and an axial ratio (c/a). It is therefore possible to index their reflections by means of charts devised by A.W.Hull and W.P. Davey (1921). These charts are made with lattice plane

spacings plotted along the axis of abcissas according to a logarithmic scale and different axial ratios c/a appear at different vertical levels on the chart. A better form of chart is obtained by plotting against log c/a (Bunn, 1945).

In order to compare the observed spacings with the theoretical values of the plots, a strip of paper is placed beneath the logarithmic scale of abcissae of the chart, and the values of the interplanar spacings d laid off along its edge. The strip with its pattern of lines is then moved about over the plot with its edge parallel to the axis of abcissae for a particular c/a(= 1.86 for Zn), until a position where its pattern coincides exactly with that of the chart. In order to be really useful these charts should be plotted on a large scale; ~~and~~ the particular chart used measured 3' by 2'.

7. Experimental Results. Zinc on various substrates.

Zinc was deposited on glass as described in Part II (1) giving thick opaque films with evaporation times between 30 secs. and 60 secs. The various one-degree orientations obtained are listed in Table 1. (see page 50).

One-degree (001) and one-degree (100). Figure 29, obtained from a Zn film deposited on glass, shows one degree (100) and one-degree (001) medium strength giving the 002 and the 100 arcs in the plane of incidence. Figure 30 shows strong one-degree (001) and one-degree (100) of zinc sublimed on to a fresh

Table 1. Orientation of Zinc Deposits.

Orientation	Number of specimens.	Substrate
1° (001) and (002)	1	Glass
	1	Rocksalt
1° (101)	1	Glass
1° (112)	22	Glass
	2	Rocksalt
	1	Mica
1° 201	1	Glass
1° (105)	1	Glass

cleavage of rocksalt in vacuo (compare with the charts showing (001) and (100) orientation, Figures 24 and 22 respectively). The pattern was identical at different azimuths with respect to the cube face showing that the orientation was one-degree and not two-degree (Complete orientation, i.e. two-degree orientation, of Zn on rocksalt is described in Part III).

One-degree (201) orientation. Figure 31 shows an arc in the plane of incidence on the 201 ring. Comparison with the plotted chart of one degree (201) orientation (Figure 26) shows that it corresponds to 1° (201) orientation although the orientation is not particularly strong. The slight strengthening

of intensity on the 200 ring in the plane of incidence might suggest some (100) orientation also present, particularly since the 200 diffraction is 1/3 of the intensity of the 201 diffraction from structure factor considerations. However if there was an appreciable amount of one degree (100) orientation present then the 112 arcs would lie on the same level as the 100 arcs (see Figure 22) but they are not; this indicates that the orientation is not one degree (100). The observed strengthening on the 200 ring in the plane of incidence is probably due to the degree of randomness of the orientation spreading out the 200 spots on either side of the plane of incidence (see Figure 26) and causing them to overlap in the plane of incidence with a resultant increase in intensity.

One degree (10ℓ) orientation. Figure 32 shows the pattern obtained off a mirror-like surface of zinc corresponding to a short evaporation time (the zinc was flashed over). The orientation is weak so it is difficult to determine the exact orientation with any degree of certainty. However the positions of the 112 and the 203 arcs indicates an orientation of the (10ℓ) type rather than of the (11ℓ) type. There is an apparent strengthening of the intensities of the 103 and the 105 rings in the plane of incidence. Comparison of the arc positions with that of Figure 27 shows reasonable agreement and

suggests one degree (105) orientation. The strengthening of the 103 ring in the plane of incidence is obviously due to the coalescing of the 103 arcs on either side of the plane of incidence, as can be seen from the 103 spot positions on the theoretical pattern for one degree (105) orientation.

One-degree (101) orientation. Weak (112) orientation sometimes causes an apparent strengthening of the 101 ring in the region of the plane of incidence if the 101 spots on either side of it (see Figure 25) are spread out sufficiently to overlap in the plane of incidence, so care has to be taken in assigning the correct orientation to the specimen. Figure 33 however shows a strengthening of the 101 ring, in the plane of incidence, which would seem to be greater than what one would expect from the above effect, and so may well be attributed to one degree (101) orientation (cf. Figure 23).

One degree (112) orientation. As can be seen from Table 1, out of the total of 30 specimens of zinc examined, 25 showed one degree (112) orientation. The electron diffraction patterns showed (112) orientation in various strengths ranging from weak orientation giving almost random rings to orientation which gave short arcs. The theoretical positions of the diffraction spots for one degree (112) orientation are shown in Figure 25.

Figure 34 shows weak one degree (112) orientation

obtained from a mirror-like surface of zinc formed by flashing zinc on to glass.

Figure 35 shows one degree (112) which is somewhat stronger; this was obtained from a deposit which was bluish-white in appearance and which showed a sheen by reflected light.

Figure 36 shows strong one degree (112) orientation, obtained from a specimen formed by evaporating zinc in vacuo on to a fresh cleavage of rocksalt.

Zinc on glass at oblique incidence. Zinc was deposited on glass so that the vapour stream was incident on the surface over a range of angles of incidence as described above.

The deposits were approximately radially symmetrical about the point where they were intersected by the normal to them from the source; a symmetrical pattern corresponding to one degree (112) orientation (Figure 37) was obtained with the beam very close to or through the foot of the normal from the atom source to the substrate. In a radial strip of the deposit, when the electron beam was normal to the radius i.e. normal to the plane of incidence of the vapour stream on that part of the specimen in the electron beam, asymmetric patterns were obtained at various angles of incidence (Figure 38 corresponds to an angle of incidence of 14°; Figure 39 to an angle of 54°). In all these cases the 112 arc remained in the plane of incidence of the pattern and was still strong. The other arcs

appearing in the pattern were practically in the same position as in the symmetrical pattern of the one degree (112) orientation.

These observations show that throughout the specimen the crystals still have (112) orientation parallel to the substrate surface, but some crystals of the one degree orientated set have grown preferentially so as to predominate in the upper layers of the deposit. It was observed that in the thinner parts of the specimen (in this specimen, at parts where the vapour stream was incident by an angle $\gtrsim 70°$ to the normal) this preferential growth had not developed.

The specimens had a marked sheen in a directed beam of light showing highly reflecting facets roughly normal to the incident vapour had been formed on the zinc crystals of the deposit. From the direction of the light reflections which were especially strong from the deposit region at 60° vapour stream incidence it was estimated that the facets were inclined at about 60° (with some spread between 50° and 70°) to the substrate thus suggesting (001) facets (which would be at 61°44' to the substrate for 112 orientation) as being the most probable.

Figure 39 at an incidence of 54° shows a strong 002 arc whose centre lies on a radius at 30° to the shadow edge. This agrees with the above deduction that the facets are {001}.

The 10ℓ arcs in Figure 39 lie on the appropriate layer lines which would correspond to (001) orientation normal to the 002 arc radius, nor on row lines tangential to the 100 ring and

parallel to the 002 radius. As a particular example the short 100 arc lies on a radius making ~115° with the radius to the 002 arc (instead of 90°). This confirms that the crystals are not in one degree (001) orientation about the direction of the vapour stream falling on this part of the specimen.

The positions of the arcs do not agree with there being (112) facets either, because they do not correspond to one degree (112) orientation about the vapour stream direction at this part of the specimen (e.g. the 100 arc is in the wrong position), nor do they correspond to only partial one degree (112) orientation about this direction.

Figures 38 and 39 show faint oxide arcs in parallel growth due to the film of ZnO formed by exposure to air in transferring the specimens to the camera.

Normal incidence. As has been shown above, patterns which are asymmetric in the intensities of the arcs were obtained only a few degrees away from normal incidence. The pattern shown in Figure 40 was obtained from a region of deposit formed at normal incidence. This presented considerable difficulty in its interpretation; there is no well-defined arc in the plane of incidence and an identical pattern was obtained at 90° to this azimuth so that it must correspond to one degree orientation. The following method, suggested by Dr.H.Wilman, was employed:-

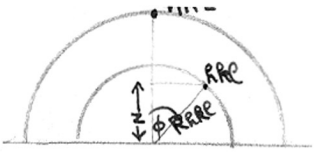

Determination of the orientation of Figure 40.

Let HKL be the orientation, hkl a general diffraction.

Now $\cos\phi = \dfrac{\underline{R}^* \cdot \underline{r}^*}{R^* r^*} = \left[\Sigma hHa^{*2} + \Sigma(hK+kH)a^*b^*\cos\gamma\right] d_{hkl}\, d_{HKL}$

For the hexagonal system $a^* = 2/\sqrt{3}a$; $c^* = 1/c$; $\gamma^* = 60°$

Substituting we get

$$\cos\phi = \left[4/3\left\{hH + kK + \tfrac{1}{2}(hK+kH)\right\} + lL/c/a)^2\right] 1/a^2\, d_{hkl}\, d_{HKL}$$

Now $R_{hkl} = \dfrac{\lambda L}{d_{RRR}}$ and $R_{110} = \lambda L/(a/2)$

so that $\cos\phi = \left[4/3\left\{hH+kK + \tfrac{1}{2}(hK+kH)\right\} + lL/(c/a)^2\right] \dfrac{4R^2_{110}}{R_{hkl}\, R_{HKL}}$

or $R_{hkl}\cos\phi = z_{hkl} = \dfrac{\left[4/3\left\{hH+kK + \tfrac{1}{2}(hK+kH)\right\} + lL/(c/a)^2\right]}{\dfrac{4R^2_{110}}{R_{HKL}}}$

where z_{hkl} is the vertical height of the hkl diffraction above the central spot.

$$\frac{z_{hkl} \cdot R_{HKL}}{4\, R_{110}} = 4/3\left\{hH+hK + \tfrac{1}{2}(hK+kH)\right\} + lL(c/a)^2$$

i.e.

$$z_{hkl}\,(R_{HKL}/4R^2_{110})\ 3/2 = 2hH + 2kK + (hK+kH) + 3/2\,\frac{lL}{(c/a)^2}$$

c/a for zinc = 1.86. Substituting we get

$$z_{hkl} = 2h\,(H/A) + 2k(K/A) + (hk/A + kH/A) + .4335\ l(L/A)$$

Call $H/A = H'$, $K/A = K'$, $L/A = L'$, so that

$$z_{hkl} = 2hH' + 2kK' + (hK' + kH') + 0.4335\ lL'.$$

Substituting into this equation the measured values of z for the 112, 101 and 100 arcs, taking into account the equivalent planes for the 100 and the 101 (defining the 112 arcs as 112), we get the following set of equations:-

112		$2.25 = 3H' + 3K' + 0.967L'$	(1)
101	101	$1.27 = 2H' + K' + 0.4335L'$	(2)
	$10\bar{1}$	$1.27 = 2H' + K' - 0.4335L'$	(3)
	011	$1.27 = H' + 2K' + 0.4335L'$	(4)
	$01\bar{1}$	$1.27 = H' + 2K' - 0.4335L'$	(5)
100	100	$0.69 = 2H' + K'$	(6)
	010	$0.69 = 2K' + H'$	(7)
	$\bar{1}10$	$0.69 = -H' + K'$	(8)
	$1\bar{1}0$	$0.69 = H' - K'$	(9)

From eqns. (1), (2) and (6) we get $H' = 0.326$, $K' = 0.038$, $L' = 1.336$

corresponding to (104) orientation

From eqns. (1), (2) and (7) we get $H' = 0.42$, $K' = 0.13$, $1' = 0.692$

corresponding to (315) orientation.

From eqns. (1), (2) and (8) we get $H'-K' = 0.29$ and $H'-K'=0.69$ which is inadmissable.

From eqns. (1), (2) and (9) we get $0.29 = H'-K'$ which is also $0.69 = H'-K'$ inadmissable

From eqns. (1), (3) and (6) we get H' = 0.45, K' = 1.59, L' = -1.336

Corresponding to $(\bar{2}7\bar{6})$ orientation which can be neglected.

From eqns. (1), (3) and (7) we get H' = 0.69, K' = 0, L'=0.207

corresponding to (301) orientation.

From eqns. (1), (3) and (8) we get H' = 0.112, K' = 0.802, L' = -0.565

corresponding to $(17\bar{5})$ orientation.

From eqns. (1), (3) and (9) we get H' = 0.69, K' = 0, L' = 0.207

corresponding to (301) orientation.

From eqns. (1), (4) and (6) we get H' = 0.13, K' = 0.42, L' = 0.695

corresponding to (135) orientation.

From eqns. (1), (4) and (7) we get H' = 0.04, K' = 0.33, L' = 1.32

corresponding to (014) orientation.

Equations (1), (4) and (8) gives an inadmissable solution

so do equations (1), (4) and (9).

Equations (1), (5) and (6) give H' = 0, K' = 0.69, L' = 0.207

corresponding to (031) orientation.

Equations (1), (5) and (7) give H' = 1.59, K' = 0.45, L' = 1.35

corresponding to $(7\bar{2}6)$ orientation which can be neglected.

Equations (1), (5) and (8) give H' = -0.01, K' = 0.68, L'=-1.35

corresponding to $(02\bar{4})$ orientation which can be neglected.

Equations (1), (5) and (9) give H' = 0.80, K' = 0.11, L' =-0.555 corresponding to $(71\bar{5})$ orientation which can be neglected.

The orientations to be considered are therefore (102), (104), (301) and (135). There is no 102 arc in the plane of incidence so that it cannot be (102) orientation; neither can it be (104) orientation since this would mean that the 203 arcs would be 28° from the plane of incidence instead of the 13° observed. The (301) orientation does not bring the 203 arcs near enough to the plane of incidence either, since they would be at 33.4° from the plane of incidence.

The only remaining orientation is (135). This is plotted and shown in Figure 28. The observed pattern agrees with this chart very well particularly for the position of the 101, 102, 112, 110, 103 arcs and accounts for the 203 arcs being nearly in the plane of incidence. ~~However there is a~~ An apparent discrepancy in the position of the 100 arcs which ~~cannot~~ might be accounted for (40° to the shadow edge instead of 57° for (135) orientation) by absorption effects in the crystals.

In the customary notation

$$r^{*2} = \Sigma h^2 a^{*2} + 2\Sigma hk\, ab \cos$$

$$= a^* (h^2 + hk + k^2) + c^{*2} l^2$$

For zinc (close packed hexagonal) $c^* = 1/c$; $a^* = 2/\sqrt{3}a$

$d_{110} = a/2$ so that $r^*_{110} = \sqrt{3}a^*$

Substituting we get

$$r^{*2}_{135} = (r^*_{110}\sqrt{2}/3)^2 \left\{ (h^2 + hk + k^2) + c^{*2}/a^{*2}l^2 \right\}$$

$$= (r^*_{110}\sqrt{2}/3)^2 \cdot 22.64.$$

Substituting the measured value of r^*_{110} we get $r^*_{135} = 5.5$ cm. The diffraction intensity falls off too rapidly to enable an arc in this position to be clearly identified.

Interpretation of the (135) orientation. This pattern is undoubtedly due to one degree orientation since the pattern was identical at an azimuth at right angles to it. It shows no strong arc in the plane of incidence but apart from this there is a similarity to the pattern characteristic of one-degree orientation, as can be seen by comparing it with Figure 41.

This (135) orientation cannot be due to (001) facets which would tend to cause modification of an initial (112) orientation towards (11ℓ) orientations (e.g. (115) orientation would give the 112 arcs in the observed pattern of 15° on either side of the plane of incidence) since (11ℓ) orientations would never allow the 101 arcs to be as close to the plane of incidence as actually observed.

Figure 42 shows a plan of the reciprocal lattice of zinc. It can be seen that the 135 vector is intermediate between the [112] vector and the [011] (≡ [101]) but does not in actual fact lie in the plane which contains the [011] and the [112] vectors but is slightly above it as seen in the diagram

(the height above the plane is $1\frac{2}{3}$ instead of $1\frac{1}{3}$).

Hence it is suggested that the orientation which apparently is one degree (135) arises from the fact that the crystals form (101) facets and thus tend to (101) orientation parallel to the surface at normal incidence, the resultant (135) orientation being the result of this preferential growth of (101) facets in the upper layers as the initial (112) orientated layer becomes thicker.

Interpretation of Figure 44. It may be observed that in Figure 43 (which shows short well defined arcs corresponding to one degree (112) orientation) the 100 arcs are in the correct position i.e. 50° to the shadow edge as illustrated in the chart of (112) orientation (Figure 25).

Figure 44 is slightly off (112) orientation with broader 112 arcs with the 100 arcs about 40° to the shadow edge. The 102 arcs are, on the other hand, nearer the plane of incidence than they should be for one degree (112) orientation (e.g. the centre of the 102 arc is 70° to the shadow edge instead of 60° as in Figure 43) in a manner which is very similar to that of Figure 28 i.e. the (135) orientation. The 100 arcs in Figure 40 are in actual fact 40° to the shadow edge instead of 57° for one degree (135) as plotted in Figure 28. Hence it is concluded that Figure 44 corresponds to a stage which is intermediate between one degree (112) orientation (Figure 41)

and the preferential growth of (101) facets as shown in the pseudo (135) orientation of Figure 40.

Interpretation of Figure 45. Figure 45 was obtained from a zinc film evaporated on to a fresh cleavage face of mica at room temperature. The same pattern was obtained at different azimuths and it is very unlikely that it corresponds to two degree orientation particularly in view of the similarity of the pattern with those obtained on glass which are without doubt cases of one degree orientation. This pattern shows the following arcs in the plane of incidence 100, 101, 200, 202 etc. One degree (100) orientation cannot be present since, for example, the 102, 103 spots are not present in the second layer line of one degree (100) orientation. It does not correspond to one degree (101) e.g. there are no 100 spots at 25° on either side of the plane of incidence. It resembles (112) orientation most closely but there is no 112 arc in the plane of incidence. There is in actual fact a strengthening of the 112 ring on either side of the plane of incidence as in the case of the (135) orientation although the effect is not so marked as in the latter case. The 10ℓ arcs are nearer the plane of incidence than they would be for one degree (112) orientation as in the case of 135 orientation so that this pattern suggests a similar modification of the (112) orientation by the preferential growth of (101) facets.

8. Discussion of results on orientation in zinc deposits.

Although zinc films have been studied extensively by means of the electron microscope, the range of orientations of zinc in films condensed from the vapour has never been clearly or satisfactorily demonstrated. Dixit (1933) evaporated zinc on to molybdenum blanks and found that the orientation first produced at temperatures about 20°C. was that in which the most densely packed plane of atoms was parallel to the surface i.e. (001) orientation; at higher temperatures (up to 300°C.) he concluded that other planes tended to be parallel to the substrate, but he has not referred to it, or realised the significance of, the strong asymmetry in his patterns which must have been due to oblique incidence of the vapour stream combined with facet development such as that described above. His observed orientations are therefore not characteristic of the lower initial layers formed on the substrate. He calculated, by supposing a layer of atoms on the surface to act as a two-dimensional gas, that the area occupied per atom in each plane was proportional, for any given metal, to the absolute temperature at which orientation on that plane was most prominent. The experimental results cannot be considered satisfactory, however, in view of the ill-defined nature of the orientations.

The author has described above a detailed investigation

of the structure of zinc films (formed by condensation of the vapour) both at normal incidence and at oblique incidence of the vapour stream. Strongly oriented films of oxide-free zinc were obtained, and the manner in which the orientations were determined has been described.

The plane with the highest atomic population in zinc is the basal plane (001); the next most densely populated planes are the (100) and the (101) planes. One-degree (001) and one-degree (100) orientations were observed simultaneously (in the same specimen) both on glass and the cleavage face of rock-salt. Weak one-degree (101) orientation was also observed. In addition to these orientations which correspond to densely packed planes lying parallel to the substrate, weak one-degree (105) and medium one-degree (201) orientations were obtained. Undoubtedly the heat received by the substrate by radiation from the filament facilitates orientation and might possibly account for these higher orientations. However the most commonly occurring orientation was that with (112) planes parallel to the surface. Out of a total of 30 specimens, 25 showed (112) orientation, although in some cases this (112) orientation was not at first apparent since it had been modified by the growth of facets in the upper layers of the deposits (the (201) & the (105) orientations might also be due to facet development)

When the electron beam was close to or through the foot of the normal from the atom source to the substrate symmetrical

patterns were obtained. However if the incident vapour was only slightly inclindd to the surface asymmetric patterns were obtained when the electron beam was normal to the direction of the vapour stream. An experiment with a directed beam of light showed that highly reflecting facets had been formed on the zinc crystals of the deposit, suggesting by the direction of their reflections the possibility of their being (001) facets. A study of the diffraction patterns from different parts of the surface (corresponding to different angles of incidence of the vapour stream) confirms the suggestion that the preferential growth of (001) facets takes place in the upper layers of the deposit thus modifying the initial (112) orientation on the substrate to give the asymmetric patterns. observed. This preferential growth of (001) facets was not observed in thin layers.

The (001) habit (i.e. the tendency to form (001) faces) of zinc has been observed previously by Matthewson and Phillips (1927) and Straumanis (1931,1932) while Finch, Wilman and Yang (1948) observed the absence of (00ℓ) rings in the diffraction patterns obtained from electrolytically deposited zinc in (110) orientation (with weak (112) orientation also present), showing that the deposit crystals had large (001) faces. Geist (1949) examined zinc crystals grown by sublimation and found that they consisted of stacks of plates parallel to the hexagonal basal plane (001). This (001) habit has also been amply verified

in the author's experiments with zinc films formed from the vapour, since the majority of the patterns showed a complete absence of (002) diffractions.

The formation of (001) facets in the above cases is supported, to some extent, by the parallel growth of ZnO shown by some of the patterns since the parallel growth of (001) ZnO on the (001) cleavage face of zinc has been amply verified (Wilman, 1948; Acharya, 1948; Finch, 1950). The parallel growth of ZnO on the etched (001) face of Zn is also demonstrated in Part IV.

The way in which the (112) orientation of zinc is modified at normal incidence of the vapour stream by the preferential growth of (101) facets in some cases is described; the crystals them tend to (101) orientation in the upper layers of the deposit resulting in orientations which are intermediate between one-degree (112) and one-degree (101), depending on the extent to which (101) facets have been formed. It may be noted that Stranski (1949) investigated the growth of Cd and Zn single crystals from the vapour and found that they gave the faces (001), (101), (100), (110), (102), the (101) faces being the most likely faces to be formed after (001) faces.

The fact that the (112) orientation parallel to the substrate predominates in these specimens is further confirmation of the contention that the crystallites (e.g. in the case of iron) orientate parallel to the surface in deposits

such as those investigated above. In the case of lead sulphide and iron (and presumably in the cases observed by Burgers etc.) this orientation parallel to the surface only appears to be modified due to the undulating nature of the surface and the low mobilities of these substances. Zinc, however, in virtue of its very high mobility, migrates over the surface and fills the hollows. Consequently one does not observe an effect similar to that observed with iron and lead sulphide; what is observed is a modification of the orientation parallel to the surface by the preferential development of the otherwise slowly growing facets.

The strongly oriented films of oxide-free zinc were obtained by evaporating zinc off a tungsten filament in a vacuum of 10^{-3} mm. It may be noted in this connection that too high a vacuum does not seem desirable since the presence of gas facilitates the formation of oriented films by effectively increasing the mobility of the deposit atoms on the substrate. The zinc first evaporated serves to "getter" the space around the zinc vapour source, the bound oxygen appearing as metal oxide on the intercepting substrate. However, in view of the small volume of the evaporation chamber (together with its freedom from gaskets, etc.) it would seem that the amount of ZnO formed would be insufficient to cover the whole of the substrate to a thickness of more than one atom layer. On

continued evaporation the zinc film would be free of oxygen. The faint oxide arcs visible in some of the patterns are due to the thin ZnO film on the surface of the zinc due to exposure to air after the film is formed.

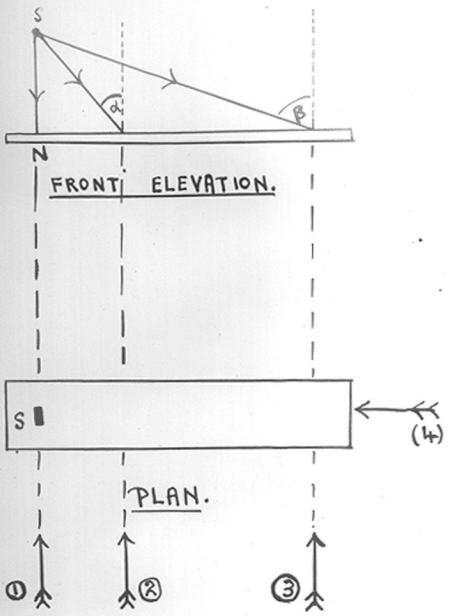

S = SOURCE OF ATOMS.

N = FOOT OF NORMAL.

ELECTRON BEAM AT RIGHT ANGLES TO VAPOUR STREAM ALONG (2) & (3).

ELECTRON BEAM ALONG VAPOUR STREAM IN (4).

Fig. 1.

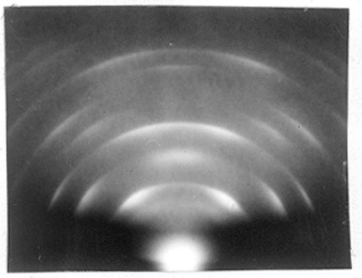

Fig. 2.

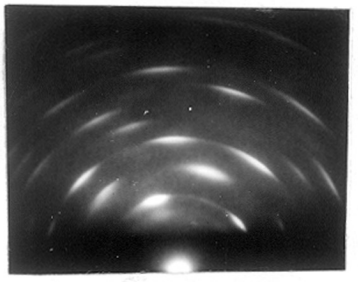

Fig. 3.

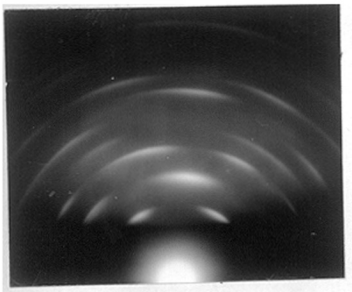

Fig. 4.

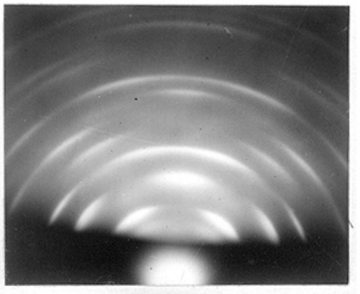

Fig. 5.

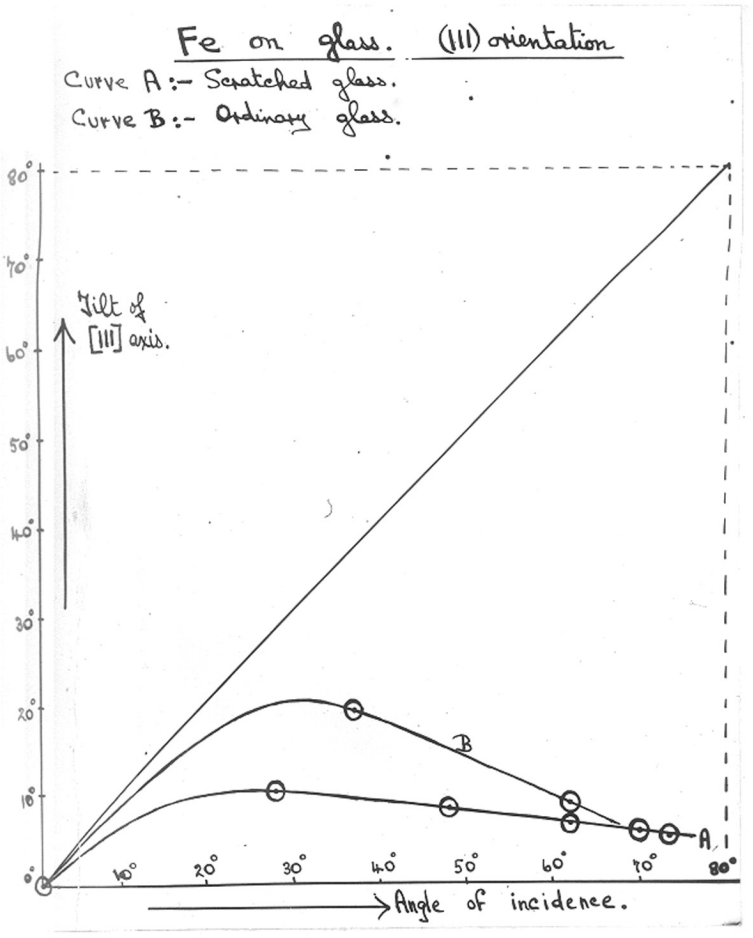

Fig. 6.

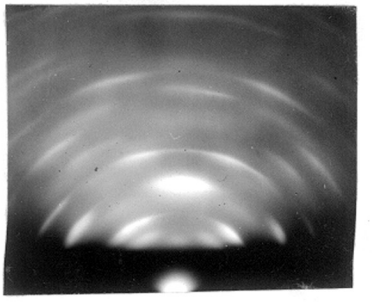

Fig. 7.

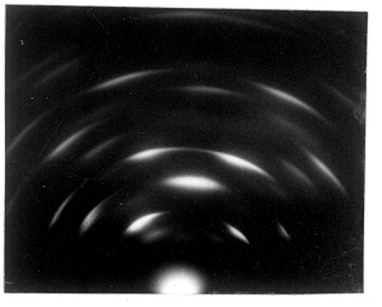

Fig. 8.

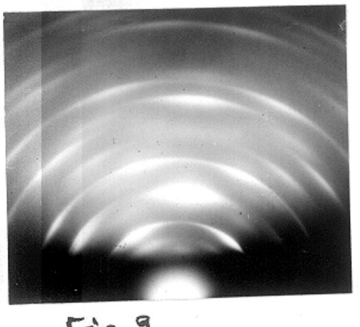

Fig. 9.

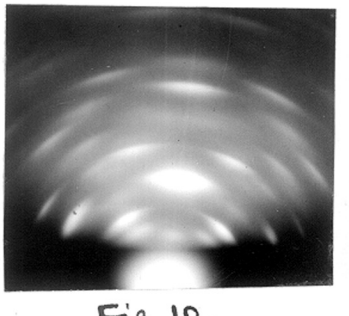

Fig. 10.

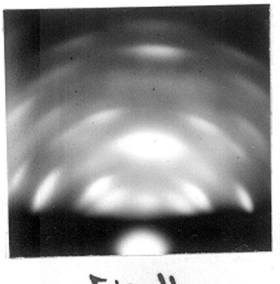

Fig. 11.

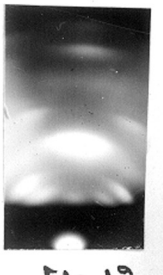

Fig. 12.

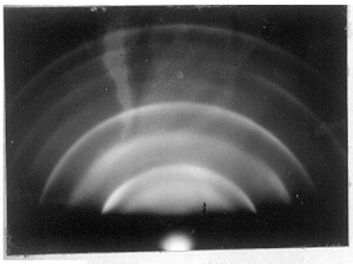

Fig. 13.

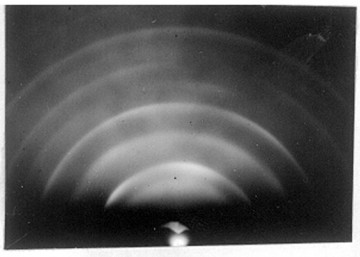

Fig. 14.

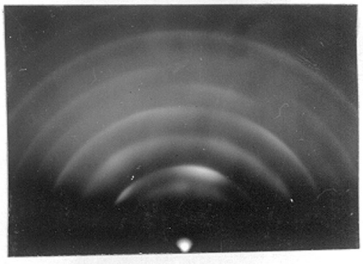

Fig. 15.

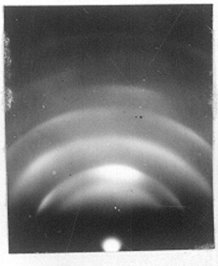

Fig. 16.

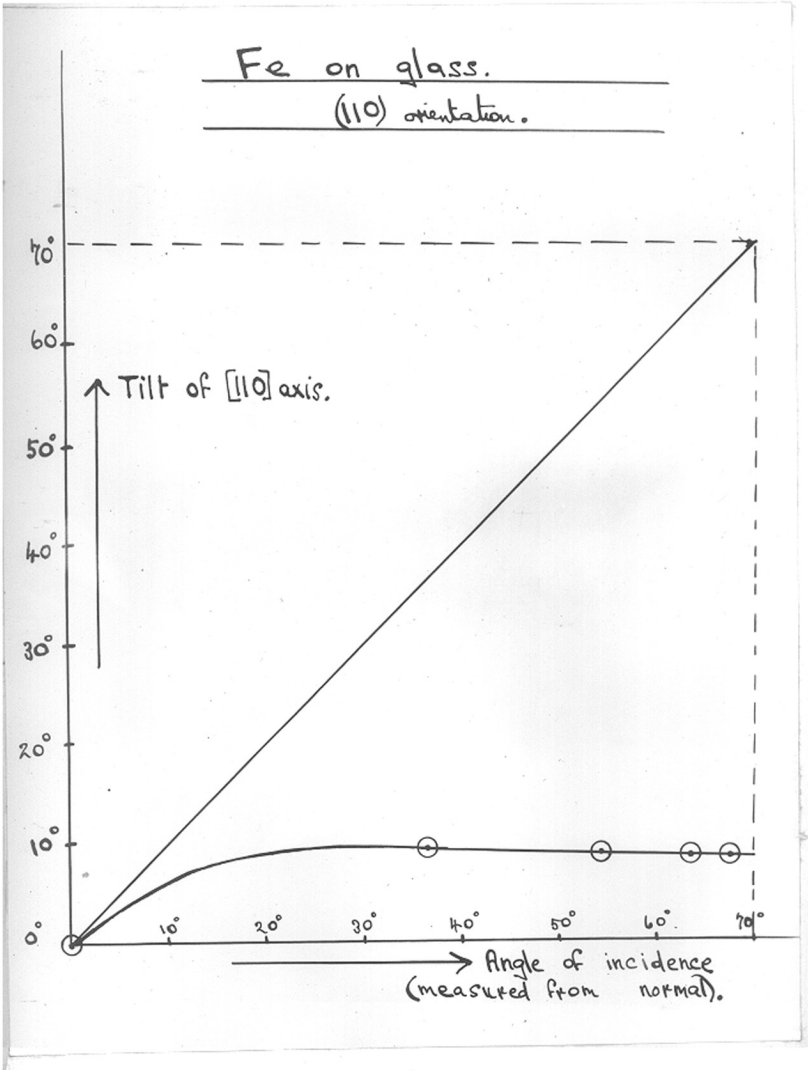

Fig. 17.

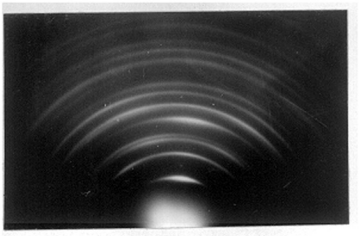

Fig.18.

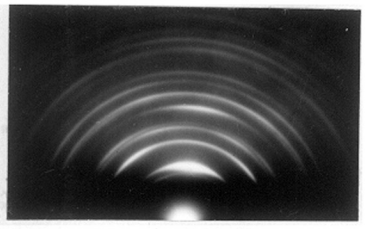

Fig.19.

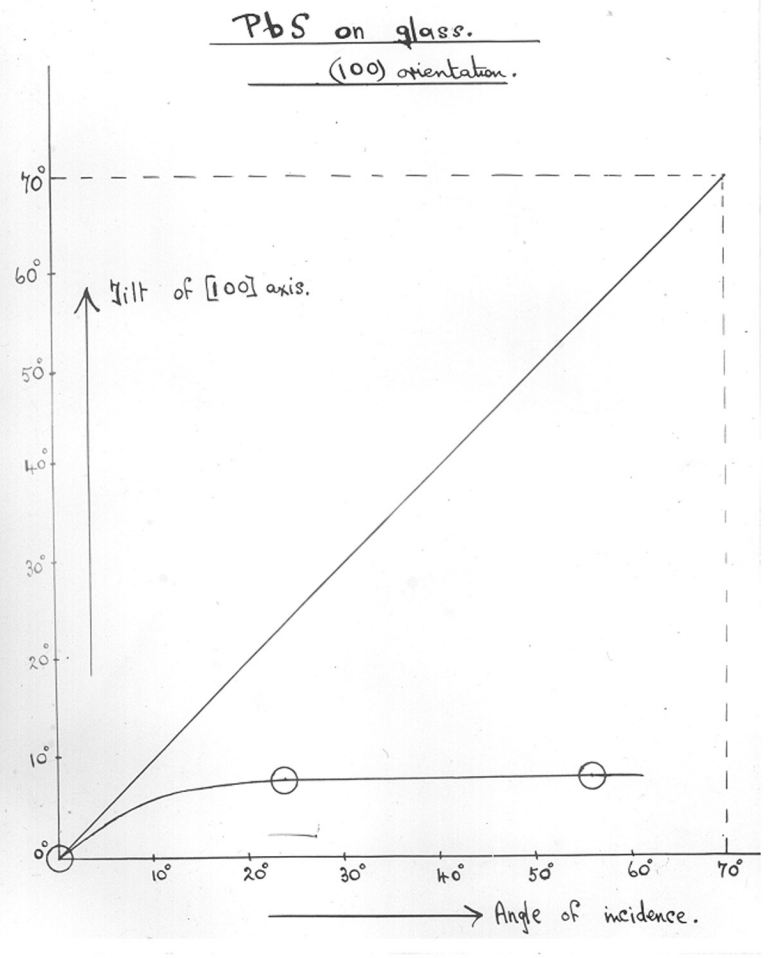

Fig.20.

DIAGRAMMATIC REPRESENTATION.

FIGURE 21

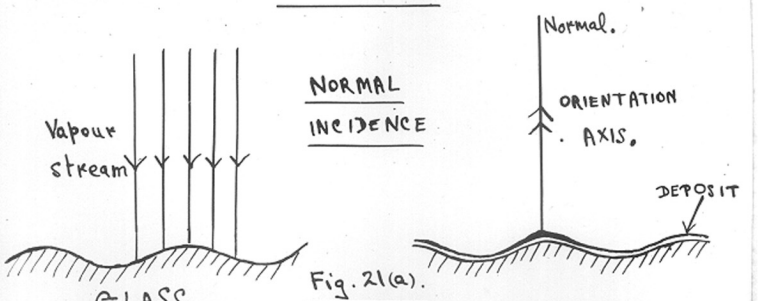

Fig. 21(a).

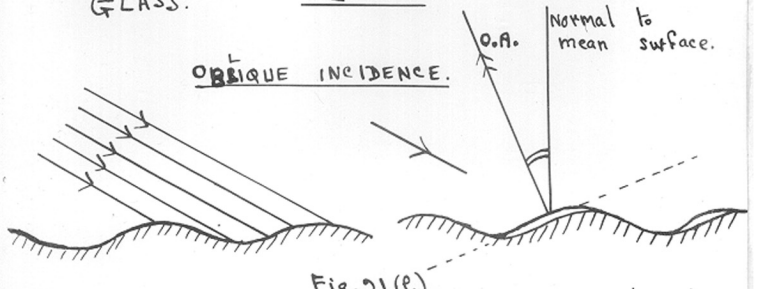

Fig. 21(b).

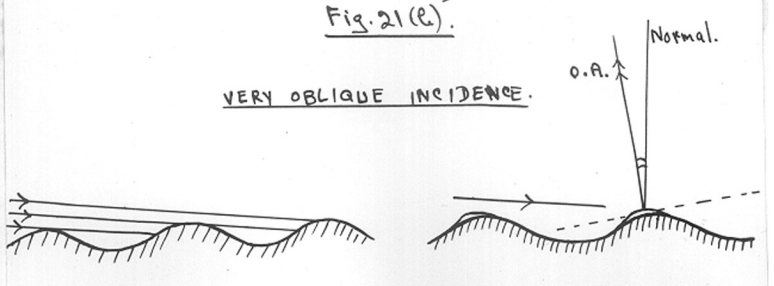

Fig. 21(c).

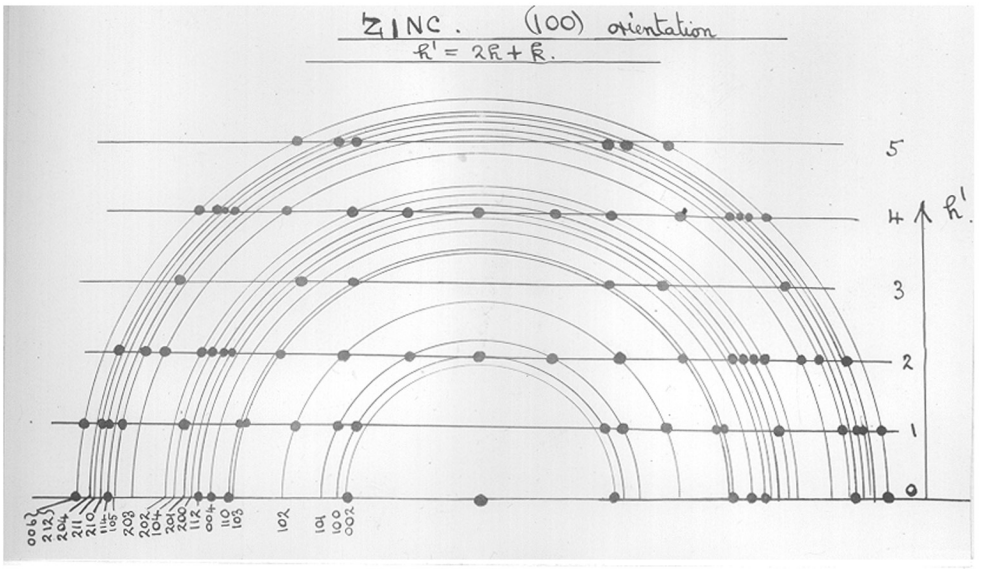
ZINC. (100) orientation
h' = 2h + k.
5
4
3
2
1
0
h'
0063
2123
204
211
210
115
105
208
202
104
200
112
004
110
105
102
101
100
002

Fig. 22.

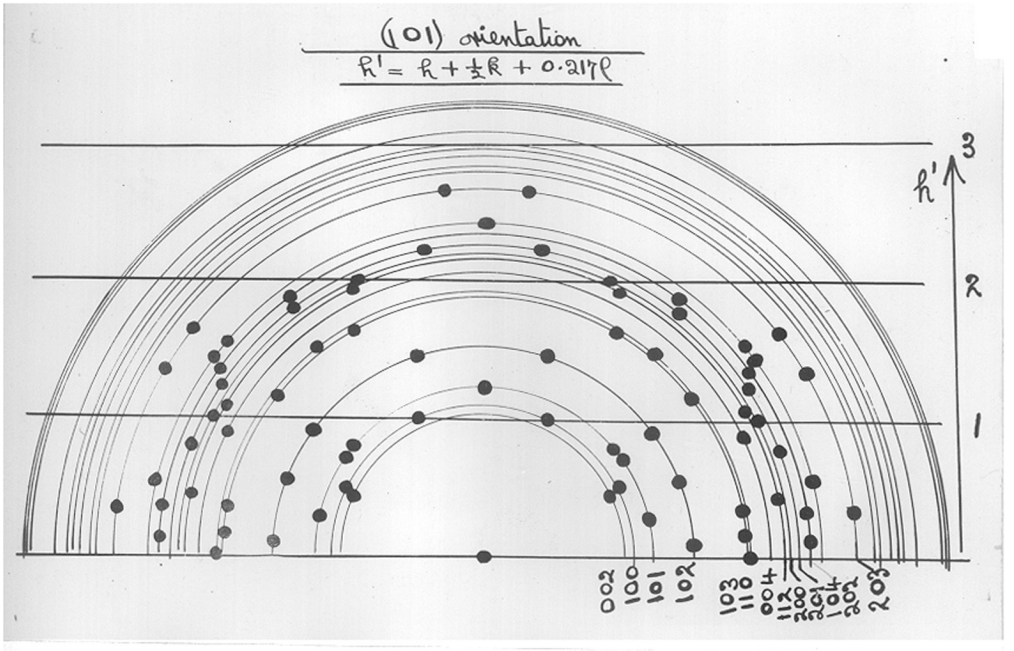
(101) orientation
h' = h + ½k + 0.217l
3
2
1
h'
002
100
101
102
103
110
004
112
201
200
203

Fig. 23.

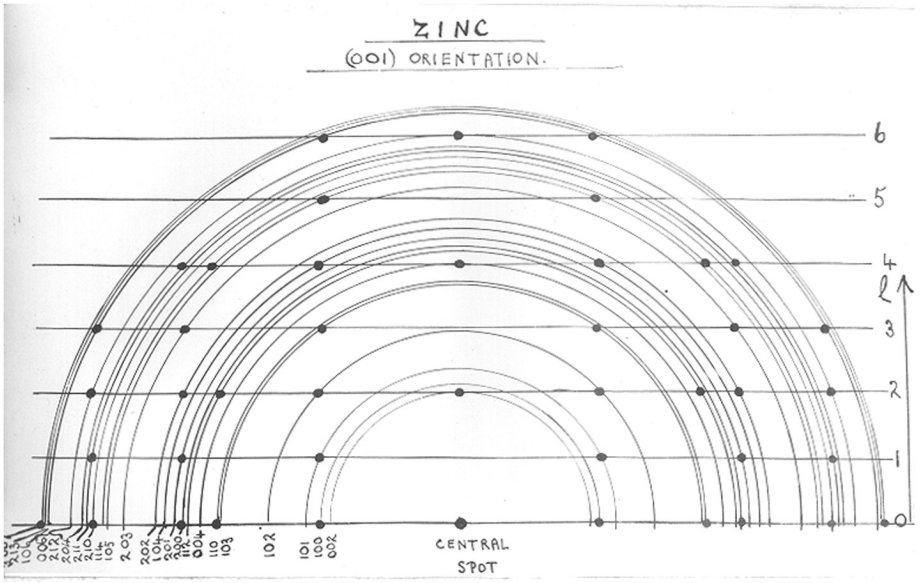
ZINC
(001) ORIENTATION.
6
5
4
3
2
1
0
l
CENTRAL
SPOT

Fig. 24.

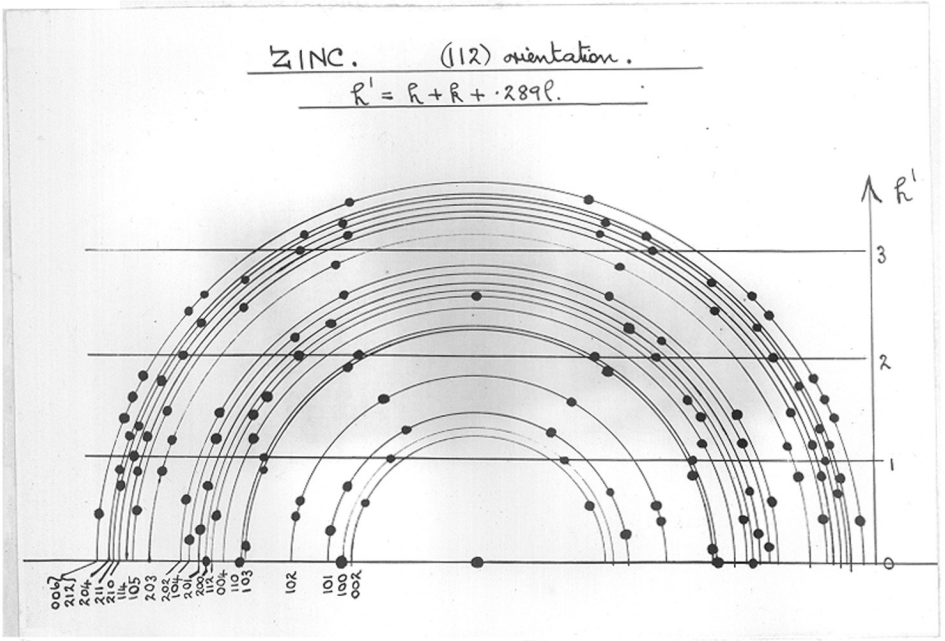
ZINC. (112) orientation.
R' = R + R + ·289P.
R'
3
2
1
0

Fig. 25.

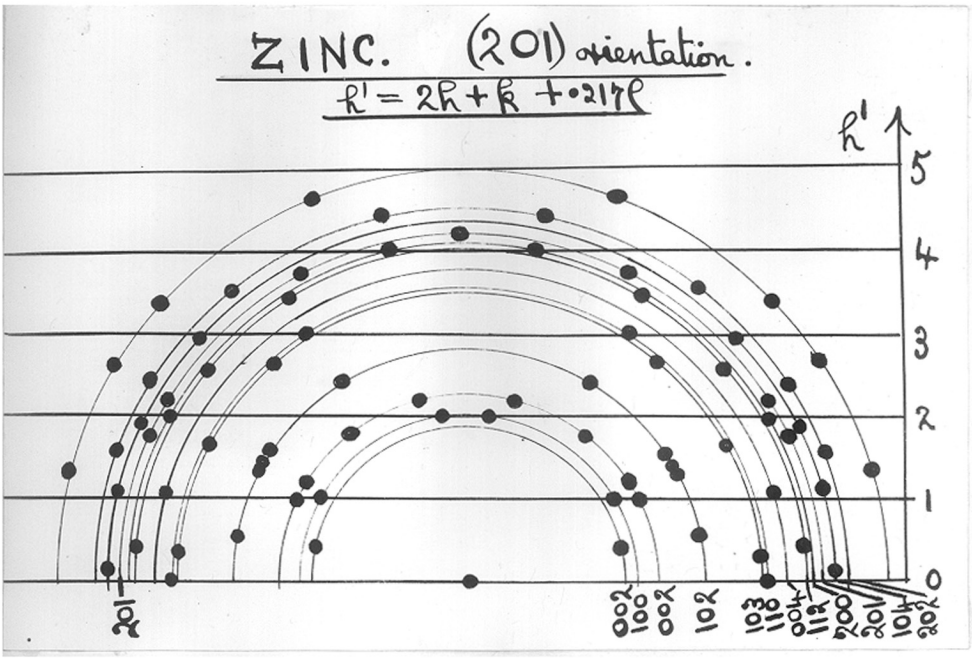
ZINC. (201) orientation.
h' = 2h + k + 0.217l
h'
5
4
3
2
1
0

Fig. 26.

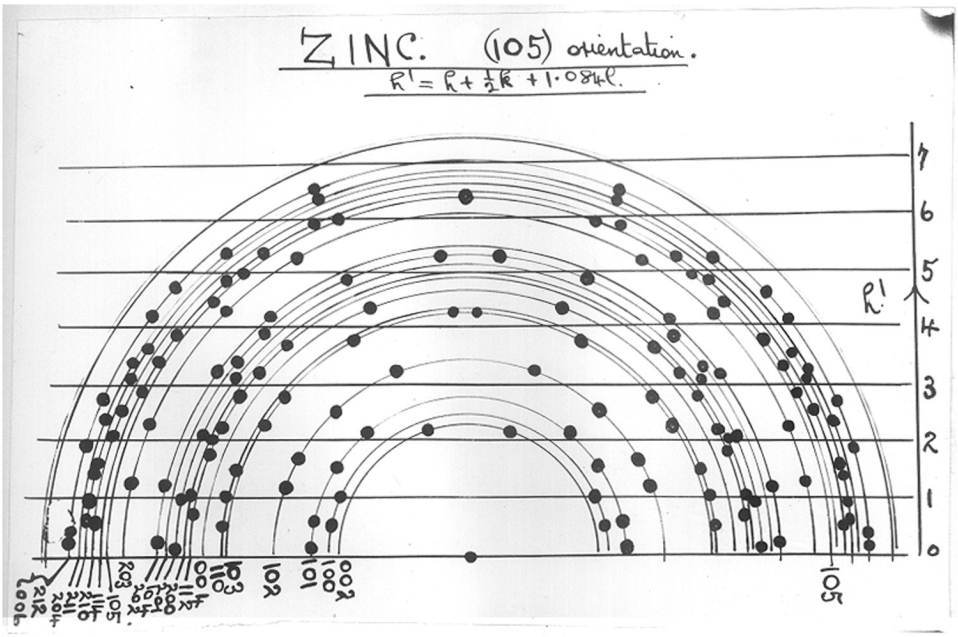
ZINC. (105) orientation.
h' = h + ½k + 1.084l.
h'
7
6
5
4
3
2
1
0

Fig. 27.

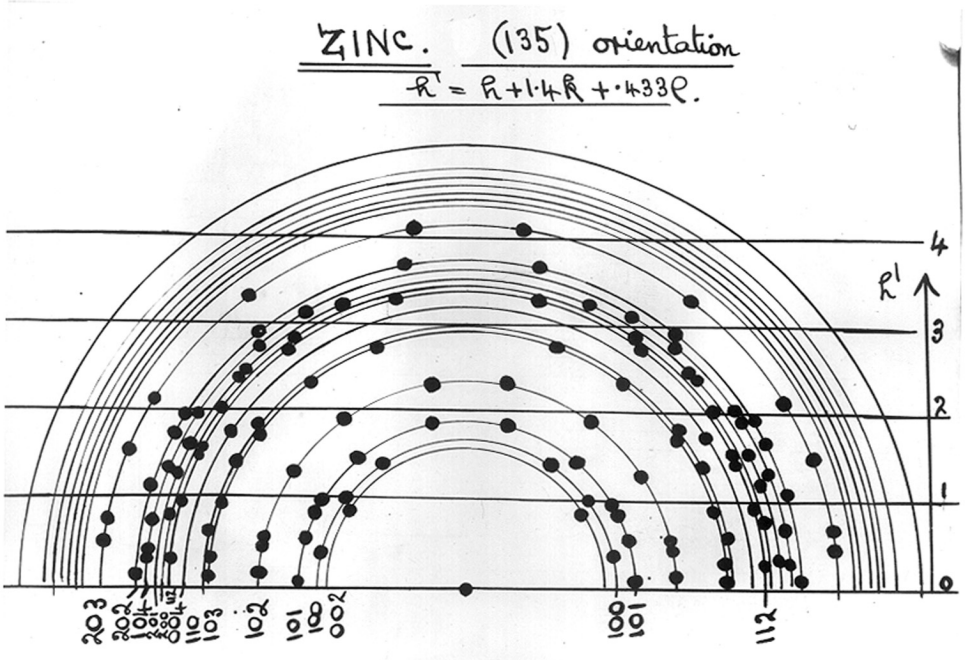
ZINC. (135) orientation
R' = R + 1·4R + ·433P.
4
3
2
1
0
R'
$20\bar{3}$
$20\bar{2}$
$10\bar{3}$
$10\bar{2}$
$10\bar{1}$
$00\bar{2}$
$10\bar{1}$
$11\bar{2}$

Fig. 28.

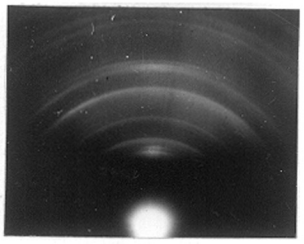

Fig. 29.

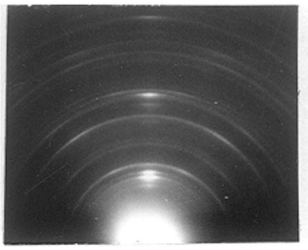

Fig. 30.

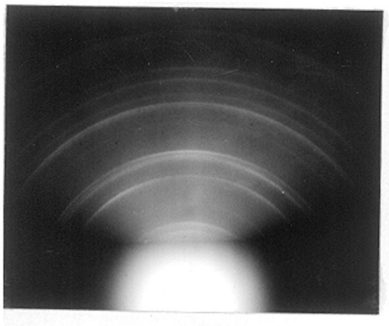

Fig. 31.

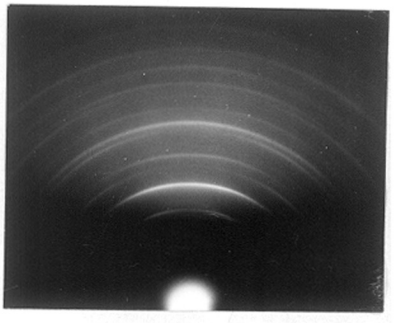

Fig. 32.

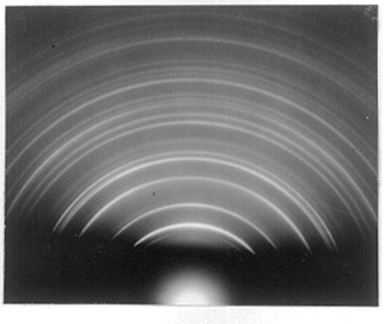

Fig. 33.

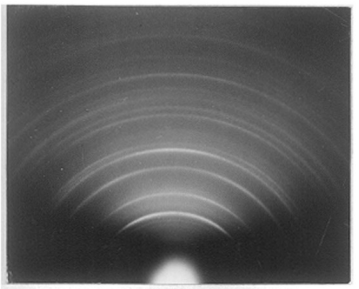

Fig. 34.

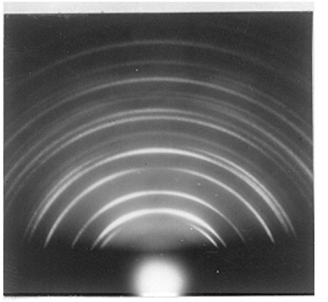

Fig. 35.

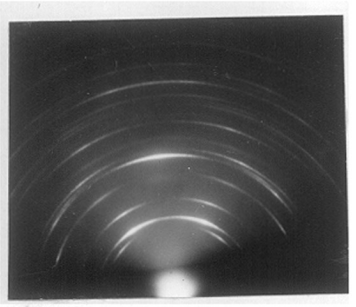

Fig. 36.

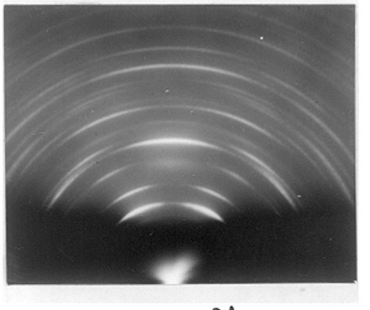

Fig. 37.

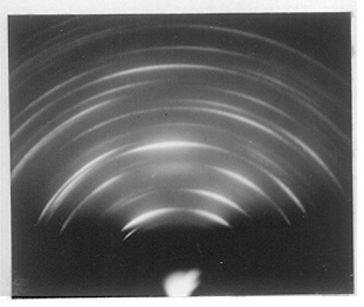

Fig. 38.

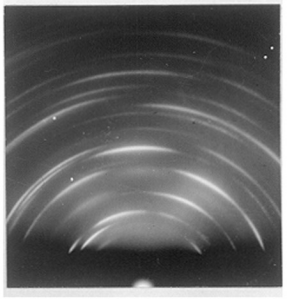

Fig. 39.

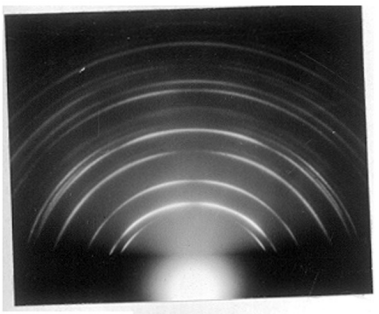

Fig. 40.

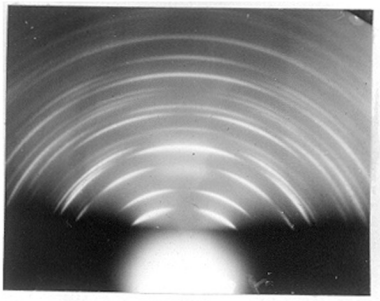

Fig. 41.

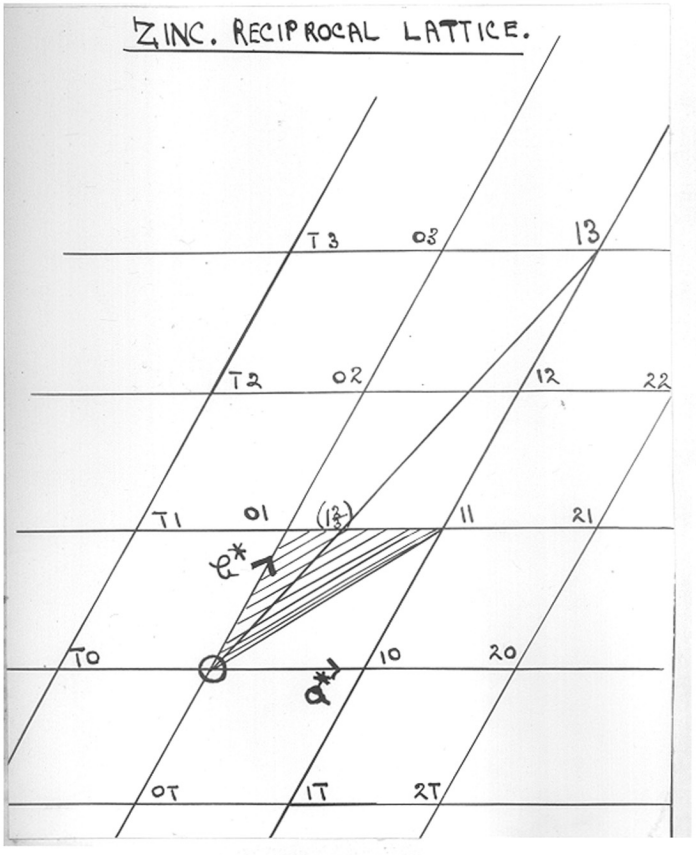

Fig. 42.

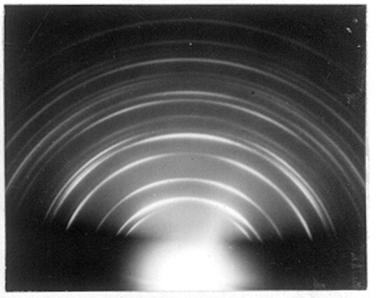

Fig. 44.

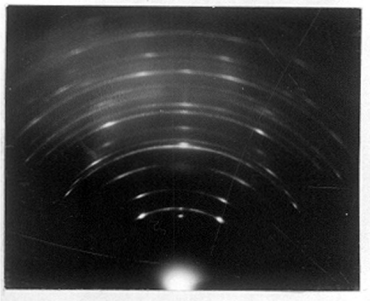

Fig. 45.

PART 3.

ZINC DEPOSITED AT NORMAL INCIDENCE ON ROCKSALT CLEAVAGE FACES.

1. Experimental Details.

Zinc evaporated from a tungsten filament on to a fresh cleavage face of rock-salt in a vacuum of 10^{-3} mm. yielded only one-degree orientations. These results have been described in Part II. Two-degree orientation of zinc was obtained by completely removing all the oxygen before depositing the zinc on to the rock salt face. A freshly cleaved specimen of rock salt was placed in a long pyrex tube attached to a backing pump, a large quantity of zinc being also placed in the tube. The walls of the tube were degassed and the tube sealed off under vacuum. The zinc was then sublimed several times to remove all (or practically all) of the oxygen (by its gettering action) in this small enclosed volume, before being sublimed on to the cleavage face to form a thin film.

2. Experimental results and their interpretation.

Figure 46 shows the pattern obtained from one of these specimens with the beam along the cube face diagonal of the (001) face. It can be seen that the main spots are on vertical

equidistant Laue zones which are those of the <100> axis of Zn, which must therefore be normal to the beam and parallel to the other cube face diagonal. In virtue of the 4-fold symmetry of NaCl, there must also be crystals with the <100> Zn row parallel to the other cube-face diagonal of the NaCl.

The spots in the plane of incidence are the 002, 100, 101, 102 (weak) and 203 (strong) diffractions. The fact that the 100 spots occur at 60° on either side of the plane of incidence confirms the presence of (100) orientation. This cannot be one-degree (100) orientation because of the absence of 101 spots on the first layer line of one-degree (100) orientation. It must therefore be two-degree (100) orientation of Zn on the (001) face of NaCl such that the b axis lies along one cube-face diagonal (at right angles to the beam) and the c axis along the other cube-face diagonal (i.e. along the beam direction).

The equivalent arrangement of the b axis along one cube-face diagonal (in the beam direction) and the c axis along the other cube face diagonal (at right angles to the beam direction) should also be observed but it is not clearly apparent from Figure 46, since the 101 spots should be on the same level as the 100 spot but the 100 spots observed are, in actual fact, slightly lower than the 100 spot being at a 100 radius apart instead of 002.

The 203 spot is very strong in the plane of incidence,

so that there is (203) orientation present, with the b axis parallel to the cube-face diagonal of the NaCl. The 101 spot is less strong, with the 102 spot less strong still. The diamond array of spots with the 102 spot at the vortex would correspond to (102) orientation but it does not extend over the plate although it reappears farther out, in the next circular Laue zone, but out of step. The 203 spot is however the centre of an extensive similar diamond shaped array of spots.

Hence it is concluded that Figure 46 corresponds to two-degree (100) orientation and two-degree (203) orientation, the (203) orientation being very much stronger than the (100) orientation. (The pattern with the beam at right angles to the above azimuth must have scanned a different portion of the specimen since it showed a strong 002 arc in the plane of incidence).

Figure 47 with the beam along the cube-face diagonal shows a pattern which is similar to Figure 46 showing (100) and (203) orientations, but in this case the (100) orientation is stronger than in the first specimen. Figure 48 shows the pattern obtained in the cube edge azimuth of the same specimen, the arc positions confirming the orientations. The rocksalt was dissolved away with water and the pattern was examined by transmission. It was found to consist of rings due mainly to zinc hydroxide (hexagonal structure).

Figure 49 was taken from a third specimen with the beam along the cube-face diagonal. This again shows (100) and (203) orientations, the (100) orientation being the stronger. The pattern also shows an elongation of the 002 spot in the plane of incidence due to refraction indicating strong (001) habit. The pattern with the beam along the cube-edge (Figure 50) shows the 101 spot in the plane of incidence to be very strong suggesting (101) orientation in this case, although the 202 diffraction is weaker than might be expected relative to the 203.

A fourth specimen was also found to consist of (100) and (203) orientations, being almost identical with the second specimen.

3. Lattice fitting of zinc on rocksalt (001).

The position of the atoms in the (100), (101) and (203) planes of zinc are plotted taking into account not only those atoms which lie in these planes but those that lie within about 1 Å. above or below the planes. These lattices are then fitted over the lattice of the (001) face of NaCl such that the b axis of Zn lies along the cube-face diagonal of the NaCl, and the c axis lies along the other cube-face diagonal. The lattice constants of zinc are:- a = 2.66 Å.; c = 4.94 Å. while NaCl has a = 5.628 Å. (Wyckoff, 1948).

Figure 51 shows the lattice fitting and suggested atomic fitting corresponding to (100) orientation. Three times the spacing of the zinc atoms along the $[01\bar{1}0]$ of Zn equals 7.98 Å., which coincides with the spacing of 2 chlorine (or sodium) atoms along [110] of NaCl (=7.96 Å.). The suggested fitting of the c axis of Zn along the other cube-face diagonal is shown where four times the spacing of the zinc atoms (=19.76Å) coincides with the spacing of 5 chlorine (or sodium) atoms. This again gives a row of high density of coincidence points.

Figure 52 shows the lattice fitting of the (203) plane of Zn on the (001) of NaCl. The large crosses indicate zinc atoms in or very nearly in the (203) plane; the smaller crosses are zinc atoms either 0.8 Å. or 1.15 Å. above or below the plane. The coincidence of atomic positions along the b axis of Zn is as before; coincidence is again obtained along this row at intervals of three times the spacing of the Cl atoms along the other diagonal, resulting in a high density of coincidence points at the interface.

Figure 53 shows the lattice fitting and suggested atomic fitting of the (101) plane of Zn on the (001) plane of NaCl. Coincidence of every third atom of Zn (to every other atom of Cl) along the b axis of Zn occurs as before. The degree of coincidence along the other diagonal is not as exact in this case as in the case of (100) and (203) orientation.

However consider the 4th row of Cl atoms parallel to the initial line of coincidence. It can be seen that a row of Zn atoms is slightly displaced from this, whereas a row of Zn atoms is slightly displaced the other way along the third row of Cl atoms. It is suggested that the stress imposed due to this slightly inexact fit will in all probability be mainly balanced out, since the compressive forces on the zinc atoms in the one row will counteract the extensive forces on the zinc atoms in the other row, resulting in reasonable stability.

4. Summary and Discussion.

Zinc evaporated from a tungsten filament on to a cleavage face of rock salt, in a vacuum of 10^{-3} mm., yielded at first only one-degree orientations. This is attributed to the fact that zinc atoms combine with the oxygen atoms en route to the substrate forming an initial layer of ZnO on the cleavage face (of the order of 1 or 2 atoms thickness). This layer is relatively immobile and consequently not orientated. Once this initial randomly oriented layer of ZnO has been formed, free zinc atoms condense on it as a new substrate but are prevented from being acted upon by the adhesive forces in the NaCl (001) face and consequently the orientation is independent of the substrate. The surface is still essentially flat however and the zinc crystals grow in orientations with dense planes parallel to the surface corresponding to an arrangement of minimum potential

energy (see Part II).

If however the oxygen atoms are removed then the mobility of the zinc atoms on the (001) face of NaCl is not hindered by any ZnO film and it was found that the zinc was invariably oriented in two-degree (100) and (203) orientations in varying proportions.

Charts are drawn showing the lattice fittings and suggested atomic fitting corresponding to these orientations. Recent work by Wilman (1950, in the press) leads him to conclude, from evidence of preferred relative orientations of crystal fragments after rotational slip, that the essential feature of epitaxial growth is the density of coincidence points between the positions of atoms in the deposit layers and the potential troughs in the substrate surface, a high density of coincidence points corresponding to high stability. This leads to the result that the condition for epitaxial orientation to occur is not that parallel lattice spacings in deposit and substrate are within say 15% of each other but that x spacings of one (say the deposit) coincide, or very nearly so, with y spacings of the other (i.e. the substrate), where x and y are low integers. This is well demonstrated by the fitting of the lattice spacing of Zn along the two cube-face diagonals in the (001) face of NaCl.

It is interesting to compare this (10ℓ) type of

orientation of Zn (hexagonal structure) on the (001) face of NaCl (face-centred cubic structure) with the orientation of ZnO (hexagonal) on ZnS (face-centred cubic) observed by Aminoff and Broome (1938) and confirmed by Uyeda, Takagi and Hagihara (1941). They obtained (203) orientation of the oxide by heating zinc blende in air.

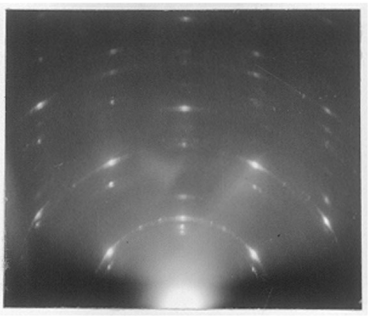

Fig. 46.

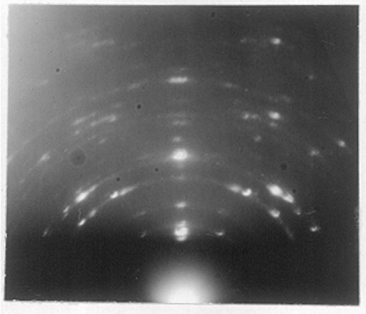

Fig. 47.

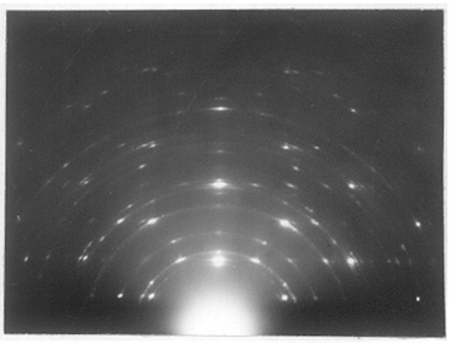

Fig. 48.

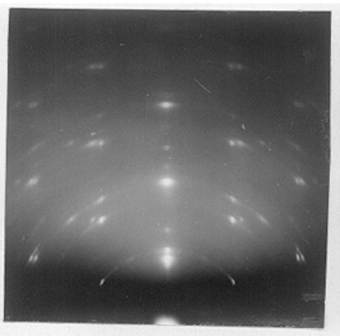

Fig. 49.

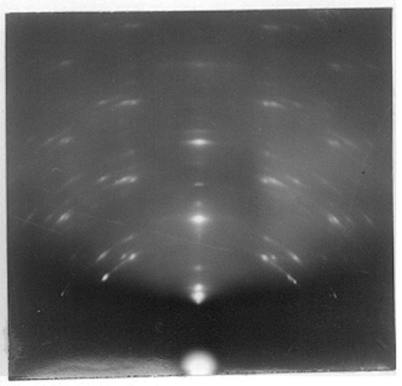

Fig. 50.

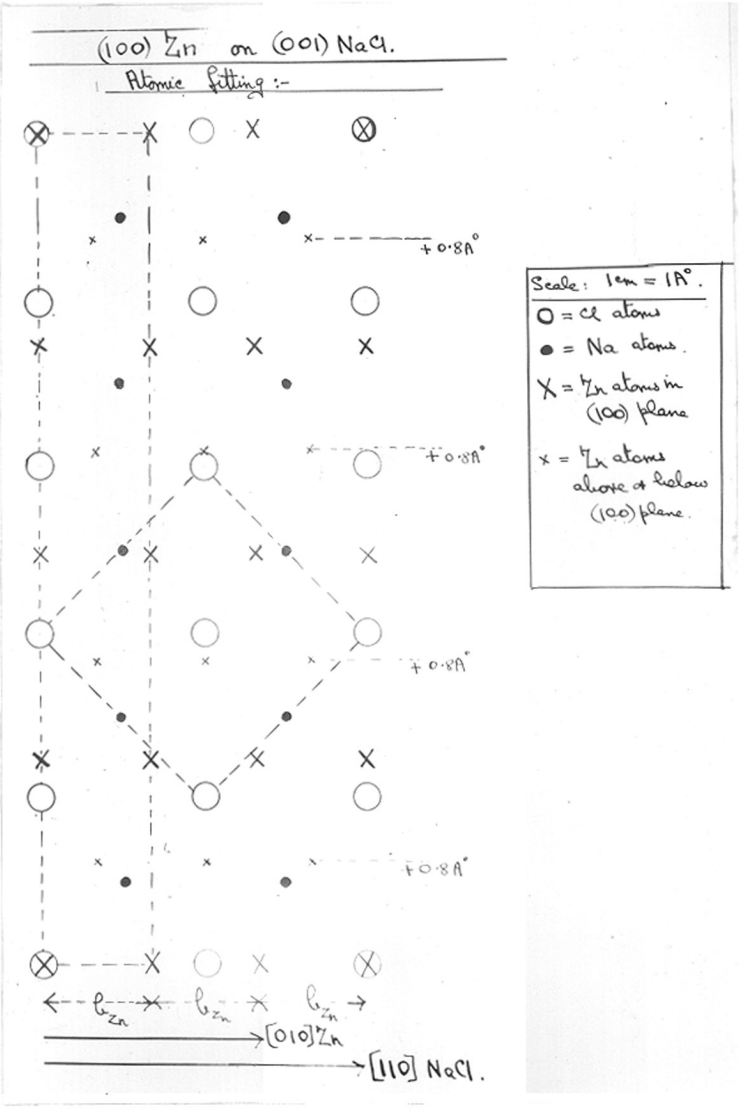
(100) Zn on (001) NaCl.
Atomic fitting :-
+0.8A°
+0.8A°
+0.8A°
+0.8A°
Scale: 1cm = 1A°.
O = Cl atoms
● = Na atoms.
X = Zn atoms in (100) plane
x = Zn atoms above & below (100) plane.
b_{Zn}
b_{Zn}
b_{Zn}
[010] Zn
[110] NaCl.

Fig. 51.

(203) orientation of Zn on (001) NaCl.

Atomic fitting :-

Scale : 1cm ≡ 1A°.

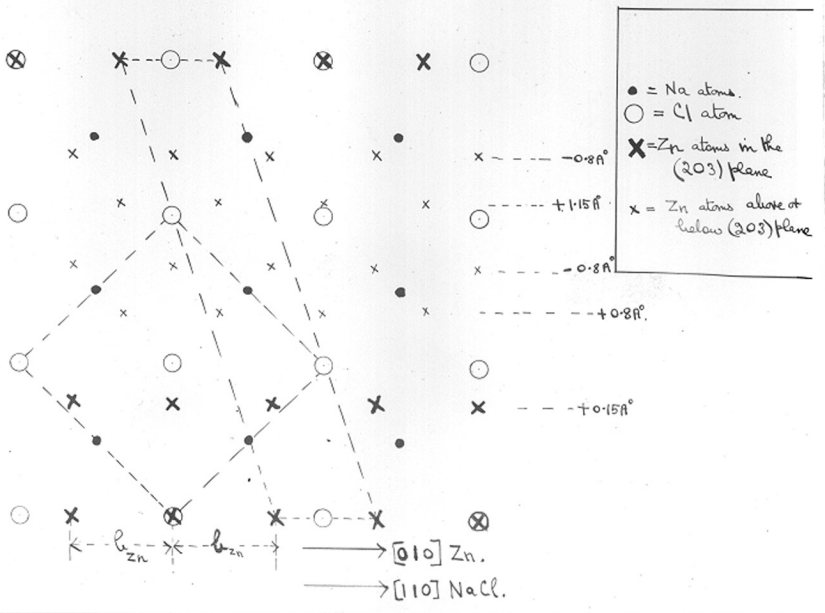

Fig. 52.

(101) orientation of Zn on (001) NaCl.

Possible atomic fitting :-

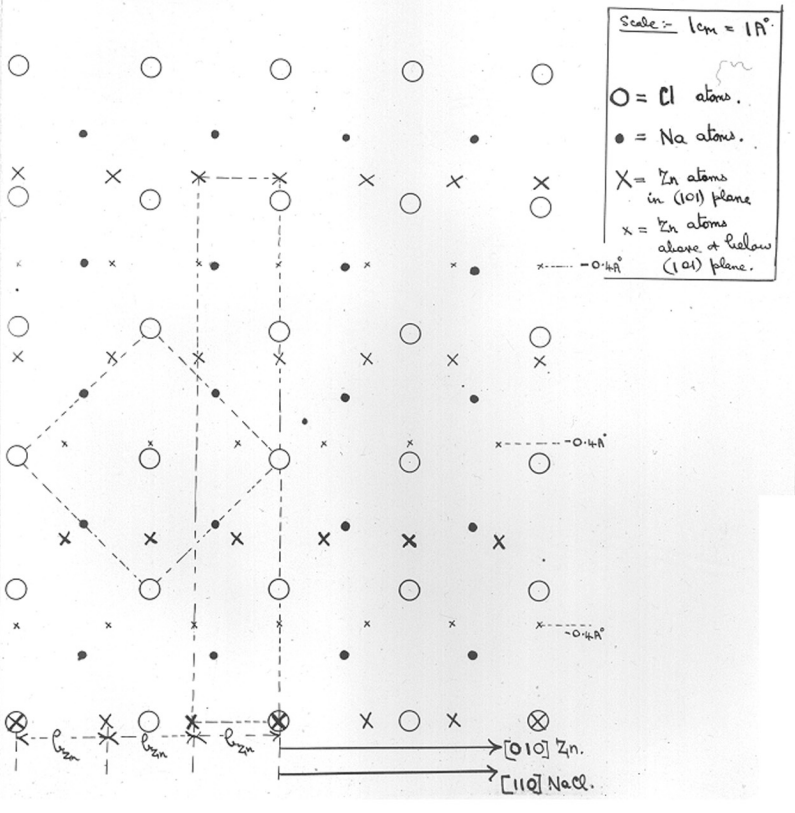

Fig. 53.

PART IV.

THE STRUCTURE OF DEPOSITS FORMED BY CHEMICAL REACTION ON SOLID SURFACES.

1. Thermal oxidation of polycrystalline zinc specimens.

Figure 41 shows the pattern obtained from a specimen of zinc on glass corresponding to medium one-degree (112) orientation. The pattern shows faint traces of ZnO formed during the exposure to air on transferring the specimen to the camera. This specimen was then heated at 350°C. for 15 minutes in air under reduced pressure (10^{-3} mm. Hg) in order to slow down the rate of reaction to facilitate the oriented growth of the oxide. The pattern obtained (Figure 54) still shows the arcs of the zinc pattern with fainter (and somewhat more diffuse) arcs corresponding to ZnO. The lattice constants of zinc are a = 2.659 Å., c = 4.937 Å., i.e. c/a = 1.602 (Wyckoff, 1948). The ZnO pattern is similar to that of the zinc pattern, only it is more condensed due to the larger lattice dimensions of the ZnO; the 112 arc of ZnO, in the plane of incidence, lies just inside the 110 radius of zinc. The pattern shows that the ZnO grows in parallel growth on the exposed faces of the zinc (usually (001) faces) such that the planes of the ZnO lattice are parallel to the planes of Zn lattice.

Figure 40 showed a zinc film in (135) orientation due to the growth of (101) facets in the upper layers of the deposit. Figure 55 shows the specimen oxidised with the ZnO in parallel growth on the exposed (101) faces of the zinc the fainter arcs being ZnO, the stronger arcs being the initial zinc pattern.

2. The Chemical Reaction of Polycrystalline Zinc with Sulphur Vapour.

Some preliminary experiments with the effect of S vapour on polycrystalline zinc led to the conclusion that the zinc had to be heated before ZnS could be formed. However if a zinc specimen was heated in the presence of S vapour with oxygen also present (10^{-3} mm. air pressure) ZnO was formed, since it apparently formed ZnO more readily than ZnS. If however the oxygen was removed from an enclosed volume (by firing some zinc to act as a getter), and the zinc specimen then heated (in this enclosed volume) to 200°C. for about five minutes the formation of zinc sulphide was observed.

Too rapid an attack by high concentration of S vapour gave rise to the face-centred cubic form of ZnS in random orientation on oriented zinc (Figure 56(a)). Only a small trace of S was required (a very small crystal was sublimed at the end of the tube) and under these conditions the parallel growth of the hexagonal form of ZnS on the polycrystalline zinc was observed.

Figure 56 shows the faint pattern of hexagonal ZnS in addition to the strong initial pattern of zinc in (112) orientation. The lattice constants of hexagonal ZnS are a = 3.811 Å., c = 6.234 Å. (Wyckoff, 1948) the fainter pattern corresponding to the structure; the 112 arc of ZnS in the plane of incidence (corresponding to the 112 arc of Zn) lying just outside the 102 radius of zinc while the three inner rings are the 100, 002 and 101 of ZnS, although the diffuseness of these rings makes it difficult to distinguish between the 100 and 002 rings. The weak intensity of the 002 diffraction in the zinc pattern indicates the prevalence of (001) faces in the zinc; so that the ZnS (hexagonal form) grows in parallel orientation on the (001) faces of the zinc.

A similar pattern showing the parallel growth of the hexagonal form of ZnS on polycrystalline zinc in (112) orientation was also obtained from another specimen treated in a similar manner.

3. Discussion.

The oxidation of metals has been studied extensively by electron diffraction but in a large number of cases the substrate has been randomly oriented or amorphous (i.e. polished metal surfaces). The oxide films in these cases are usually randomly oriented (except where the temperature of oxidation is high enough to cause recrystallisation). For instance, Smith

(1936) examined films of NiO on Ni, Cu_2O on Cu, and Fe_3O_4 on Fe (formed by heating the metals in air) but in no case was preferred orientation observed due to the amorphous nature of the highly polished surfaces. Bound and Richards (1939) examined the atmospheric oxidation of evaporated films of a number of alloys and metals but in no case was preferred orientation of the oxide observed due to the fact that the metals crystals themselves were randomly oriented. Miyake (1936), and Hickman (1948) investigated by electron diffraction (and by means of the electron microscope) the thermal oxidation of a large number of metals but in most of these cases the substrate was randomly oriented giving rise to randomly oriented oxide crystals except in those cases where the film, on thickening, recrystallised. While these experiments give useful information on the sizes and shapes of the crystallites, the structure of the oxide, and the mechanisms by which the crystallites grew, a better understanding of the substrate effects is obtained by studies of the relationships of the orientation of oxide films on <u>oriented</u> polycrystalline metal specimens and on known planes of metal single-crystals.

Burgers and van Amstel (1936) found that the oriented layers of polycrystalline barium films yielded on oxidation likewise oriented oxide layers, the orientation of the oxide being such that a direction of closest packing of the metal

atoms in the face-centred oxide lattice (i.e. [110] direction) was parallel to a corresponding direction in the body-centred metal lattice (i.e. a [111] direction). Nelson (1937) described the growth of the air-formed film of Fe_3O_4 on polycrystalline iron in (111) orientation, and suggested that the cubic face planes of the oxide and metal were parallel with the [110] in the (100) of the oxide parallel to the [100] in the (100) of the iron, this arrangement corresponding to a matching of the atomic positions in the cube face. It may be pointed out, however, that there was no evidence to show the existence of cube faces in the polycrystalline iron.

The conditions under which the growth of oriented zinc oxide on oriented polycrystalline zinc are described in the text the essential feature being a slow rate of reaction which facilitates oriented overgrowth and enables the thin oriented film of oxide to be observed since this initially oriented film gives way to randomly oriented layers of oxide as the oxide layer thickens. This is due to the fact that as the oxide film increases in thickness, the effects produced by the metallic substrate become less pronounced the outer surface of the oxide layer assuming a random orientation.

The parallel growth of hexagonal ZnO on polycrystalline zinc specimens with the (112) planes parallel to the surface is described, the ZnO growing on the exposed (001) and (101) faces of the zinc.

It was found that polycrystalline zinc specimens when exposed to S vapour in a vacuum of 10^{-3} mm. did not form ZnS (until the zinc was heated to about 200°C.; at this temperature and at this pressure it formed ZnO more readily than ZnS. Removal of the oxide however gave rise to a film of oriented ZnS (hexagonal modification) on polycrystalline zinc. The hexagonal ZnS grew on the exposed (001) faces of the zinc crystals in (112) orientation such that the lattices were parallel.

The hexagonal modification of zinc sulphide is usually only found in the mineral state (wurtzite) since it is unstable at low temperatures the transition point being 1020°C (Crenshaw 1913; Kruger, 1939). It is suggested that this hexagonal form is produced in the initial layers by the influence of the zinc (hexagonal) substrate since the zinc sulphide in thick layers was found to correspond to the cubic form of zinc sulphide in random orientation.

The mineral (wurtzite) is designated in thenomenclature of Ramsdell (1947) by 2H, wher H designates a hexagonal unit cell while the number states the total number of hexagonally closest-packed individual layers which are stacked within the length of the unit cell. Three other new polymorphs of ZnS have been observed in minerals by Frendel and Palache (1950) besides the cubic form (sphalerite). These are designated by wurtzite - 4H, wurtzite - 6H, and wurtzite - 15R.

4. Thermal oxidation of the etched cleavage face of a zinc single-crystal.

The freshly cleaved surface of a zinc single-crystal is covered by a very thin film of ZnO within a few seconds. This film was removed by a light etch in sulphuric acid (concentrated) The crystal was then washed in distilled water to remove any zinc sulphate and then dried in absolute alcohol. It was then transferred to a bath of propyl alcohol, care having been taken in the above processes to prevent the face being exposed to air. The crystal was then transferred to the camera, the propyl alcohol in virtue of its low vapour pressure protecting the surface until the pressure in the camera became too low for oxidation to take place.

Figure 57 shows the spot pattern obtained from an etched (0001) face of Zn with the beam along $[01\bar{1}0]$.

Figure 58 shows a pattern obtained from an etched cleavage heated in air at a pressure of 10^{-3} mm. Hg at 370°C. for half an hour. The pattern shows a hexagonal array of arcs corresponding to the complete (two-degree) (001) orientation of ZnO on the etched (001) cleavage face, the arced spots showing a slight disorientation. Superimposed on the spot pattern is the ring pattern of ZnO showing that some of the crystals were randomly oriented.

The effect of sulphur on the orientation of the oxide on the etched cleavage face of zinc. The oxide-free etched surface of a zinc single-crystal cleavage face (prepared in the manner described above) was placed in carbon disulphide for two minutes (since a longer time resulted in the formation of randomly-oriented face-centred cubic zinc sulphide). The pattern did not reveal oriented zinc sulphide but only zinc spots corresponding to the etched surfaces. However, Figure 59 shows the pattern obtained after oxidation at 370°C.; the rings are those of randomly oriented zinc oxide with a faint but well-defined spot in the plane of incidence on the 101 ring. In addition to this there are several orders of strong arced spots in the plane of incidence which do not correspond to the normal ZnO pattern. These are discussed later.

A zinc cleavage face with the initial film of oxide removed by a light etch was placed in warm benzene for 15 mins. The diffraction pattern revealed only traces of ZnO. On heating this surface in air for one hour at 370°C. a pattern was obtained (Figure 60) which shows (101) orientation in addition to the main (001) orientation of the ZnO on the (001) face of the zinc. The 101 arc can be seen outside the strong 002, and the 202 arc can be seen outside the strong 002, and should be compared with the pure (001) orientation of Figure 58.

An attempt to form oriented ZnS on the cleavage face of zinc by heating the crystal in the presence of S vapour was

unsuccessful since ZnO was formed instead. However, the pattern obtained (Figure 61) shows one-degree (201) orientation in addition to the (001) orientation. Thus the three innermost rings are the 100, 002, 101 of ZnO and there is an arc in the plane of incidence on the 002 ring; the next ring is the 102 then another group of three strong rings occur viz. 110, 103, and a third ring which is a closely-spaced ring group consisting of 3 rings (200, 112, 201). The position of the arc in the plane of incidence on the third ring suggests 201 orientation.

Polymorphic Zinc Oxide. Figure 59 shows several orders of arced spots in the plane of incidence; these spots were also observed in a pattern obtained from another cleavage face similarly tested. There are three possible explanations of these spots:- (1) they correspond to an abnormal ZnO structure, (2) they correspond to (103) orientation of an abnormal ZnS structure, (3) they do not arise from the presence of either ZnO or ZnS. The arc positions rule out (2) and it was not found possible to account for them by assuming the presence of some other substance (e.g. $ZnSO_4$). The radius of the second order spot in the plane of incidence is, within the accuracy of measurement of 1 in a 1,000, equal to the radius of the 003 ring of ZnO.

Since R_{00_3} (ZnO) = 3/2 x R_{00_2} (ZnO)

we have dx (2nd order) = 2/3 . d_{00_2} = c/3 (ZnO)

dx (1st order) = 2/3.c(ZnO) = 3rd order of 2c

i.e. 6th order of 4c.

It is therefore suggested that these spots may be due to a new polymorph of zinc oxide with a structure such that the basal dimensions remain the same, but the c of the polymorph being two thirds of the c of normal ZnO.

5. Discussion.

Wilman (1948), Acharya (1948), (cf. Finch, 1950), established that the relatively perfect (001) cleavage face of zinc became covered with an extremely thin, optically invisible layer of highly oriented zinc oxide crystals within a minute or so after cleavage (as had been previously observed by Finch and Quarrell, 1933). These results suggest that the thickness of the ZnO was only a few atoms over most of the surface, although the ZnO showed projections 20 A. high in some parts due presumably to the local preferential oxidation where the surface was rougher. No such oxide layers were detected by Acharya on antimony, bismuth or tin surfaces when freshly cleaved. His results on the thermal oxidation of zinc cleavage faces showed that the initial spontaneously-formed oxide layer remained almost unchanged even after 2 hours heating at 400°C., only after further heating for a long period of time did growth of unoriented zinc oxide crystals become appreciable. If, however, the zinc cleavage faces were exposed for a short time to mild attack by sulphur vapour, then they rapidly gave

rise at 400°C. to a layer of zinc oxide partly in (001) and partly in (101) orientation. Clear evidence of the increased rate of oxidation with roughness of the zinc surface was found by comparison of observations with the cleavage plane and with the much rougher (001) faces of the (102) twinned crystal. Acharya found that when the fresh cleavage face was treated with benzene no change in the pattern could be observed the pattern still showing the clear Kikuchi bands (because of the smooth surface) of the zinc and the spots of ZnO. However, on heating at 400°C. for ½ hour a ring pattern was obtained showing partly random orientation and partly preferential (001) and (101) orientation in addition to the strong pattern due to the initial (001) oriented ZnO. He suggested that traces of sulphur in the benzene must have attacked the cleavage face in the same manner as in the experiments with H_2S gas resulting in a very thin layer of zinc sulphide which, on heating in air, gave (101) orientation in addition to the (001) orientation of the oxide normally observed.

A technique for etching away the air-formed film of ZnO is described above and the parallel growth of (001) - oriented ZnO also on the cleavage face roughened by etching is demonstrated. The initial film of oxide was removed and the cleavage face treated with benzene known to contain a trace of thiophene; on subsequent oxidation the pattern revealed (101)

and (001) orientation of the oxide although no intermediate pattern of ZnS was observed. Traces of (101) orientation were also found in the oxide pattern when the etched cleavage had been treated with carbon disulphide prior to oxidation.

These results confirm, to some extent, the contention that traces of S (either in the benzene, or from H_2S gas or from the CS_2) modify in some manner the subsequent formation of the oxide on the cleavage face of zinc, although the manner in which this takes place is not yet evident. It is suggested that some such mechanism might account for the traces of (201) orientation observed when a cleavage face was heated in partial vacuum in the presence of sulphur vapour.

In the course of these experiments arced spots were observed in the plane of incidence in the patterns of the oxide on more than one occasion. It is suggested that they may be due to a new polymorph of ZnO with the same basal dimensions as the normal oxide lattice but with c equal to 2/3 of the c of normal ZnO.

It is interesting to note that the new polymorphs of zinc sulphide viz. wurtzite-4H, wurtzite-6H and wurtzite-15R (Frondel and Palache, 1950) when heated in air at 800°C. for 16 hours were found by X-ray study to be converted in every instance to the ordinary form of ZnO (Previtt, Hopkins and Frondel, 1950). ZnO has a wurtzite type structure (2H) based

on hexagonal close-packing of the oxygen atoms; thus it was thought possible that higher polymorphs of ZnO would be derived from the corresponding ZnS forms, but this did not prove to be the case.

6. The oxidation of a zinc-blende cleavage face.

In view of the interesting nature of the reaction between heated zinc-blende crystals and oxygen, and in view of the discrepancies in some of the earlier results of Aminoff and Broome (see Part IV (7)), crystals of zinc-blende having fresh cleavage faces, (110), were heated in a furnace at 650°C. The oxidation of zinc-blende at a lower temperature range is described in Part V.

It was found that crystals cleaved from a block of sphalerite reddish brown in colour shattered to pieces on heating due, undoubtedly, to imperfections in structure (the reddish brown colour is probably due to the presence of iron). However cleaved portions of a pale yellow crystal did not shatter on heating and Figure 63 shows the pattern obtained from such a cleavage face, after oxidation at 650°C. for 1/4 hour, resulting in a thick oxide film showing interference colours. The electron beam was along the cube-edge azimuth in the (110) face of the ZnS. Figure 62 shows the pattern obtained with the electron beam along the cube face diagonal of the ZnS. Both patterns show elongation of the spots towards

the shadow edge indicating the smooth nature of the surface. Both patterns show a strong arc in the plane of incidence which is found by measurement to be the 103 arc of ZnO. Figure 62 with the beam along the cube-face diagonal of the ZnS shows rows of closely spaced spots at a measured angle of 58.4° with the shadow edge i.e. at an angle of 31°36' with the plane of incidence. The spot spacing along these rows corresponds to the c of ZnO.

Now let the angle between the normal to the (103) plane of ZnO and the c axis be ϕ. Then in the customary notation

$$\underline{r}^*_{103} = \underline{a}^* + 3\underline{c}^*$$

i.e. $$\underline{c}.\underline{r}^*_{103} = \underline{c}.\underline{a}^* + 3\underline{c}.\underline{c}^* = 3$$

Now $$\cos\phi = \frac{\underline{c}.\underline{r}^*}{cr^*} = \frac{\underline{c}.\underline{r}^* d_{103}}{c}$$

Substituting we have $\cos\phi = 3/c\ d_{103}$

Substituting the lattice constants of ZnO into the expression

$$\frac{1}{d^2_{103}} = \frac{4}{3a^2} + \frac{9}{c^2}$$

for hexagonal structures we get $d_{103} = 1.474$ Å., so that $\phi = 31°39'$. The observed value of 31°36' is in excellent agreement with this, so that it is concluded that the ZnO is in (1013) orientation on the (110) cleavage face of the ZnS.

Etched cleavage face. A cleavage face was etched in hot dilute nitric acid (nitric acid S.G. 1.420: water = 1:3) for two minutes, and then washed in distilled water. The diffraction patterns obtained were the customary patterns of sharp diffraction spots due to the roughened etched surface. When this specimen was heated in air at 570°C. for 1 hour a pattern of arcs corresponding to ZnO was observed in addition to the spot pattern of the initial (110) ZnS face (Figure 64 and Figure 65 with the beam along cube edge and the cube face diagonal respectively).

(103) orientation of ZnO can be seen to be present but in addition to this it can be seen from Figure 65 that some of the arced spots lie on row lines making angles of 55° and 125° with the shadow edge. The spacing along these rows corresponds to the (001) spacing of ZnO. The angle between a (111) face and the (110) face of ZnS is 35° so that the above arcs (Figure 65 with the beam along the [110]) are evidently due to the (001) orientation of ZnO on the (111) faces of ZnS produced by etching.

7. Discussion.

Aminoff and Broomé (1936) oxidised the natural (111) and (110) cleavage faces of sphalerite (ZnS) by heating the crystals in air. They found that the ZnO formed was so oriented that the c axis was perpendicular to the octahedr on face

(i.e. the (111)) and the 'a' edge parallel to the [110] octahedron edge. They point out that the c axis should make an angle of 35°16' with the normal to (110) plane of ZnS i.e. 54°44' with the [001]. However in 1938 they stated that the c axis of ZnO formed on the (110) face made an angle of 57°36' ± 1° with the [001] of ZnS; while the c axis of the ZnO formed on the (111) face made an angle of 54°44' with the [001] ZnS corresponding to (001) orientation of the oxide, and the c axis of the ZnO on the (001) face made an angle of 51°36' with the [001] ZnS, corresponding to (203) orientation of the oxide. There seems to be considerable discrepancy between these two sets of results (1936 and 1938) on the (110) cleavage face.

Yamaguti (1935) studied the oxidation of zinc blende and found that the oxidation product (ZnO) was in complete orientation such that the (103) planes of ZnO were parallel to the cleaved (110) surface of ZnS and moreover the [010] axis of the ZnO was parallel to the [110] of the ZnS.

Now the calculated angle between the c axis and the (103) plane of ZnO is found to be 58°24' so that the (103) orientation observed by Yamaguti is in agreement with the 1938 results of Aminoff and Broome. Seifert (1940) from the theoretical consideration of these results concludes that they do in actual fact correspond to (103) orientation of ZnO on the (110) ZnS and not to ZnO tetrahedra parallel to those of ZnS. He points

out that there is a 16% difference in lattice dimensions in the "a" direction of the ZnO and the ZnS at the interface. He also concludes that there would be a better fit with the (405) planes parallel to the (001) planes of ZnS than in the experimentally observed (203) orientation on the (001) face, pointing out that the reason for this observed orientation was not clear.

The (103) orientation of ZnO on the (110) face of ZnS has since been observed by Uyeda, Takagi and Hagihara (1941) and is confirmed by the results of the author (Figures 62 and 63)

Uyeda, Takagi and Hagihara (1941) investigated the oxide formation on the $\{111\}$, $\{\bar{1}\bar{1}\bar{1}\}$, $\{110\}$ and $\{100\}$ faces in the natural and etched states and also on the cleaved $\{110\}$ surfaces. From the results of these investigations they concluded that the orientation of zinc oxide crystals on the minute etch faces of zinc blende is determined by the following rules:-

1. The c axis of ZnO is almost parallel to one of the four [111] axes of the ZnS which makes the smallest angle with the surface normal.

2. An a xis of the ZnO is exactly parallel to a [110] axis of ZnS.

3. A simple net plane of the zinc oxide is parallel to the underlying zinc blende surface which may also be a simple net plane. It was also concluded that (4) A zinc oxide grows more readily when the corresponding $\langle 111 \rangle$ axis of ZnS is directed

outward from the surface than it would if directed inwards. The results obtained by Aminoff and Broome (1938) can be seen to conform with the first three rules.

Now it is well known that an etched surface is not always parallel to the apparent surface in microscopic dimensions. Uyeda, Takagi and Hagihara found that with hydrochloric acid etching the minute faces formed corresponded to a negative triakis tetrahedron, most of the faces making angles with the negative tetrahedral faces (111). The polyhedron which corresponded to nitric acid etching was a combination of positive and negative triakis tetrahedron. It was found that in this case the minute (001) faces were quite predominant on the apparent (001) surface.

The author etched the (110) cleavage face of ZnS with nitric acid and then oxidised the face by heating it in air. The resulting patterns showed the (001) orientation of ZnO on the (111) faces of the ZnS produced by the etching process in addition to the (103) orientation on the remaining (110) portions of the surface.

It is not quite clear from the account of Uyeda, Takagi and Hagihara whether or not they observed this, since as has been pointed out they found the faces corresponded to triakis tetrahedra after nitric acid etching in which the faces are <u>not quite</u> (111) faces. However they seem to contradict this

by saying that with the (110) surface etched by nitric acid the c axis of the ZnO was exactly parallel to the [111] axis of ZnS, in which case they must have observed (001) orientation of the ZnO on the (111) planes of ZnS.

However, the author's results make it clear that (111) faces are produced by nitric acid etching, the etching process being probably faster than in the experiments of Uyeda, Takagi and Hagihara; the zinc oxide then grows on these minute (111) faces in 001 orientation.

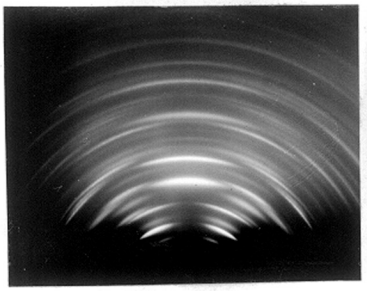

Fig. 54.

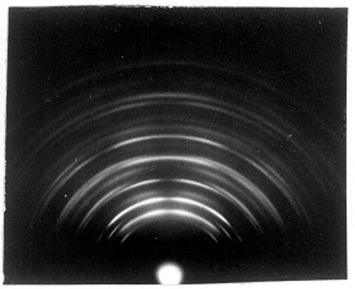

Fig. 55.

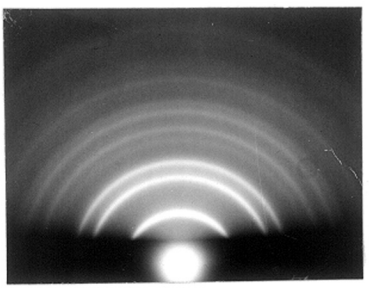

Fig. 56a.

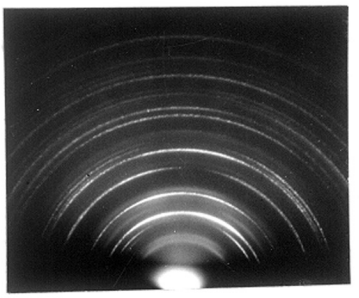

Fig. 56.

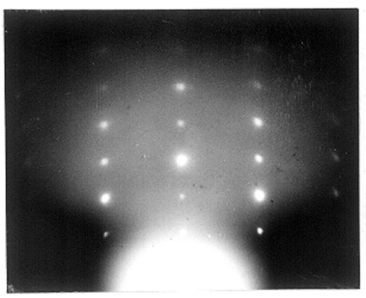

Fig. 57.

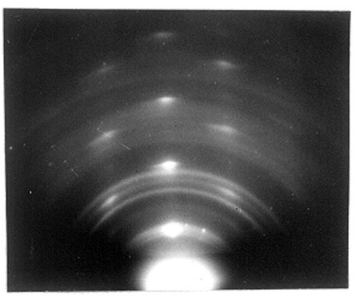

Fig. 58.

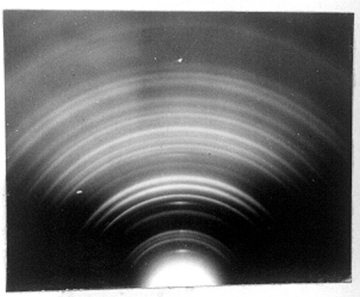

Fig. 59.

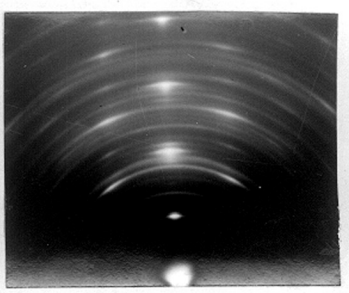

Fig. 60.

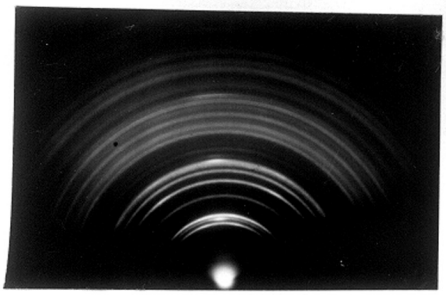

Fig. 61.

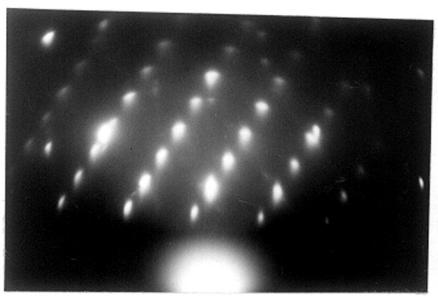

Fig. 62.

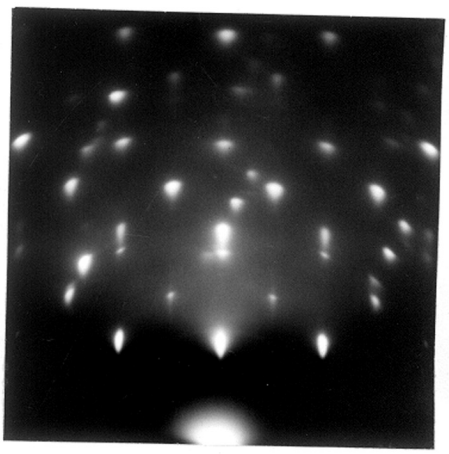

Fig. 63.

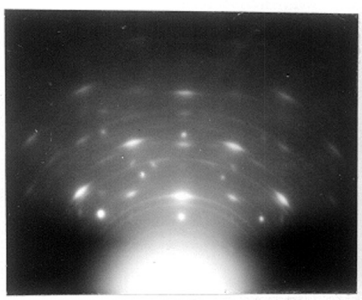

Fig. 64.

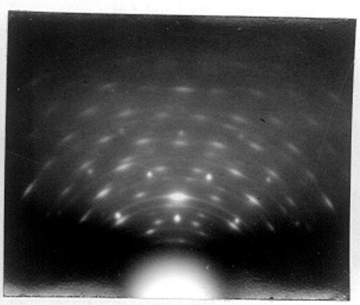

Fig. 65.

PART 5.

EPITAXIAL STRAIN AND DISORIENTATION IN CRYSTALS GROWING ON SINGLE CRYSTAL SUBSTRATES.

1. The Oxidation of Zinc Blende.

A diffraction pattern from a fresh cleavage face of a transparent pale yellow zinc blende crystal showed the high perfection and atomically smooth nature of the surface. The crystal was then raised from room temperature to approximately 520°C. in air during 45 minutes and kept at this temperature for 30 minutes. It was then allowed to cool for about 10 minutes before removal and transference to the camera.

Figure 66 shows the pattern obtained from this surface with the electron beam along the cube-face diagonal of the ZnS substrate while in Figure 67 the beam is parallel to the cube-edge. There is a pronounced arcing (6°) shown in Figure 66 while there is no appreciable arcing shown in Figure 67. This clearly shows that there is a rotation about an axis parallel to the cube face diagonal of the {110} ZnS surface. Apart from this arcing the diffraction patterns confirm the {103} ZnO orientation described previously in Part 4.

The ZnO layer was removed by immersing the crystal in dilute nitric acid (HNO_3, S.G. 1.42 : H_2O = 1:3) for about

60 seconds. Figures 68 and 69 show the resulting patterns with the beam along the cube-edge and cube-face diagonal of the ZnS respectively. These sharp spot patterns show that after removing the ZnO-ZnS surface layer, the zinc blende substrate was still undistorted at a short distance below the interface.

2. The abrasion of a {110} ZnS cleavage face along the cube-edge

It has been pointed out (Wilman, 1950) that directed disorientations, apparently of rotational-slip type, are caused when single crystals are abraded in suitable directions, and this was tested in the case of zinc blende in connection with the above results. The abrasion was carried out by applying a light pressure ($\sim$100 grams) by hand to the crystal against the outer parts of a flat rotating disc covered with No.0000 emery paper. The disc was 20 cm. in diameter, and rotated at a speed of about 300 revs./min. although this was reduced by the friction of the crystal on it. The abraded surface was traversed by fine scratches parallel to the direction of abrasion.

This abraded surface, after washing in distilled water, gave at first diffraction patterns consisting only of general scattering. When the crystal was immersed in dilute nitric acid for about 10 seconds and then washed in distilled water a pattern showing faint rings corresponding to randomly oriented

ZnS crystals was obtained.

The specimen was then etched for 15 seconds in hot nitric acid (1:2) and washed in distilled water. Figures 70 and 71 show the resulting patterns with the electron beam along the cube face diagonal and cube-edge respectively. Figure 70 corresponds to the normal pattern in this azimuth except that it consists of long arcs and is displaced as a whole by a 30° rotation about the undeflected beam. This rotation is to the right in Figure 70. This corresponds to a 30° rotation of the lattice about the cube-face diagonal which was normal to the direction of abrasion. Figure 71, with the beam along the abrasion direction shows the normal pattern (though arced) with additional arcs lying on layer lines normal to the shadow edge, showing that the rotation axis was then in the surface and normal to the beam.

The specimen was etched again in hot nitric acid of the same strength as before for 10 secs. Figure 72, with the electron beam along the cube-face diagonal, shows the normal pattern (but arced) rotated by 10° about the undeflected beam. Figure 73, with the electron beam parallel to the abrasion direction, shows the normal pattern in this azimuth with additional sharper spots on vertical layer lines.

Figure 74 shows the pattern obtained with the beam along the cube-face diagonal after the surface had been etched for a further 10 secs., showing now only 4° lattice rotation

about the cube-face diagonal. The pattern with the beam along the cube-edge direction is shown in Figure 75.

A further etch for 15 secs. gave rise (with the beam along the cube-face diagonal) to the normal pattern unrotated as a whole but with the spots spread out into short tadpole-shaped arcs extending up to 4° from the normal spot positions (Figure 76). Figure 77 shows the corresponding pattern with the beam along the cube-edge azimuth.

3. Discussion.

The oxidation of a fresh cleavage face of zinc blende at 520°C. is described. Apart from the pronounced arcing (6°) shown in Figure 66, apparently not observed previously, the diffraction patterns confirm the {103} ZnO orientation indicated by the experiments of Yamaguti (1935), Aminoff and Broome (1936, 1938), Uyeda, Takagi and Hagihara (1941) (see also Seifert, 1940). The patterns from the crystal before oxidation showed the high perfection and atomically smooth cleavage surface of the crystal. After etching away the ZnO-ZnS surface layer with nitric acid the sharp spot patterns obtained showed the ZnS substrate to be still undistorted at a short distance below the interface.

Wilman (1950) demonstrated the common occurrence of rotational slip as a new kind of deformation process in crystals. The above results (Figures 66 and 67) are explained satisfactorily

(Evans and Wilman, 1950) as being due to this kind of deformation caused by the epitaxial stress between the substrate and overgrowth crystals, due to their different lattice constants at the interface. Thus the strong arcing in Figure 66, but the inappreciable arcing in Figure 67, shows clearly that the lattice disorientation is, in this case, simply a rotation about an axis parallel to the cube-face diagonal of the $\{110\}$ ZnS surface. This could therefore correspond to rotational slip of the $\{103\}$ orientated ZnO crystals, or of parts of the ZnS substrate, on the planes which are normal to this rotation axis i.e. $\{11\bar{2}0\}$ in the ZnO (since $\langle 100\rangle$ ZnO is parallel to $\langle 1\bar{1}07$ ZnS) or $\{1\bar{1}0\}$ in the ZnS. In the ZnS at least this plane is a direction of especially perfect cleavage, and thus according to the results obtained by Wilman (1950) should be a direction of easy rotational slip, and it should thus be similarly easy on the corresponding $\{11\bar{2}0\}$ planes of the ZnO which has a structure differing from that of the zinc blende only in the hexagonal type of superposition of its (0001) layers. This constitutes the first clear example of rotational slip caused by epitaxial stresses.

The fact that none of the previous workers (Yamaguti etc. had observed the arcing of the ZnO pattern can be attributed to the effect of a higher temperature of oxidation (red heat) which they used. Support of this view is provided by the author's

observation that no arcing of the ZnO pattern was observed when a ZnS crystal was heated in air at 670°C. (as described in Part 4). The higher temperature favours recrystallisation whereas at the lower temperature (as the patterns show) the crystals attained a moderate size before slip took place.

Other examples of rotational slip caused by epitaxial stresses have since been observed by several workers in this laboratory. Goswami (1950) observed rotational slip on the {110} planes of cadmium deposited electrolytically on the {110} face of copper, while Gharpurey (1950) has observed rotational slip on the cube-faces of (110)-orientated silver deposited from the vapour on to a (001) rock salt cleavage face.

In order to present a possible picture of a way in which rotational slip arises, consider Figure 78a. ABCD and A'B'C'D' represent the corners of neighbouring rotational-slip lamellae as part of a ZnO overgrowth crystal before the stress is relieved by its subdivision. Suppose the part near CD adjoining the substrate is held under tension (or compression) parallel to CD owing to the atomic forces of the substrate on the overgrowth crystal. Farther from the substrate, i.e. along AB, the lattice dimensions must tend to their normal values. It thus seems possible that relief of the tension (or compressio near CD, by a slip at the overgrowth-substrate interface, may occur unevenly over the contact surface, so that, for example,

the lamellae ABCD may remain held near C and contract (or expand) from D towards C, while A'B'C'D' may be held near D' and contract (or expand) in the direction C'D'. This motion, oppositely directed in the two parts of the crystal, may thus result in a relative rotational slip which in general will not be fully reversed as the interface slip proceeds, thus there will be left both a residual rotational-slip deformation and a residual but reduced strain near the interface (Figure 78b).

The nearly uniform intensity along the arcs in Figure 66 suggests that, in actual fact, a fine lamellar sub-division of the ZnO crystals occurred, initiated by a sudden release along one lamellar region and thereby passing on rotational motion to neighbouring regions as in normal rotational slip, but also triggering their potential release at the interface region.

In order to test the possibility of rotational slip on the above planes in the ZnO and ZnS structures, experiments were made on the effect of abrasion of zinc blende cleavage faces. No ZnO crystals were available large enough for such experiments but the similarity of structure of the ZnS and the ZnO allows the results to be considered applicable also to the ZnO. Abrasion of a zinc blende $\{110\}$ cleavage face parallel to the cube edge in the surface resulted in a surface which yielded at first only ZnS rings in the electron diffraction

pattern. After this surface was etched in nitric acid the pattern consisted of arcs and showed a mean lattice rotation of 30° about the cube-face diagonal which was normal to the direction of abrasion.

This result is similar to that of Raether (1947) with NaCl, though Raether followed Germer's (1936) interpretation of the rotation, which entirely neglected the possibility of lateral cohesion between the rotated cleavage blocks on their common faces normal to the rotation axis. At the perpendicular azimuth (i.e. along the abrasion direction) the normal pattern was obtained though arced, with additional arcs lying on layer lines normal to the shadow edge, showing that the rotation axis was then in the surface and normal to the beam.

After further stages of etching, similar patterns were obtained but showing the reduced range of the lattice rotation at the increased depth below the original surface, until after a final etch the pattern was mainly the normal pattern unrotated as a whole but with short tadpole-shaped arcs extending from the normal spot positions. It was thereby confirmed that rotational slip occurred easily on the $\{110\}$ planes normal to the surface of the zinc blende, and by inference also on the corresponding $\{11\bar{2}0\}$ planes of the ZnO.

In zinc blende the translational slip has been said to occur on $\{111\}$, probably along $\langle 112 \rangle$, and if this is

accepted the above lattice rotation could equally be due to flexural translational slip. Similarly the rotation observed by Raether (1947) in NaCl could also be explained as being due to such slip along $\langle 1\bar{1}0 \rangle$ in the $\{110\}$ planes inclined upwards and forwards along the abrasion direction. In PbS (Germer, 1936; Beukers, 1939) slip is on $\{001\}$ alone and this interpretation can therefore explain the observed rotation.

In order to make a more critical test of whether flexural slip or rotational slip is the primary process accounting for such large lattice rotations the anodically polished 110 surface of a copper crystal was abraded along particular directions and the results are described in Part 6.

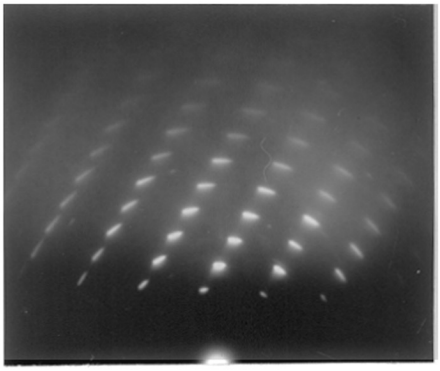

Fig. 66.

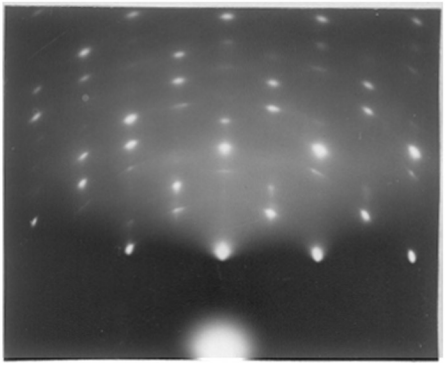

Fig. 67.

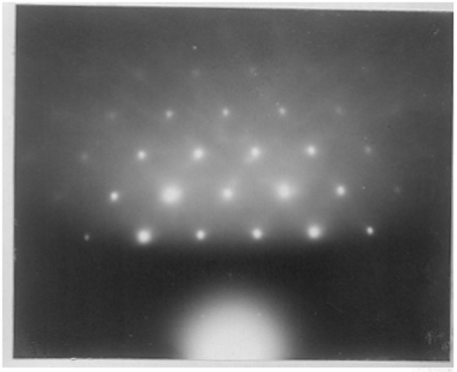

Fig. 69.

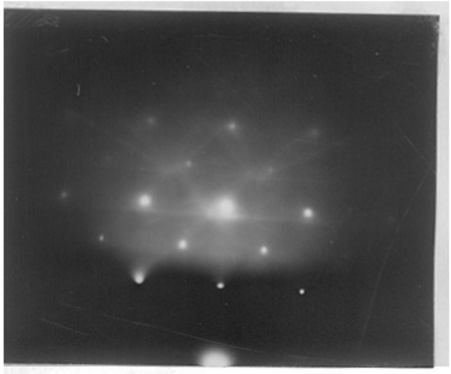

Fig. 68

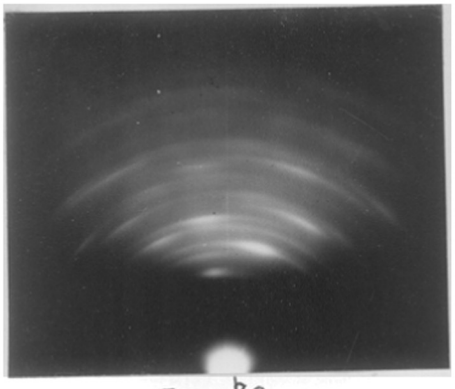

Fig. 70.

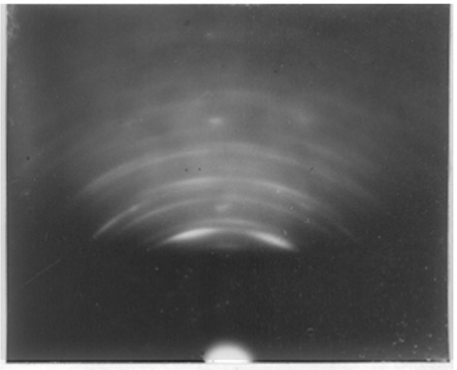

Fig. 71.

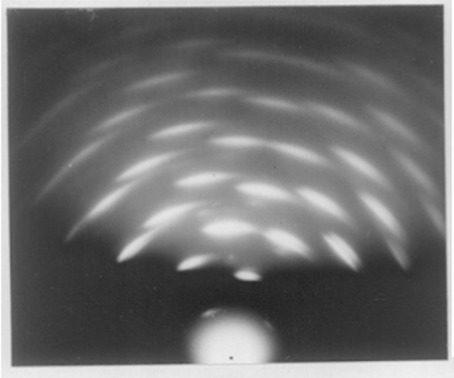

Fig. 72.

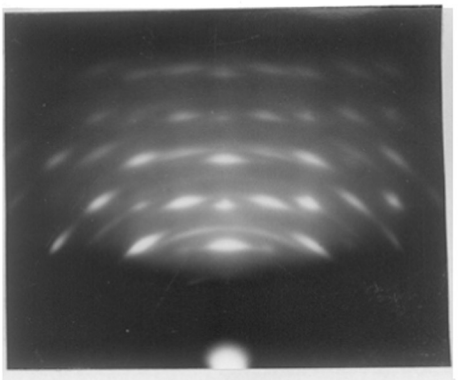

Fig. 73.

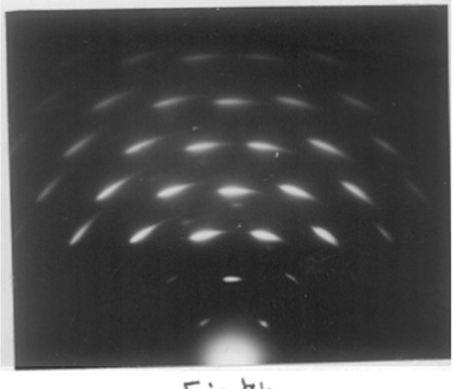

Fig. 74.

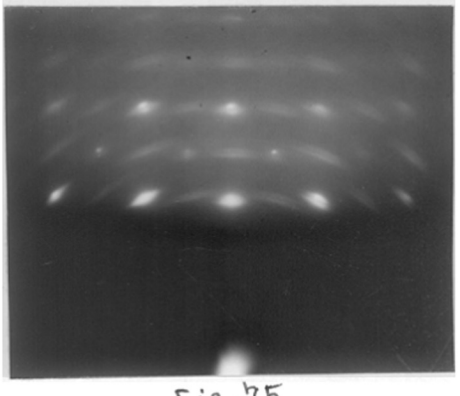

Fig. 75.

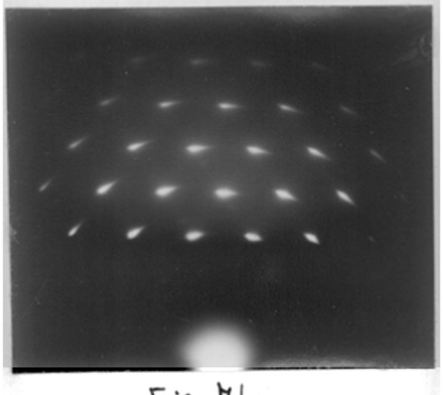

Fig. 76.

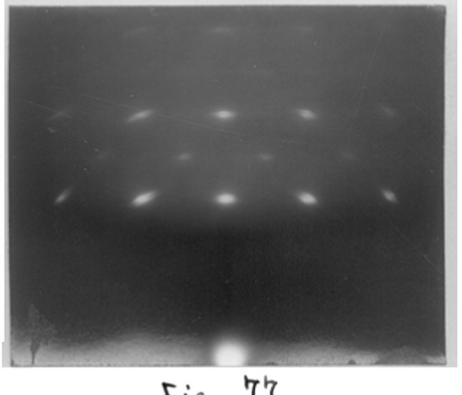

Fig. 77.

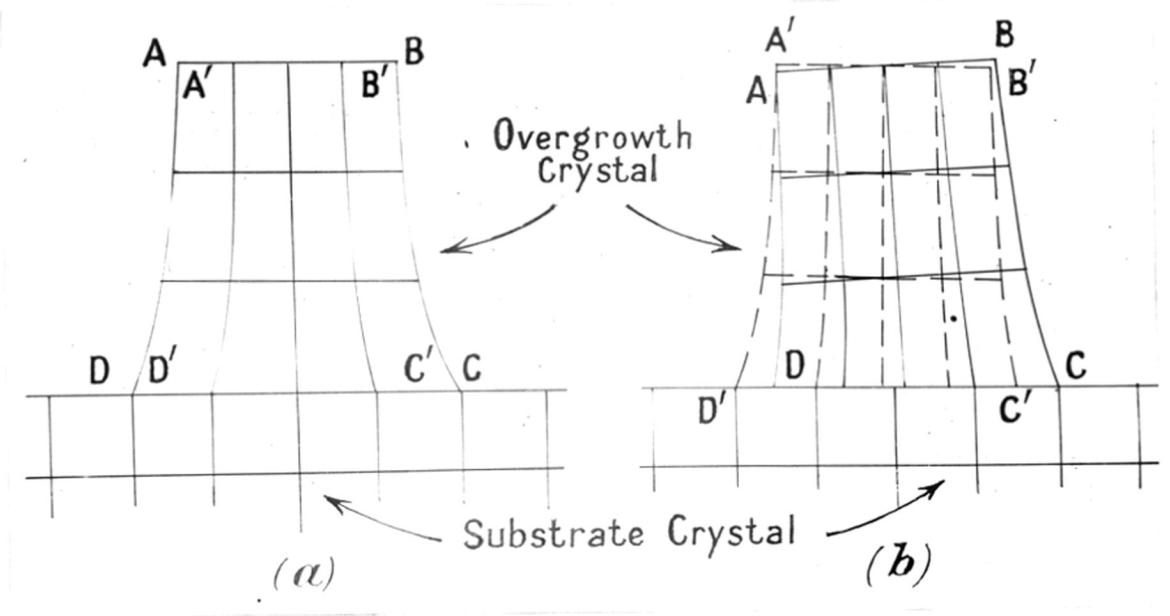

Fig. 78.

PART 6.

THE DEFORMATION OF A COPPER CRYSTAL BY UNIDIRECTIONAL ABRASION.

1. Experimental Details.

A section about 1 cm. long was sawn off carefully from a single-crystal cylindrical rod of copper of diameter about 1 cm. A fine-toothed saw was used, care being taken to avoid undue stress in clamping and sawing the crystal. The crystal had been grown by slow cooling from the melt in hydrogen.

The crystal was smoothed on emery paper and polished anodically in a bath of one part of orthophosphoric acid (S.G. 1.75) to one of distilled water. It was then washed in distilled water, dilute phosphoric acid, distilled water and finally in 5% KCN solution to remove traces of oxide before a last rinse in water followed by acetone. It was immediately immersed in propyl alcohol to prevent contamination and then transferred to the diffraction camera. Patterns were recorded from this surface, with a specimen-plate distance about 23 cm., which defined the crystal orientation relative to the surface. The surface was then adjusted to a $\{110\}$ plane to within about 2° by further abrasion on a sequence of grades of emery cloth and paper down to No.0000. A final anodic polish removed the mechanically distorted surface layers and smoothed the surface

still further.

Figure 79 was obtained from this surface with the electron beam parallel to the cube-edge. The sharpness of the Kikuchi-line patterns shows the high perfection of the crystal, while the very limited spot pattern (except at particular azimuths as in Figure 79) shows that the surface was highly smooth on an atomic scale.

The copper crystal was abraded in a manner similar to that with the zinc blende crystal, the copper crystal being transferred to an adjacent new part of the emery paper when the abrasion track began to show removal of copper. The total period of abrasion was about 30 secs. carried out in intermittent stages of about 10 secs. each. Abrasion along the cube-face diagonal in the copper surface was done on 0000 emery. Along the cube-edge and the $\langle \bar{1}12 \rangle$ direction there seemed to be a higher resistance to abrasion so that a coarser grade was used initially (Grade 3 followed by 0), before a final light abrasion with 0000 paper.

The abraded surfaces, as observed visually, were traversed relatively uniformly by fine scratches parallel to the direction of abrasion; and after 10 seconds immersion in 2% KCN in water to remove oxide, they yielded electron diffraction patterns consisting only of diffuse scattering, apparently due to the coarse roughness of the surface. All the abraded surfaces

were examined at a camera length of 47 cms. and the patterns were recorded at the main azimuths after the crystal had been etched away to various depths below the initial surface, so as to reveal the nature and extent of the lattice deformation caused by the abrasion. It was found that the above degree of abrasion caused a surface disorientation which decreased with increasing depth below the surface, until at a depth of the order of 10μ the single crystal was scarcely perceptibly distorted.

For brevity the electron beam direction in the following descriptions will be designated as in azimuth "A" when its plane of incidence is along the abrasion direction and "B" when it is at right angles to this in the surface, irrespective of the directions of these relative to the crystal lattice.

2. Abrasion on $\{110\}$ along $\langle 1\bar{1}0\rangle$

The surface which initially gave Figure 79 was abraded as above with 0000 emery along the $\langle 1\bar{1}0\rangle$ direction. The abraded surface gave at first electron diffraction patterns consisting of only general scattering. After etching during 1 minute in 5% KCN (followed by the usual rinse in water, acetone and propyl alcohol) ring patterns were obtained at all azimuths, but the rings were strengthened in certain regions. With the beam in azimuth A the pattern, Figure 81, was symmetrical about the plane of incidence, on which lay the

centres of the strengthened 200 and 400 arcs. This indicated that many of the crystal fragments were then orientated with their cube faces roughly parallel to the surface. Figure 80 at azimuth B is asymmetrical, however, with the strongest part of the 200 and 400 rings lying on a radius 10° from the plane of incidence, instead of 45° as they would have been if from the original crystal. Thus most of the crystal fragments were rotated by 35° about an axis normal to the abrasion direction, from the orinetation of the initial crystal, though the length of these asymmetric arcs, especially the 200 arc, shows that some of the fragments had been rotated by up to 90° or more from the initial orientation. Further etching for 45 seconds in 5% KCN gave no change in the diffraction pattern, nor did 5 minutes more in 10% KCN.

After a deeper etch with nitric acid (one part of HNO_3 of spec.grav. 1.42 to two of water) Figures 82 and 83 were obtained in the azimuths B and A respectively. The now clear and separate arcs are still in the same positions as the strengthened parts of the rings in Figures 80 and 81, showing still more clearly that at this order of depth below the initial surface the deformation consisted mainly of rotation (35° to 90°) of the lattice fragments about an axis in the surface and normal to the abrasion direction. The arcing (subtending about 35° to 90°) in the symmetrical pattern Figure 83, and the presence of diffractions such as those of 311

type in Figure 82 show, however, that there was a variation of lattice orientation from the initial orientation within a range of $\pm$ 15° about an axis in the A azimuth.

Figures 84 and 85 were obtained after a few seconds further etching in the nitric acid solution, and correspond to the underlying single-crystal which had remained undistorted.

The crystal was etched further still, resmoothed by electropolishing, and again abraded with 0000 emery along $\langle 1\bar{1}0 \rangle$ as before. In this case the nitric acid etch led to clear electron diffraction patterns, Figures 86 and 87, showing a large proportion of practically undisturbed copper crystal with also many fragments rotated by up to 35° about the B azimuth direction. There was displacement of up to about the A azimuth axis, as shown by faint arcs of hkl type ($1 \neq 0$) in Figure 86 and by the arcing of the diffractions which appeared on the vertical "layer lines" in Figure 87 corresponding to the main rotation about the B direction concluded from Figure 86.

3. Abrasion on $\{110\}$ along $\langle 001 \rangle$.

When the crystal had been re-surfaces by electrolytic polishing so as to give electron diffraction patterns characteristic of only the undisturbed crystal, it was abraded with 0000 emery along $\langle 001 \rangle$ and again examined after light then deeper etching. Several such trials were unsuccessful in showing any well-marked stages intermediate between the initial stage

which gave general scattering and that giving practically single-crystal spot patterns. A coarser grade of emery was therefore used (3, then 0 and 0000) with the aim of exerting a greater tangential force on the freshly electropolished copper crystal, whose surface had now become about 10° incline away from the {110} plane.

Removal of the surface layers was tried by electropolishing with the hope of securing greater control on the amount removed. Two minutes such treatment followed by the usual removal of any oxide present by 5% KCN led to Figures 88 and 89 being obtained in the (new) B and A azimuths. Figure 88 shows a diffuse spot pattern due to the slight displacement (round the corresponding powder-pattern ring position) of the normal spots, which are elongated owing to refraction at the smooth but undulating surface. The sharp arcs represent the same (but sharper) spot pattern displaced by a mean rotation of 12° about the beam, thus parts of the crystal had rotated about an axis parallel to the surface or nearly so, in the B azimuth direction i.e. normal to the abrasion direction. These arcs tail off in intensity towards higher angular deviations, showing that some parts of the crystal had rotated by up to 25° from the initial orientation. Figure 89 at azimuth A shows the main diffuse spot pattern (elongated normal to the shadow edge due to reflection at the smooth surface) corresponding to the initial crystal orientation and in addition

there are a set of sharper arcs whose centres lie on the nearly vertical spot rows. The "layer lines" which correspond to the lattice rotation indicated by Figure 88 thus show that the rotation axis was not in the surface but was normal to the $\{1\bar{1}0\}$ planes which were parallel to the abrasion direction and were at 80° to the surface.

4. Abrasion on $\{110\}$ along $\langle \bar{1}12 \rangle$.

The crystal surface, after extensive initial electropolishing, was abraded along the $\langle \bar{1}12 \rangle$ direction by 3,0 and 0000 emery, and after removal of the surface layers by two minutes electropolishing yielded Figures 90 and 91 in the B and A azimuths respectively.

Figure 90 shows a hexagonal disposition of arcs swept out by a 12° rotation (about the undeflected-beam spot) of the spot pattern which was yielded initially by the crystal surface. Here the electron beam was normal to a set of $\{1\bar{1}1\}$ planes which were nearly normal to the surface and parallel to the abrasion direction. Thus in Figure 90 the 220 spot is nearly vertically above the undeflected spot and other diffractions of the same type lie on radii 60° to left and right of this. A neighbouring part of the surface yielded a similar strong hexagon pattern of arcs but these subtended about 25° at the central spot. In Figure 91 the pattern of strong arcs in a

centred $\sqrt{2}$-rectangle pattern corresponds to a mean crystal orientation having a $\{110\}$ plane normal to the beam, this orientation being derived from that of the initial crystal by a rotation of the order of 20° about the cube diagonal which was normal to the abrasion direction. There are also in Figure 91 some rows of spots or quite short arcs corresponding to the initial crystal orientation, in which the surface was about 10° inclinéd from the $\{110\}$ plane, about the $\langle 1\bar{1}0\rangle$ axis.

Thus Figures 90 and 91 together show that abrasion parallel to a set of $\{1\bar{1}1\}$ planes which were inclined at 80° to the surface, resulted in a rotation (up to 25° or more) of the lattice in the surface regions, about the normal to this set of $\{1\bar{1}1\}$ planes.

5. Abrasion on $\{110\}$ along a direction at 55° to cube edge.

Attempts were made to investigate the effect of abrading the copper face which was roughly $\{110\}$ along a direction which was midway between $\{1\bar{1}0\}$ and $\{1\bar{1}1\}$ planes disposed nearly normal to the surface. However, no clear transition stages between the orientation of the underlying single crystal and the practically randomly disoriented surface layer were observed.

6. Discussion.

The above experiments establish that abrasion of an approximately {110} copper crystal surface causes an extensive lattice rotation in the surface regions of the crystal, often up to 25° and sometimes 90° or more, about a well-defined axis which is normalmto the {001}, {1$\bar{1}$0} or {1$\bar{1}$1}planes, whichever of these planes is approximately normal to the surface and parallel to the abrasion direction. We must now consider how these results can be interpreted.

In all the face-centred-cubic metals, including copper, the translational slip at room temperature has been found by many observers to be only on {111} along ⟨1$\bar{1}$0⟩ , though in aluminium at 450° Boas and Schmid (1931) found slip to be on {001} along {1$\bar{1}$0} . Since in elongation, compression or flexure (including "kinking" - cf. Mugge, 1898, Orowan, 1942) a lattice rotation occurs about an axis in the slip plane and normal to the translational slip direction, then if slip were on {111} along ⟨1$\bar{1}$0⟩ none of these processes can account for any of the above three results obtained from copper while if slip occurred on {001} along ⟨1$\bar{1}$0⟩ this could only account for the one case of rotation about ⟨110⟩. Twist slip (Mugge, 1898, Johnsen, 1914, Buerger, 1930) about the translational-slip direction could also only be a possible explanation of this one case of the three observed. Multiple glide combinations appear

also to be unlikely to lead to the observed direction, thus to explain these by translational slip new and hitherto unobserved directions of slip have to be postulated.

It was concluded that such abrasion results on the above are due to rotational slip occurring on densely-populated atomic planes which are more or less parallel to the abrasion direction and normal or steeply inclined to the surface. Moreover, the possibilities of rotational slip on the here observed $\{001\}$, $\{1\bar{1}0\}$ and $\{1\bar{1}1\}$ planes is fully supported by the direct microscopic observations of such rotated laminae in the case of the "deformation bands" which have been studied in detail by Barrett (1938, 1940, 1943, see also 1947). Barrett and Levenson (1939, 1940) and Barrett and Steadman (1942) and which appear to be parallel rotational-slip lamellae (displaced azimuthally on their common interfaces) in their initial stages (Wilman, 1950a,b). In aluminium the lamellae were parallel to the $\{001\}$ planes (in Cu also) and sometimes to $\{110\}$, and in iron they were parallel to $\{001\}$ (which is the fracture plane) or sometimes $\{111\}$; thus in none of these cases were they parallel to the normal translational slip planes (which are indeed not shown up by etching) nor the reported twin planes which are $\{111\}$ in Al, $\{112\}$ in Fe.

Barrett has pointed out that the true translational slip directions cannot be deduced with certainty merely by

observation of slip strictions, since at high deformation there is a similar good definition of the boundary lines between deformation bands, though then the lattice orientations in the neighbouring bands or lamellae have rotated away from each other so that the lamellae are no longer in contact on similar net planes as initially. This is evidently due, as he suggested, to the different forces acting on different parts of the crystal, causing different combinations of the normal translational-slip systems to operate in these adjoining regions. (Barrett also apparently considered this to apply to the initial formation of the lamellae). Barrett and Levenson (1939) have published photo-micrographs showing the effect of high deformation in causing flexure of the lamellae, and such flexure may be the cause of the slight arcing in the above Figures 83, 87, 89, 91 from the abraded copper crystal with the beam parallel to the abrasion direction. A few degrees deviation of the abrasion direction from the $\{001\}$, $\{1\bar{1}0\}$ or $\{1\bar{1}1\}$ planes of the copper would be likely to accentuate flexure of the lamellae.

We may sum up the results considering these in conjunction with Barrett's observation of "deformation bands" lamellae in corresponding directions, as confirming the following view of the deformation caused by abrading a single-crystal surface unidirectionally. The abrasive particles are pressed into the surface as they move over it, and they force

fragments of the crystal away from the surface, leaving channel-shaped depressions (scratches) behind them. At the sides and perhaps also the bottom of these the crystal lattice has been partly fragmented in a coherent rotational-slip manner owing to the frictional drag of the abrasive particles tangential to the densely-populated planes which approximate to the sides of the channels. The very thin rotational-slip lamellae are in coherent contact on their common interface planes and are only slightly rotated each from the adjacent ones in general, as in the case of rotational-slip in $K_4Fe(CN)_6.3H_2O$ and gypsum (Wilman, 1950a,b), thus they give rise to continuous "tailed" arcs in the electron-diffraction patterns, and they are difficult to identify even microscopically. These lamellae are usually parallel to densely-populated atomic planes which are inclined steeply or perpendicularly to the surface and tend to be parallel to the abrasion direction or nearly so, and they are largely disorientated still further by flexure (and by translational-slip causing homogeneous lattice rotations) near the immediate surface regions.

This picture differs essentially from that implied by Germer (1936) and Beukers (1939) for the interpretation of similar rotations in PbS abraded on {001} along <001> (and accepted by Raether (1947) in connection with NaCl similarly abraded), in that the fragmentation is not attributed to normal

cleavage (note that copper has no known cleavage plane) and furthermore the evidence provided shows that cohesional contact between them, and regularity of displacement of, the neighbouring lamellar fragments is largely maintained in the rotational-slip as previously described (Wilman, 1950a,b). Thus it appears likely that the thin lamellae would be difficult to recognise with certainty even in electron microphotographs of unidirectionally abraded crystal faces (cf. Raether, 1947) unless perhaps after very slow etching. So far only a general system of scratch channels has been observed, except when wide scratches are made by relatively large abrasive particles or pointed objects such as needles, in which cases translational slip bands inclined to the abrasion direction may sometimes occur (Whitehead, 1949).

One further and exceedingly useful conclusion which can be drawn from the above results from copper is that, at least in the crystal used, there was neither a mosaic structure (cf. Wood and Tapsell, 1946) nor an orientated segregation of traces of impurities to such an extent as to impair or obscure the fundamental origin of the observed characteristic directions of rotational slip. This origin (see Wilman, 1950a,b) is from the form of the normal crystal structure itself and the orientation relative to the direction of abrasion and that of the abraded surface, though it is clearly shown by the present

results that the rotational slip is on densely-populated net planes which may be inclined considerably away from the normal to the surface.

These results obtained by H.Wilman and the author are now being published in the Proc. ~~Phys~~. Roy. Soc. together with similar results obtained by H.Wilman and D.N.Layton in abrasion of iron single-crystals showing rotation on {001}, {110} and {111} planes.

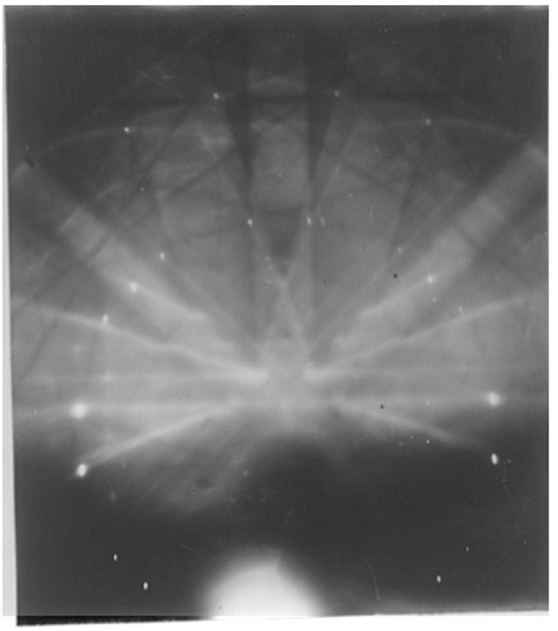

Fig. 79.

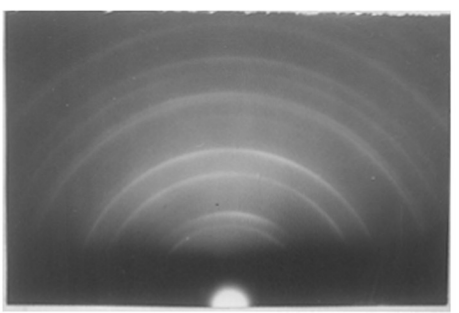

Fig. 80.

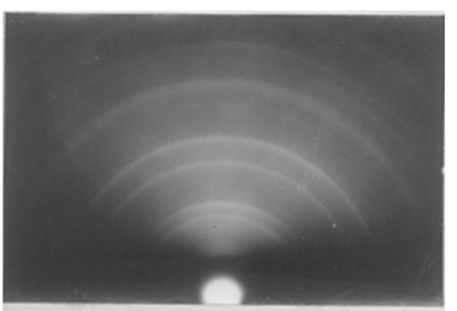

Fig. 81.

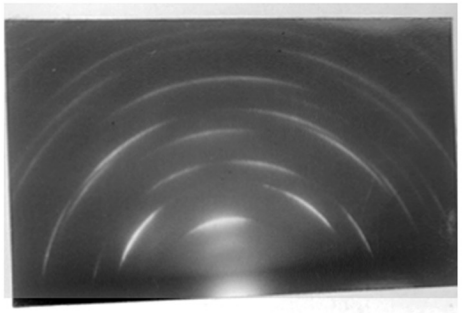

Fig. 82.

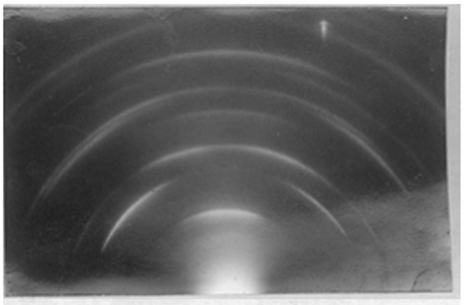

Fig. 83.

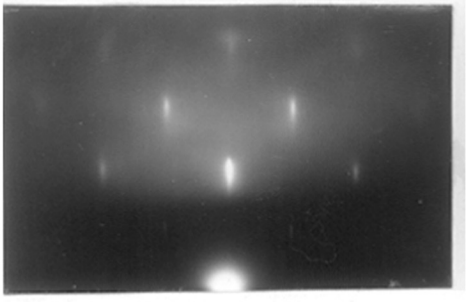

Fig. 84.

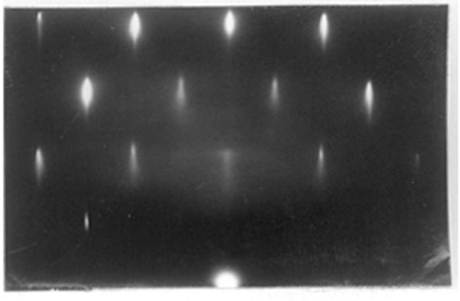

Fig. 85.

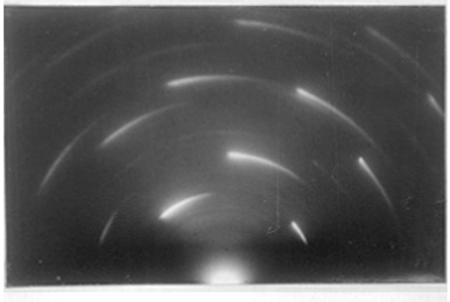

Fig. 86.

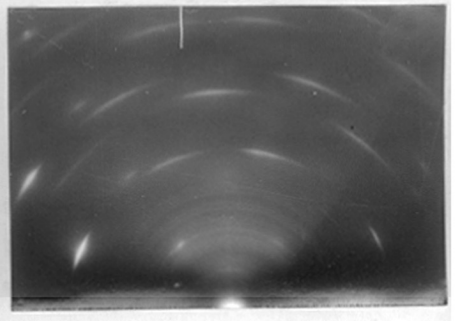

Fig. 87.

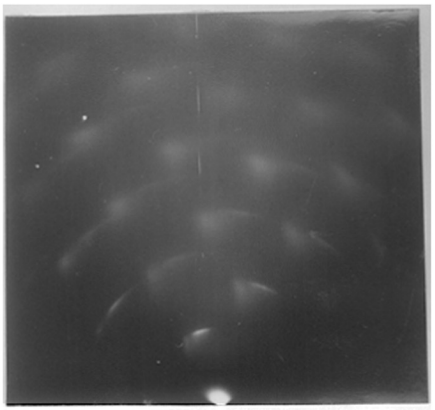

Fig. 88.

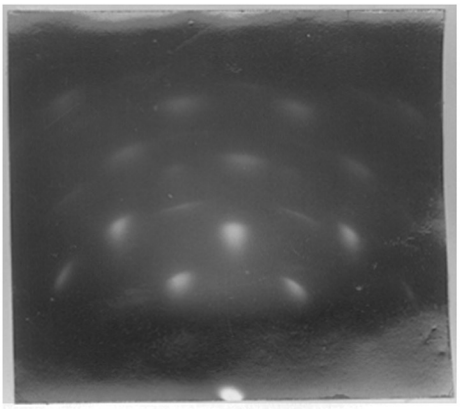

Fig. 89.

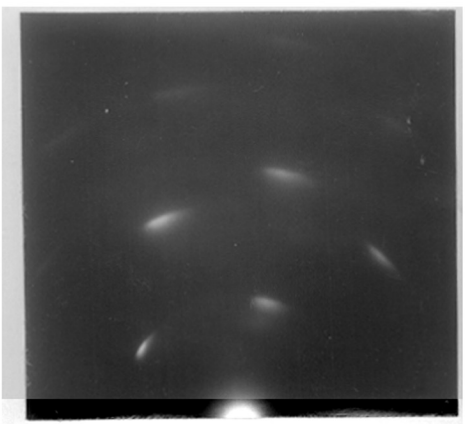

Fig. 90.

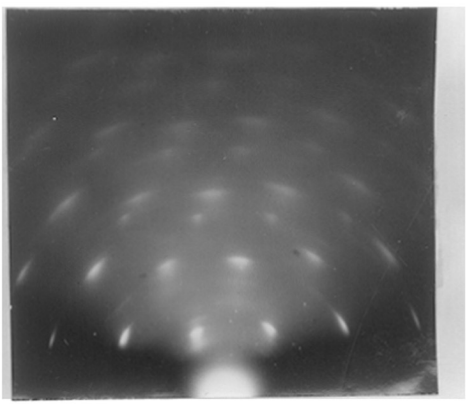

Fig. 91.

PART 7.

SUMMARY.

a. The structure of one-degree oriented films of iron, lead sulphide and zinc, formed by condensation of the vapour on to inert substrates, is investigated in order to find out how the main experimental conditions influence the orientation of the deposit crystals.

(111) is the most commonly occurring orientation of iron deposited on glass; (110) orientation was also found to occur on one occasion. The results indicate that neither the rate of evaporation nor the fine-scale texture of the surface are critical factors. (100) orientation of PbS on glass was observed.

When the vapour stream is inclined to the surface the orientation axis tilts only partly towards it, and the manner in which the tilt varies with the angle of incidence is explained. The results lead to the conclusion that when only this partial tilt of the orientation axis occurs the crystal are oriented with a densely-populated atom plane parallel to the substrate surface, but differently inclined parts of the undulating surface recieve different amounts of deposit material per unit area since the mobility of the deposit material (e.g. iron and lead sulphide) is too low for the

substance to migrate, to any appreciable extent, over the substrate surface. This natural explanation, quite apart from any question of facet development, suffices to account for the partial tilt of the orientation axis observed in the above cases and by previous workers with other substances.

Zinc deposits on glass usually grow in (001), (101) and (112) orientations, (112) orientation being by far the most frequently occurring orientation. The conditions under which these oriented films were obtained, and the methods used for determining the orientations, are described. Pronounced (001) habit of zinc is shown by many of the specimens.

Zinc has a much higher mobility than either iron or lead sulphide. It migrates over the substrate surface to fill the hollows, and consequently one does not observe an effect similar to that observed with those substances. However in virtue of this high mobility the initial (112) orientation of the zinc crystals parallel to the substrate surface is usually modified by the preferential growth of (001) facets in the upper layers of the deposit, giving rise to asymmetric patterns. The preferential growth of (101) facets is also suggested as causing in some cases a modification of the initial (112) orientation in the upper layers of the deposit.

b. The conditions under which two-degree (100) and

(203) orientations of zinc (deposited from the vapour) on the (001) face of rock-salt were obtained are described. The lattice fitting corresponding to these orientations illustrate the contention that a high denisty of coincidence points between the positions of the atoms in the deposit layer and the potential troughs in the substrate surface is the essential feature of epitaxial growth, a high density of coincidence points corresponding to high stability.

c. The influence of the substrate on the orientation of the oxidation product is illustrated by the oxidation of oriented polycrystalline zinc specimens and of a zinc single-crystal cleavage face.

The parallel growth of hexagonal ZnO on polycrystalline zinc specimens with (112) planes parallel to the surface is described, the ZnO growing on the exposed (001) and (101) faces of the zinc. The parallel growth of the hexagonal modification of ZnS on the exposed (001) faces of zinc crystals in (112) orientation is also described.

A technique for etching away the air-formed film of ZnO is described and the parallel growth of (001) -oriented ZnO on the etched cleavage of Zn is illustrated. Contamination of the cleavage surface with sulphur prior to oxidation results in (101) orientation in addition to (001) orientation. Traces of what might be a new polymorph of ZnO are found.

d. It was found that a fresh {110} cleavage face of zinc blende, on oxidation at 650°C., yielded ZnO in {103} orientation while the cleavage face etched by nitric acid yielded ZnO in (001) orientation on the {111} facets of the zinc blende exposed by the etching in addition to the {103} orientation. These results remove certain ambiguities in the results of previous workers.

e. The oxidation of a freshly cleaved {110} surface of ZnS at 520°C. showed rotational slip of the {103} oriented ZnO crystals on the $\{11\bar{2}0\}$ planes of the ZnO or the {110} in the ZnS, constituting the first clear example of rotational slip caused by epitaxial stress. This indication that such slip occurs particularly easily on the ZnO $\{11\bar{2}0\}$ planes is confirmed by the strong lattice rotation produced about the $\langle 110 \rangle$ axis of zinc blende by mechanical abrasion of a {110} face along [001].

Extensive rotational slip is also demonstrated in a copper crystal on {001}, $\{1\bar{1}0\}$ and $\{1\bar{1}1\}$ planes by abrasion of an anodically polished {110} face in directions parallel to these planes respectively, which were normal to the surface or nearly so. In this case there is no likely alternative explanation of the lattice deformation in terms of multiple translational slip.

Acknowledgements.

The author wishes to thank Professor G.I.Finch, M.B.E., F.R.S., for his encouraging interest in the work, and Dr.H.Wilman for suggesting the problems and supervising this research.

The author also wishes to thank Mr.P.R.Rowland of Guy's Hospital Medical School, London, S.E.1, for preparing and making available the copper crystal used in the experiments described in Part 6.

The author is indebted to the Ministry of Education for a grant under "The Further Education and Training Scheme", during the tenure of which this work was carried out.

References.

Acharya, H.K., 1948, Ph.D.Thesis, University of London.

Allen, A.T. and Crenshaw, J.L., 1913, Z.anorg Chem., 79, 130.

Aminoff, G. and Broome, B., 1936, Nature (Lond.), 137, 995.

Aminoff, G. and Broome, B., 1938, Kungl.Svenska Vetenskapakad Handl., 3rd series, 16.

Andrade, E.N.daC. and Martindale, J.G., 1935, Phil.Trans. Roy. Soc., 235, 69.

Bannon, J. and Googan, C.K., 1949, Nature, 163, 62.

Bardeen, J., Brattain, W.H. and Shockley, W., 1946, J.Chem.Phys., 14, 714.

Barrett, C.S., 1938, Amer.Inst.Min.Metall.Engrs., Tech.Pub. 977 (and 1939, Trans.A.I.M.E., 135, 296);

1940, ibid., No.1141 (and 1940, Trans.A.I.M.E., 137, 128);

1943, "The Structure of Metals" Mc.Graw Hill, (New York and London).

1947, Phys.Rev., 72, 243.

Barrett, C.S. and Levenson, L.H., 1939, Amer.Inst.Min.Metall. Engrs. Tech.Pub. 1038. (and 1939, Trans.A.I.M.E., 135, 237);

ibid., No.1104 (and 1940, Trans.A.I.M.E., 145, 231).

Barrett, C.S. and Steadman, F.W., 1942, Amer.Inst.Min.Metall. engrs. Tech.Pub. 1430) (and 1942, Trans.A.I.M.E., 147, 57).

Bateson, S. and Bachmeyer, A.J., 1946, Nature, 158, 133.

Beeching, R., Phil.Mag., 1936, 22, 938.

Beek, O., Smith, A.F. and Wheeler, A., 1940, Proc.Roy.Soc., A. 62, 177.

Benard, J., 1948, Pittsburgh Int.Conference on Surface Reactions, 147.

Beukers, M.C.F., 1939, Rec.Trav.Chim. Pays-Bas, 58, 485.

Boas, W. and Schmid, E., 1931, Z.Physik, 71, 703.

Bosworth, R.C.L., 1935, Proc.Roy.Soc., A.150, 58.

Bound, M. and Richards, D.A., 1939, Proc.Phys.Soc., 51, 256.

Brattain, W.H. and Becker, J.A., 1933, Phys.Rev., 43, 428.

Bruck, L., 1936, Ann.Phys., Leipzig, 26, 233.

Buerger, M.J., 1930, Amer.Miner., 15, 45, 174, 226.

Burgers, W.G. and Dippel, C.J., 1934, Physica, 1, 549.

Burgers, W.G. and van Amstel, J.J.A.P., 1936, Physica, 3, 1037.

Bunn, C.W., 1945, "Chemical Crystallography" (Oxford Univ.Press).

Cahn, J.W., 1949, Journ.Inst.Metals, 76, 121.

Capdecombe, L., 1945, Journ.des Etats de Surface, p.247 (Paris).

Chariton, J.B. and Seminov, M.N., 1924, Z.Physik, 25, 287.

Cockcroft, J.D., 1928, Proc.Roy.Soc., 119, 295.

Crenshaw, J.L., 1913, See Allen and Crenshaw.

Davisson, C. and Germer, L.H., 1927, Phys.Rev., 30, 707.

Dixit, K.R., 1933, Phil.Mag., 16, 1049.

Drabble, J.D., 1949, Ph.D.Thesis, Univ. of London.

Elleman, A.J., 1948, Ph.D.Thesis, Univ. of London.

Evans, D.M. and Wilman, H., 1950, Proc.Phys.Soc., A.63, 298.

Evans, U.R., 1948, Pittsburgh In.Conf. on Surface Reactions.

1948. "Metallic Corrosion" (London, Edward Arnold).

Finch, G.I., 1938, Journ.Chem.Soc., 1137.

Finch, G.I., 1950, Proc.Phys.Soc., B.63, 465.

Finch, G.I. and Quarrell, A.G., 1934, Proc.Phys.Soc., 46, 148.

1939, Proc.Roy.Soc., A.141, 398.

Finch, G.I., Quarrell, A.G. and Wilman, H., 1935, Trans.Farad. Soc., 31, 1051.

Finch, G.I. and Whitmore, E.J., 1938, Trans.Farad.Soc., 34, 640.

Finch, G.I. and Wilman, H., 1937, Erg.exakt.Naturwiss., 16, 353.

Finch, G.I., Wilman, H. and Yang, L., 1947, Disc.Farad.Soc., 43a, 144.

Finch, G.I. and Sun, C.H., 1936, Trans.Farad.Soc., 32, 852.

Fordham, S. and Khalsa, R.G., 1939, J. Chem. Soc., p.406.

Frank, F.C. and Merwe, J.H.van der., 1949, Proc.Roy.Soc., A.198, 205.

Frenkel, J., 1924, Z.Physik, 26, 117.

Frondel, C. and Palache, C., 1950, Amer.Min., 35, 116.

Garforth, F., 1949. See Mott and Cabrera.

Geiling, S., and Richter, T., 1949, Acta.Cryst., 2, 305.

Geist, D., 1949, Acta Cryst., 2, 13.

Gen, M.I., Zelmanoff, I and Schalkinoff, A.I., 1933, Phys.Zeits. Sowjet., 4, 825.

Germer, L.H., 1936, Phys.Rev., 50, 659.

Goche, O. and Wilman, H., 1939, Proc.Phys.Soc., 51, 625.

Hass, G., 1942, Kolloid Zeits., 100, 230.

Hickman, J.W., 1948, Pittsburgh Int.Conf. Surface Reactions, 142

Hull, A.W. and Davey, W.P., 1921, Phys.Rev., 17, 549.

Johnsen, A., 1914, Jahrb.Radioaktivitat u.Electronik, 11, 226.

Kirchner, F., and Lassen, H., 1935, Ann.Physik, 24, 173.

Kirchner, F., 1932, Z.Phys., 76, 755.

Konig, H., 1948, Optik, 3, 101; (1949, Science Abst., No.642).

Kruger, F.A., 1939, Z.Krist., 102, 136.

Lassen, H., 1934, Phys.Z., 35, 172.

Lassen, H. and Bruck, L., Ann.Phys., 22, 65.

Laue, M.von, 1948, "Materiewellen und ihre Interferenzen"

Levinstein, H., 1949, Journ.App.Physics, 20, 306.

Lotmar, W., 1947, Helv.Phys.Acta., 20, 441.

Lustman and Mehl, 1942, Trans.Electrochem.Soc., 81, 369.

Matthewson, C.H. and Phillips, A.J., 1927, Proc.Inst.Metals Divn Amer.Inst.Min.Metall.Engrs., p.143.

Mehl, R.F. and Mc Candless, E.L., 1937, Trans.A.I.M.E., 125,531.

Mehl, R.F., Mc Candless, E.L. and Rhines, F.N., 1934, Nature, 134, 1009.

Menzer, G., 1938, Naturwiss., 26, 385.

Merwe, J.H. van der., 1949, Discn.Farad.Soc., No.5, p.201.

Miayamato, S., 1933, Trans.Farad.Soc., 29, 794.

Miyake, S., 1938, Sci.Pap.Inst.Phys.Chem.Res., Tokyo, 34, 565.

Mott, N.F., 1949, Research, 2, 162.

Mott, N.F. and Cabrera, N., 1949, Rep.Prog.Physics, 12, 163.

Mugge, O., 1898, Neues Jahrb.Mineral Geol. Palaeont, I, 71.

Nelson, H.R., 1937, J.Chem.Phys., 5, 252.

Neuhaus, 1941, Z.Krist., A.103, 297; 105, 287; (Willems, 1943, 105, 53, 144, 149)

Orowan, E., 1942, Nature, 149, 643.

Pfeil, L.B., 1929, J.Iron Steel Inst., 119, 501.

Picard, R.G. and Duffendack, O.S., 1943, Journ.App.Phys., 14, 291.

Pilling, N.B. and Bedworth, R.E., 1923, J.Inst.Metals, 29, 529.

Prewitt-Hopkins, J. and Frondel, C., 1950, Amer.Min., 35, 116.

Raether, H., 1947, Metaux et Corrosion, 22, 2 (No.257).

Ramsdell, L.S., 1947, Amer.Min., 32, 64.

Royer, L., 1928, Bull.soc.franc.Mineral., 51, 7.

Rudiger, O., 1937, Ann.Physik, 30, 505.

Seifert, H., 1937, Fortsch.Mineral., 22, 185.

Schwab, G.M., Trans.Farad.Soc., 1947, 43, 715.

Smith, N., 1936, J.Amer.Chem.Soc., 58, 173.

Stranski, J.N., Disc.Farad.Soc., No.5, p.13.

Straumanis, M., Z.Physikal.Chem. (B), 13, 316.

Tammann, 1930, J.Inst.Metals, 49, 39.

Thomson, G.P., 1927, Nature, 120, 802.

Thomson, G.P., 1931, Proc.Roy.Soc., A.133, 1.

Thomson, G.P. and Cochrane, W., 1939 "The Theory and Practice of Electron Diffraction" (Macmillan).

Thomson, G.P., 1948, Proc.Phys.Soc., 61, 403.

Uyeda, R., Takagi, S. and Hagihara, H., 1941, Proc.Phys.Math. Soc., Japan, 23, 1049.

Valensi, G., 1935, Met.Corr., 12, 196.

Vernon, W.H.J., 1924, Trans.Farad.Soc., 19, 886.

Volmer, H., 1932, Trans.Farad.Soc., 28, 359.

Wagner, C., 1933, Zeits.Phys.Chem., (B) 21, 35.

Was, D.A., Physica, 6, 390.

Weber, A.H. and O'Brien, D.F., Phys.Rev., 60, 574.

Weber, A.H. and Friedrich, L.W., Phys.Rev., 66, 248.

Weber, A.H. and Keagh, C.T., Journ.App.Physics, 19, 1077.

Whitehead, J.R., 1949, Research, 2, 146.

Willems, J., 1943, Z.Kristall., 105, 149.

Williams, R.C. and Wyckoff, R.W.G., 1945, Science, 101, 594.

Wilman, H., 1940, Proc.Phys.Soc., 52, 323.

Wilman, H., 1947, Discn.Farad.Soc., 43a, 248.

Wilman, H., 1948, Proc.Phys.Soc., 60, 117.

Wilman, H., 1950a, Nature, 165, 321.

Wilman, H., 1950b, Proc.Phys.Soc. (in press).

Wood, R.W., 1916, Phil.Mag., 32, 365.

Wood, W.A. and Tapsell, H.J., 1946, Nature, 158, 415.

Wyckoff, R.W.G., 1948, "Crystal Structure" (Interscience Pub.)

Yamaguti, T., 1935, Proc.Phys.Math.Soc.Japan, 17, 443.